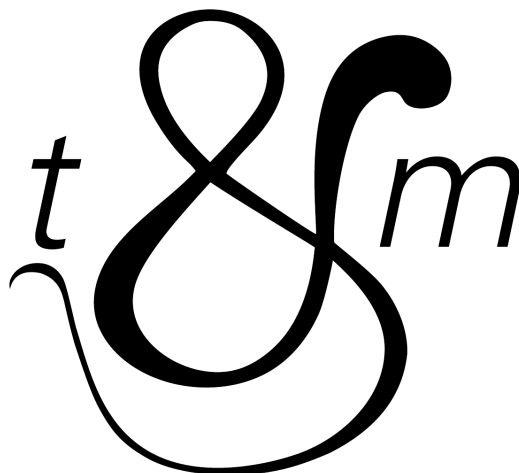


TIME AND MATTER

Proceedings of the 3rd International Conference on
TIME AND MATTER

4 – 8 October 2010
Budva, Montenegro



Edited by
Martin O'Loughlin
Samo Stanič
Darko Veberič



University of Nova Gorica Press

Proceedings of the 3rd International Conference on TIME AND MATTER
4 – 8 October 2010, Budva, Montenegro

Edited by: prof.dr. Martin O'Loughlin, prof.dr. Samo Stanič and
doc.dr. Darko Veberič

Cover design: Eva Kosel

Typeset by: doc.dr. Darko Veberič

Published by: University of Nova Gorica Press, Vipavska 13,
SI-5000 Nova Gorica, Slovenia

Publication year: 2011

Printed by: A-media d.o.o., Šempeter pri Gorici, Slovenia; 80 copies

ISBN 978-961-6311-71-7

CIP - Kataložni zapis o publikaciji
Narodna in univerzitetna knjižnica, Ljubljana

53(082)

INTERNATIONAL Conference on Time and Matter (3 ; 2011 ;
Budva)

Proceedings of the 3rd International Conference on Time
and Matter, 4 – 8 October 2010, Budva, Montenegro / edited
by Martin O'Loughlin, Samo Stanič, Darko Veberič. – Nova
Gorica : University, 2011

ISBN 978-961-6311-71-7

1. O'Loughlin, Martin John

256448768

Copyright © 2011 by University of Nova Gorica Press

All rights reserved. This book, or parts thereof, may not be reproduced in any form or by any means, electronic or mechanical, including photocopying, recording or any information storage and retrieval system now known or to be invented, without written permission from the Publisher.

International Advisory Committee:

Danilo Zavrtanik (University of Nova Gorica), Chair
Ikaros Bigi (University of Notre Dame)
Jeremy Butterfield (University of Cambridge)
Dennis Dieks (Utrecht University)
Martin Faessler (LMU Munich)
Don Howard (University of Notre Dame)
Cecilia Jarlskog (Lund University)
Hermann Nicolai (MPI für Gravitationsphysik)
Leonard Susskind (Stanford University)
Gabriele Veneziano (Collège de France)
Bruce Winstein (University of Chicago)
Hans Dieter Zeh (University of Heidelberg)

Local Organizing Committee:

Samo Stanič (University of Nova Gorica), Chair
Alexandre Creusot (University of Nova Gorica)
Gordana Medin (University of Montenegro)
Martin O'Loughlin (University of Nova Gorica)
Jovan Mirković (University of Montenegro)
Andreja Sušnik (University of Nova Gorica)
Darko Veberič (University of Nova Gorica)
Danilo Zavrtanik (University of Nova Gorica)

Organiser:

Laboratory for Astroparticle Physics, University of Nova Gorica
Vipavska 13, SI-5000 Nova Gorica, Slovenia
Email: tam@ung.si Phone: +386 5 3315 368 Fax: +386 5 3315 385

Previous conferences:

- ☞ Venice, Italy, 11 – 17 August 2002
Proceedings: World Scientific Publishing Company (April 30, 2006)
ISBN-10: 9812566341
- ☞ Bled, Slovenia, 26 – 31 August 2007
Proceedings: University of Nova Gorica Press (2008)
ISBN: 978-961-6311-48-9

The conference was sponsored by



University of Nova Gorica

Preface

The concepts of time and matter form the fundamental framework for our perception and understanding of the phenomena that take place in the world around us – phenomena which can, both at the macroscopic and microscopic level, be described as interactions between objects with certain properties.

The concept of time provides a basis for a quantitative description of the interaction dynamics, providing a parameter that describes the evolution of relations between physical objects.

The concept of matter provides the basis for representing the objects themselves. Matter is represented by the stress-energy tensor together with the intrinsic properties of charge and spin as dictated by the standard model of particle physics. Via the theory of general relativity, given to us by Einstein almost a century ago, this matter in turn creates the same space-time arena in which everything moves and interacts.

However, this simple and apparently intuitive picture remains incomplete with many unanswered questions that are at the forefront of research in almost all branches of physics. Is this framework of time and matter truly suitable for a precise and complete description of all possible physical phenomena, or is this description merely an approximation to a more fundamental underlying reality in which time and matter play new and possibly as yet undiscovered roles? We believe that time had its beginning at the Big Bang, but it is not yet clear in exactly what way this happened or if a meaning can be given to “Before the Big Bang”. Is time at extremely fine temporal resolution really continuous, is it perhaps discrete, or is it just an effective parameter? We also have solid experimental evidence that we are lacking a complete understanding of all possible forms of matter (Figure 1). On the cosmological level this is most evident in ongoing searches for the constituents of dark matter and dark energy while on the microscopic level there is a continual probing of the standard model of particle physics in the hope of finding the elusive Higgs boson or other more exotic new physics.

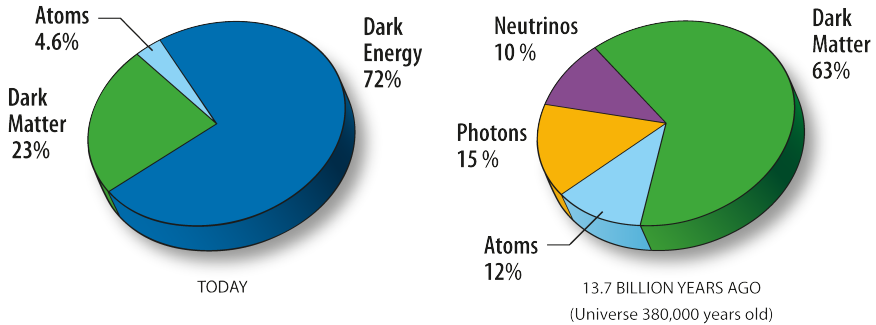


Figure 1: Estimated distribution of dark matter and dark energy in the universe today (left) and $13.7 \cdot 10^9$ years ago (right) obtained from spacecraft-based Wilkinson Microwave Anisotropy Probe (Credit: NASA/WMAP Science Team, 2011).

The primary aim of the third Time and Matter (TaM) conference held in Budva, Montenegro, during September 2010, was to provide a meeting place for ideas from various fields of physics and philosophy involving the concepts of time and matter.

With the recent experimental advances in collider-based particle physics, both at the energy and at the luminosity frontier (Figure 2), we are entering a renaissance for new physics searches at microscopic scales, with direct searches for new particles and rare decay modes and indirect searches for physics beyond the standard model through precision measurements of its parameters. A number of presentations of recent results of these searches were given at TaM 2010, complemented by experimental observations and theoretical treatment of time and matter on macroscopic scales, in astrophysics and cosmology. Both approaches are essential in order to increase our understanding of time and matter.

It is our belief that the TaM 2010 conference was a success both in bringing together people who are at the forefront of research into diverse aspects of the physical world and in promoting new ideas that are being pursued beyond the borders of specialized scientific communities. We hope that the acquaintances made at the conference may turn into friendships and/or research collaborations, and that the various aspects of time and matter that have been discussed may provide fruitful and stimulating material for new ideas and approaches, further clarifying the mysteries of the world in which we live.

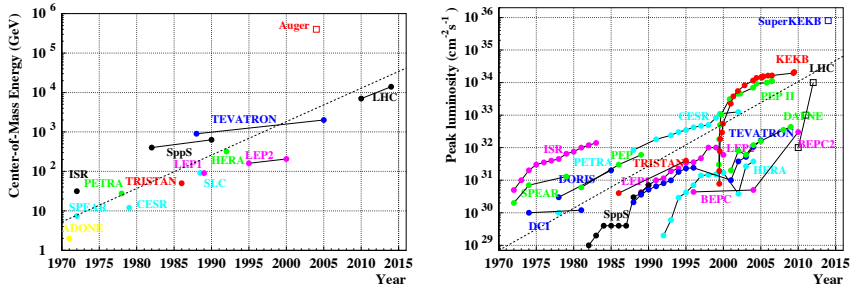


Figure 2: Both the centre-of-mass energy (left) and the luminosity trends (right) of lepton and hadron particle colliders exhibit an exponential increase over 4 to 5 orders of magnitude in the last four decades. The centre-of-mass energies of the interactions of extreme energy cosmic rays with air nuclei, detected by the Pierre Auger Observatory, are shown as a reference.

The presentations at “Time and Matter 2010” were grouped into six sections: problems of matter and dark matter; coherence, de-coherence and entanglement; CP and CPT violation; quantum gravity and cosmology; philosophical perspectives on time and fundamental physics. Twelve of the contributed papers are presented in these proceedings. On behalf of both the local organizing committee and the international advisory committee I would like to express our thanks to all the speakers for their interesting lectures and for the written contributions. The next “Time and Matter” conference is planned to take place in 2013 in Slovenia.

Samo Stanič and Martin O’Loughlin
for the Local Organizing Committee

Contents

<i>Search for solar axions with the CAST experiment</i> B. Lakić	1
<i>Bits, Time, Carriers, and Matter</i> S.S. Mizrahi	17
<i>CP Violation in B Meson Decays - Present and Future</i> P. Križan	33
<i>Improved search for the neutron electric dipole moment at the Paul Scherrer Institut</i> P. Schmidt-Wellenburg	47
<i>Prospects for hunting non-perturbative physics at the Pierre Auger Observatory</i> T.C. Paul	51
<i>Results from the Pierre Auger Observatory</i> T.C. Paul	69
<i>LHCb Status and Prospects</i> R. Lefèvre	87
<i>Various Facets of Spacetime Foam</i> Y.J. Ng	103
<i>A short introduction to Asymptotic Safety</i> R. Percacci	123
<i>Singular Homogeneous Plane-Waves, Matrix Big-Bangs and their non-Abelian Theories</i> L. Seri	143
<i>Cosmic time with quantum matter?</i> H. Zinkernagel	157
<i>Epistemic and ontic interpretation of quantum mechanics: Quantum information theory and Husserl's phenomenology</i> T. Bilban	161

t & *m*

Search for solar axions with the CAST experiment

B. LAKIĆ^{1*}, S. AUNE², K. BARTH³, A. BELOV⁴, S. BORGHI³,
 H. BRÄUNINGER⁵, G. CANTATORE⁶, J.M. CARMONA⁷, S.A. CETIN⁸,
 J.I. COLLAR⁹, T. DAFNI⁷, M. DAVENPORT³, C. ELEFThERIADIS¹⁰,
 N. ELIAS³, C. EZER⁸, G. FANOURAKIS¹¹, E. FERRER-RIBAS²,
 H. FISCHER¹², J. FRANZ¹², P. FRIEDRICH⁵, J. GALÁN⁷, A. GARDIKIOTIS¹³,
 E.N. GAZIS¹⁴, T. GERALIS¹¹, I. GIOMATARIS², S. GNINENKO⁴,
 H. GÓMEZ⁷, E. GRUBER¹², T. GUTHÖRL¹², R. HARTMANN¹⁵,
 F. HAUG³, M.D. HASINOFF¹⁶, D.H.H. HOFFMANN¹⁷, F.J. IGUAZ^{2,7},
 I.G. IRASTORZA⁷, J. JACOBY¹⁸, K. JAKOVČIĆ¹, D. KANG¹²,
 T. KARAGEORGOPOULOU¹⁴, M. KARUZA⁶, K. KÖNIGSMANN¹²,
 R. KOTTHAUS¹⁹, M. KRČMAR¹, K. KOUSOURIS¹¹, M. KUSTER^{5,17},
 P. LANG¹⁷, C. LASSEUR³, J.M. LAURENT³, A. LIOLIOS¹⁰, A. LJUBIČIĆ¹,
 V. LOZZA⁶, G. LUTZ¹⁵, G. LUZÓN⁷, D.W. MILLER⁹, A. MIRIZZI¹⁹,
 J. MORALES⁷, T. NIINIKOSKI³, A. NORDT^{5,17}, T. PAPAEVANGELOU²,
 M.J. PIVOVAROFF²⁰, G. RAITERI⁶, G. RAFFELT¹⁹, T. RASHBA²¹,
 H. RIEGE¹⁷, A. RODRÍGUEZ⁷, M. ROSU¹⁷, I. SAVVIDIS¹⁰,
 Y. SEMERTZIDIS¹³, P. SERPICO³, P.S. SILVA³, S.K. SOLANKI²¹,
 R. SOUFLI²⁰, L. STEWART³, A. TOMÁS⁷, M. TSAGRI¹³, K. VAN BIBBER²⁰,
 T. VAFAIADIS^{3,10}, J. VILLAR⁷, J.K. VOGEL^{12,20}, L. WALCKIERS³,
 Y. WONG³, S.C. YILDIZ⁸, AND K. ZIOUTAS^{3,13}

(CAST COLLABORATION)

¹ *Rudjer Bošković Institute, Zagreb, Croatia*

² *IRFU, Centre d'Études Nucléaires de Saclay (CEA-Saclay), Gif-sur-Yvette, France*

³ *European Organization for Nuclear Research (CERN), Genève, Switzerland*

⁴ *Institute for Nuclear Research (INR), Russian Academy of Sciences, Moscow, Russia*

⁵ *Max-Planck-Institut für Extraterrestrische Physik, Garching, Germany*

⁶ *Instituto Nazionale di Fisica Nucleare (INFN), Sezione di Trieste and Università di Trieste, Trieste, Italy*

⁷ *Instituto de Física Nuclear y Altas Energías, Universidad de Zaragoza, Zaragoza, Spain*

⁸ *Dogus University, Istanbul, Turkey*

* biljana.lakic@irb.hr

- ⁹ *Enrico Fermi Institute and KICP, University of Chicago, Chicago, IL, USA*
¹⁰ *Aristotle University of Thessaloniki, Thessaloniki, Greece*
¹¹ *National Center for Scientific Research "Demokritos", Athens, Greece*
¹² *Albert-Ludwigs-Universität Freiburg, Freiburg, Germany*
¹³ *Physics Department, University of Patras, Patras, Greece*
¹⁴ *National Technical University of Athens, Athens, Greece*
¹⁵ *MPI Halbleiterlabor, München, Germany*
¹⁶ *Department of Physics and Astronomy, University of British Columbia, Vancouver, Canada*
¹⁷ *Technische Universität Darmstadt, IKP, Darmstadt, Germany*
¹⁸ *Johann Wolfgang Goethe-Universität, Institut für Angewandte Physik, Frankfurt am Main, Germany*
¹⁹ *Max-Planck-Institut für Physik (Werner-Heisenberg-Institut), Föhringer Ring 6, 80805 München, Germany*
²⁰ *Lawrence Livermore National Laboratory, Livermore, CA, USA*
²¹ *Max-Planck-Institut für Sonnensystemforschung, Katlenburg-Lindau, Germany*

Abstract: Axions are hypothetical particles arising in models which may solve the CP problem of strong interactions. They are practically stable neutral pseudoscalar particles and also viable candidates for the dark matter in the Universe.

Most of the axion experimental searches are based on the axion coupling to two photons. As a consequence of this coupling, axion could transform into photon and vice versa in external electric and magnetic fields. Axions could be produced in the solar core by conversion of thermal photons in the Coulomb fields of nuclei and electrons - the Primakoff process, and back-converted into photons in a laboratory magnetic field.

CERN Axion Solar Telescope (CAST) is designed to search for these axions by using a Large Hadron Collider prototype dipole magnet which follows the Sun during sunrise and sunset throughout the year. To explore as wide as possible range of axion masses, the operation of CAST is divided in two phases. During the phase I the experiment operated with vacuum inside the magnet bores and scanned axion masses up to 0.02 eV. In order to extend the sensitivity to higher axion masses, the magnet bores are filled with a buffer gas at various densities. In the first part of the CAST phase II, ^4He was used as a buffer gas. In the ongoing second part of the phase II, CAST has been using ^3He to cover axion masses up to 1 eV. So far, no evidence of axion signal has been found and CAST set the most stringent experimental limit on the axion-photon coupling constant over a broad range of axion masses.

Introduction

A long-standing problem in the quantum chromodynamics is the presence of a CP violating term in the Lagrangian:

$$L_{\text{strong CP}} = \bar{\theta} \frac{\alpha_S}{8\pi} G_a^{\mu\nu} \tilde{G}_{a\mu\nu}, \quad (1)$$

where $G_a^{\mu\nu}$ is the color field-strength tensor, $\tilde{G}_{a\mu\nu}$ its dual, and $\bar{\theta}$ is given by $\bar{\theta} = \theta + \text{Arg det } M$. The parameter θ is related to the nontrivial structure of the QCD vacuum, while $\text{Arg det } M$, with M being the quark mass matrix, is the well known CP violating contribution from the electroweak sector.

The strong CP violation should be easily observed in measurements of the electric dipole moment of the neutron (nEDM). However, the existing experimental limit on nEDM requires $\bar{\theta} \leq 10^{-9}$. The strong CP problem why is this parameter $\bar{\theta}$, coming from the strong and weak interactions, is so small?

In 1977, Peccei and Quinn [1] proposed an elegant solution to the strong CP problem: they introduced a new global chiral $U(1)_{\text{PQ}}$ symmetry spontaneously broken at a scale f_a , and axion emerges as the associated pseudo-Goldstone boson. As a result, the parameter $\bar{\theta}$ is re-interpreted as a dynamical variable and is absorbed in the definition of the axion field: $\bar{\theta} \rightarrow a(x)/f_a$. There is no more CP violation in the theory, and the CP violating term (1) is replaced with

$$L_a = \frac{\alpha_S}{8\pi f_a} a(x) G_a^{\mu\nu} \tilde{G}_{a\mu\nu}. \quad (2)$$

The only thing left is to prove experimentally the existence of axions.

Axions

Axion properties

Axions are practically stable neutral pseudoscalars with phenomenology determined by the scale f_a . They generically couple to gluons (2) and mix with neutral pions (see Fig. 1). The axion mass can be expressed in the form $m_a = m_\pi f_\pi / f_a = 6 \text{ eV} (10^6 \text{ GeV} / f_a)$, where m_π and f_π are the pion mass and decay constant, respectively. Axions can couple to photons, nucleons and electrons. Most of the axion experimental searches are based on the axion interaction with two photons:

$$\mathcal{L}_{a\gamma} = -\frac{1}{4} g_{a\gamma} F_{\mu\nu} \tilde{F}^{\mu\nu} a = g_{a\gamma} \mathbf{E} \cdot \mathbf{B} a, \quad (3)$$

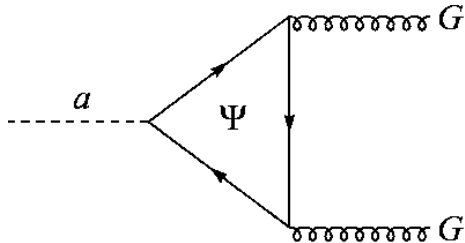


Figure 1: Coupling of axions with gluons via a triangle loop.

where F is the electromagnetic field-strength tensor, \tilde{F} its dual, a the axion field, \mathbf{E} electric and \mathbf{B} magnetic field. The axion-photon coupling constant $g_{a\gamma}$ can be written as

$$g_{a\gamma} = \frac{\alpha}{2\pi f_a} \left(\frac{E}{N} - \frac{2(4+z+w)}{3(1+z+w)} \right) = \frac{\alpha}{2\pi f_a} \left(\frac{E}{N} - 1.92 \pm 0.08 \right), \quad (4)$$

where $z \equiv m_u/m_d$ and $w \equiv m_u/m_s$ are quark-mass ratios and E/N is the model-dependent parameter. As a consequence of this interaction, axions could transform into photons and vice versa in external electric and magnetic fields.

In the originally proposed axion model it was assumed that the scale f_a is equal to the electroweak scale $f_{\text{weak}} = 250$ GeV. After ruling out this model experimentally, the idea of “invisible” axions was introduced. If we assume that $f_a \gg f_{\text{weak}}$, axions become very light and very weakly coupled particles. The best known invisible axion models are the KSVZ (Kim, Shifman, Vainshtein, Zakharov) [2] and DFSZ (Dine, Fischler, Srednicki, Zhitnitskiĭ) [3] model. The major difference between the two models is that in the KSVZ model there is no coupling (at the tree level) of axions with electrons.

Cosmological and astrophysical limits

Due to its properties (neutral, low mass, weak coupling), axions are viable dark matter candidates. In the early Universe, they could have been produced by the coherent “misalignment” mechanism or by thermal interactions, leading to both a cold and a hot dark matter component. In order

to avoid the overclosure of the Universe, axion mass is limited to the range $10^{-5} \lesssim m_a \lesssim 1$ eV.

Axions, as well as other low-mass weakly-interacting particles, could be produced in hot stellar interiors and transport energy out of stars. The couplings of these particles with matter and radiation are bounded by the requirement that stellar lifetimes do not conflict with the observations. For the axion-photon coupling, the most restrictive astrophysical limit, $g_{a\gamma} \lesssim 10^{-10} \text{ GeV}^{-1}$, is derived from globular clusters [4] by comparing the number of horizontal branch (HB) stars with the number of red giants.

Experimental searches ($a - \gamma$ coupling)

Searching for axions is very challenging. The most promising approaches rely on the coupling of axions to two photons, allowing for axion-photon conversion in external electric or magnetic fields. There are several different techniques to search for axion-photon conversion [5]:

1. Laser experiments

- Photon regeneration (“invisible light shining through walls”): if a laser beam propagates through the bore of a magnet with an optical barrier inside, then photons may be regenerated from the pure axion beam after passing through the barrier.
- Photon polarization: the polarization of light propagating through a transverse magnetic field suffers dichroism and birefringence.

2. Search for dark matter axions

- Microwave cavity experiments (the ADMX experiment): galactic halo axions may be detected by their resonant conversion into a microwave signal in a high-Q cavity permeated by a static magnetic field.

3. Search for solar axions

- Crystal detectors and Bragg condition: experiments with crystal detectors exploit the coherent conversion of axions into photons when the axion angle of incidence satisfies the Bragg condition with the crystal plane.
- Helioscope: CERN Axion Solar Telescope (CAST) is the most sensitive experiment of this type (see next section).

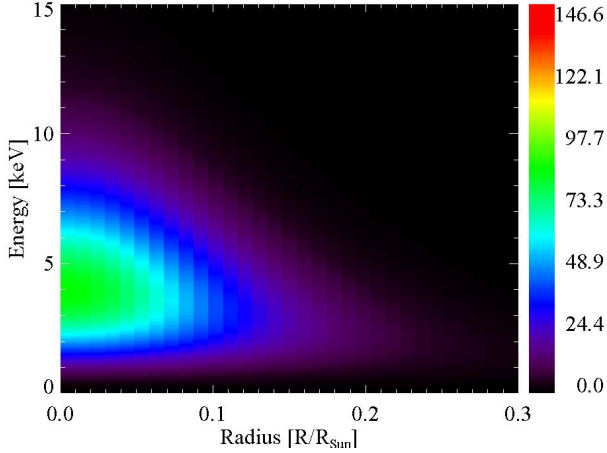


Figure 2: Solar axion flux as a function of energy and solar radius.

CAST physics

The CAST experiment is based on the axion helioscope technique [6] where a dipole magnet is oriented towards the Sun. Axions could be produced in the solar core by conversion of thermal photons in the Coulomb fields of nuclei and electrons - the Primakoff process, and back-converted into photons in a laboratory transverse magnetic field. The expected solar axion flux at the Earth is $\Phi_a = 3.75 \cdot 10^{11} (g_{a\gamma} / (10^{-10} \text{GeV}^{-1}))^2 \text{cm}^{-2} \text{s}^{-1}$ with an approximate spectrum

$$\frac{d\Phi_a}{dE_a} = 6.02 \cdot 10^{10} \left(\frac{g_{a\gamma}}{10^{-10} \text{GeV}^{-1}} \right)^2 \frac{(E_a / \text{keV})^{2.481}}{\exp(E_a / 1.205 \text{keV})} \text{cm}^{-2} \text{s}^{-1} \text{keV}^{-1} \quad (5)$$

and the average energy $\langle E_a \rangle = 4.2 \text{keV}$. (see Fig. 2). The expected number of photons (X-rays) reaching a detector is $N_\gamma = \int (d\Phi_a / dE_a) P_{a \rightarrow \gamma} S t dE_a$ where $P_{a \rightarrow \gamma}$ is the axion-photon conversion probability, S the effective area and t the measurement time. The axion-photon conversion probability in a vacuum can be written as $P_{a \rightarrow \gamma} = (g_{a\gamma} B / q)^2 \sin^2(qL)$ where L is the magnet length, B the magnetic field and $q = m_a^2 / 2E_a$ the axion-photon momentum difference. The probability is maximal if the axion and photon remain in phase over the magnet length, i.e., when the coherence condition $qL < \pi$ is satisfied. Therefore, the experimental sensitivity is restricted to a range of axion masses (for example, $m_a \lesssim 0.02 \text{eV}$ for $L = 10 \text{m}$ and

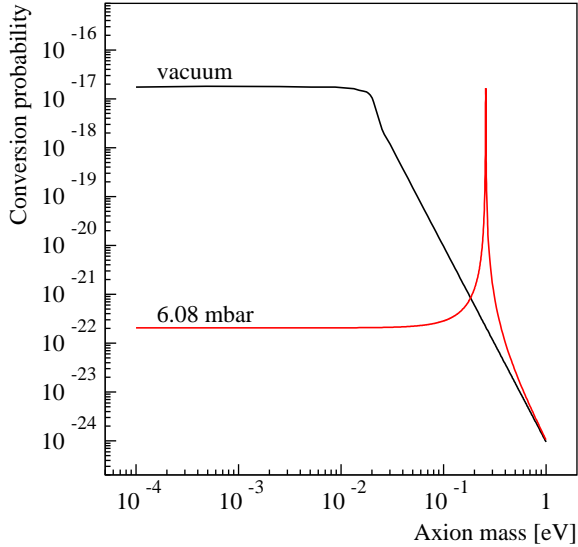


Figure 3: Axion-photon conversion probability versus axion mass. The black line corresponds to the case when vacuum is inside the conversion region and the red line to one particular helium pressure setting. The coupling constant of $1 \cdot 10^{-10} \text{ GeV}^{-1}$ is assumed.

$E_a = 4.2 \text{ keV}$). In order to extend the sensitivity to higher axion masses, the conversion region has to be filled with a buffer gas which provides an effective photon mass m_γ . In that case, the conversion probability takes the form [7]

$$P_{a \rightarrow \gamma} = \left(\frac{B g_{a\gamma}}{2} \right)^2 \frac{1}{q^2 + \Gamma^2/4} \left(1 + e^{-\Gamma L} - 2 e^{-\Gamma L/2} \cos(qL) \right) \quad (6)$$

where $q = |m_a^2 - m_\gamma^2|/2E_a$ and Γ is the inverse absorption length for photons in a gas. As a result, the coherence is restored for a narrow mass window around $m_a = m_\gamma$ (see Fig. 3).

The first implementation of the axion helioscope principle was performed in Brookhaven [8] and later in a more sensitive search in Tokyo [9, 10, 11]. The most sensitive helioscope experiment CAST [12, 13, 14] has been taking data since 2003, both with vacuum and gas (first ^4He and later ^3He) inside the conversion region.



Figure 4: CAST magnet.

CAST Experimental setup

The external magnetic field in the CAST experiment is provided by a Large Hadron Collider (LHC) prototype dipole magnet [15] with the magnetic field $B = 9.0$ T (see Fig. 4). Inside the magnet there are two parallel, straight pipes with the length $L = 9.26$ m and cross-sectional area $S = 2 \times 14.5$ cm². The operating temperature is 1.8 K which is provided by a full cryogenic station. The magnet is mounted on the rotating platform with $\pm 40^\circ$ horizontal and $\pm 8^\circ$ vertical movement. As a result, the Sun can be tracked for 1.5 hours both at sunrise and sunset during the whole year. At both ends of the magnet, different detectors are searching for X-rays coming from axion conversion inside the magnet when it is pointing to the Sun. The time the Sun is not reachable is used for background measurements. Periodical GRID measurements show that CAST points to the Sun within the required precision. As an additional check, the Sun can be filmed twice per year using a camera placed on the magnet. The overall tracking precision is $\sim 0.01^\circ$.

For the data taking with ^4He , a gas system was designed to operate in range 0 – 16.4 mbar at 1.8 K. The system provided a homogenous and stable density along the magnet bores, with adequate accuracy and reproducibility of density settings. At the ends of the bores, four X-ray windows were installed. The windows were designed to provide high X-ray transmission (polypropylene 15 μm), resistance to sudden rise of pressure (strongback mesh) and minimum helium leakage.

Before 2007, CAST utilized the following X-ray detectors: a conventional Time Projection Chamber (TPC)[16], an unshielded Micromegas de-

tector [17] and an X-ray mirror telescope in combination with a Charged Coupled Device (CCD) [18]. The X-ray focusing system and Micromegas were looking for sunrise axions, while the TPC was occupying both bores on the other end of the magnet looking for sunset axions. The X-ray telescope can focus the photons to a $\sim 9 \text{ mm}^2$ spot on the CCD, thus significantly improving the experimental sensitivity.

CAST operation, results and prospects

The operation of the CAST experiment has been foreseen to proceed in several phases:

- **Phase I:** during 2003 and 2004 the experiment operated with vacuum inside the magnet bores, thus exploring the axion mass range up to 0.02 eV. Data analysis showed the absence of excess photons when the magnet was pointing to the Sun, and therefore set an upper limit on the axion-photon coupling of $g_{a\gamma} < 8.8 \cdot 10^{-11} \text{ GeV}^{-1}$ at 95% C.L. [13]. This result is the best experimental limit for the range of axion masses up to 0.02 eV, also superseding the astrophysical limit derived from energy-loss arguments on horizontal branch stars (Fig. 5).
- **Phase II with ^4He :** during 2005 and 2006 the magnet bores were filled with ^4He . The gas pressure was increased from 0 to 14 mbar in appropriate steps to cover equally the accessible mass range. With 160 different pressure settings, the range of axion masses up to 0.39 eV was scanned. The resulting upper limit on the axion-photon coupling constant [14] is shown in Fig. 5. The measurement time at each pressure setting was only a few hours, resulting in small event numbers and therefore large statistical fluctuations of the line contour. For the first time, the limit has entered the QCD axion model band in the electronvolt range.
- **Phase II with ^3He :** In 2008, CAST started taking data with ^3He inside the magnet bores. The data taking will continue until the middle of 2011. The range of axion masses up to $\sim 1.2 \text{ eV}$ will be scanned. The first preliminary results for the axion mass range $0.39\text{eV} < m_a < 0.64 \text{ eV}$ are shown in Fig. 5.

Apart from the main line of research, CAST could also be sensitive to axions from M1 nuclear transition [19, 20], Kaluza-Klein [21] and low energy axions [22].

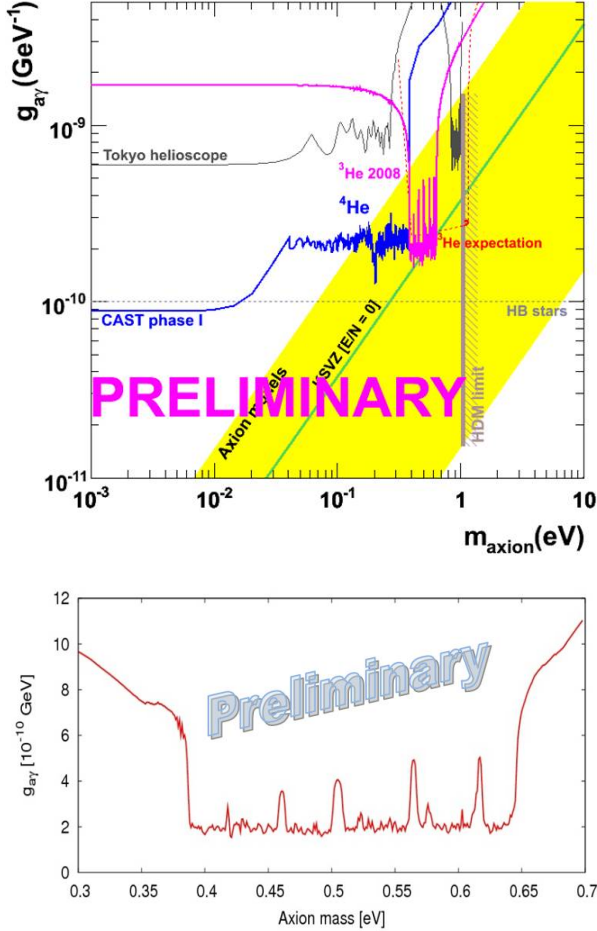


Figure 5: Exclusion limit on the axion-photon coupling constant versus axion mass. Top: Combined result from the CAST phase I and ^4He part of phase II (blue line) and preliminary limit from the first part of ^3He run (pink line) are compared with results from the Tokyo experiment and horizontal branch stars limit. The HDM line refers to the hot dark matter limit [27, 28]. The yellow band represents typical theoretical models while the red dashed line shows CAST prospects for the ^3He run. Bottom: Preliminary ^3He limit in linear scale.

Upgrades for the CAST ^3He phase

During 2007, the CAST experiment performed several upgrades in order to prepare for the more demanding ^3He part of phase II data taking. The most important upgrade was a design and installation of a sophisticated and complex ^3He gas system [23]. The system provides high accuracy in measuring the gas quantity, flexible operation modes (stepping and ramping), absence of thermo-acoustic oscillations and protection of cold, thin X-ray windows during a quench. To scan over a range of axion masses, CAST needs to control precisely the gas density in the magnet bores. This required computational fluid dynamics simulations of the system as well as different physical phenomena such as hydrostatic effect, convection and buoyancy.

Before starting ^3He data taking, CAST detectors were upgraded as well: a new shielded bulk Micromegas replaced the unshielded one, while the TPC detector was replaced by two shielded Micromegas detectors (bulk and microbulk) [24, 25, 26]. Upgraded detectors have a very low background level, therefore improving the experimental sensitivity in the ongoing ^3He part of phase II.

Conclusions and outlook

CAST provides the best experimental limit on the axion-photon coupling constant over a broad range of axion masses. CAST phase II has entered the QCD axion model band and explores the mass range where QCD axions would provide a hot dark matter component similar to neutrinos.

CAST Collaboration has gained a lot of experience in axion helioscope searches. The ongoing R&D on superconducting magnets can lead to much more sensitive helioscopes (see Fig. 6). Future helioscope experiments and microwave cavity searches (e.g. the ADMX experiment) could cover a big part of the QCD axion model region until 2020.

Acknowledgments

We acknowledge support from MSES (Croatia) under grant no. 098-0982887-2872.

References

- [1] R.D. Peccei and H.R. Quinn, Phys. Rev. Lett. **38** (1977) 1440; Phys. Rev. D **16** (1977) 1791.

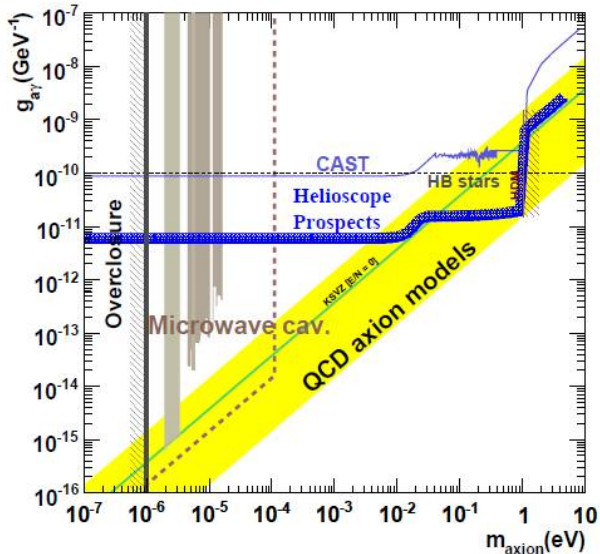


Figure 6: Prospects for future helioscope searches.

- [2] J.E. Kim, Phys. Rev. Lett. **43** (1979) 103; M.A. Shifman, A.I. Vainstein, and V.I. Zakharov, Nucl. Phys. B **166** (1980) 493.
- [3] M. Dine, W. Fischler, and M. Srednicki, Phys. Lett. B **104** (1981) 199; A.R. Zhitnitsky, Sov. J. Nucl. Phys. **31** (1980) 260.
- [4] G.G. Raffelt, Lect. Notes Phys. **741** (2008) 51.
- [5] K. Nakamura et al. (Particle Data Group), J. Phys. G **37** (2010) 075021.
- [6] P. Sikivie, Phys. Rev. Lett. **51** (1983) 1415 [Erratum-ibid. **52** (1984) 695].
- [7] K. van Bibber et al., Phys. Rev. D **39** (1989) 2089.
- [8] D.M. Lazarus et al., Phys. Rev. Lett. **69** (1992) 2333.
- [9] S. Moriyama et al., Phys. Lett. B **434** (1998) 147.
- [10] Y. Inoue et al., Phys. Lett. B **536** (2002) 18.
- [11] Y. Inoue et al., Phys. Lett. B **668** (2008) 93.
- [12] K. Zioutas et al. (CAST Collaboration), Phys. Rev. Lett. **94** (2005) 121301.
- [13] S. Andriamonje et al. (CAST Collaboration), JCAP **04** (2007) 10.
- [14] E. Arik et al. (CAST Collaboration), JCAP **0902** (2009) 008.
- [15] K. Zioutas et al., Nucl. Instrum. Meth. A **425** (1999) 480.
- [16] D. Autiero et al., New. J. Phys. **9** (2007) 171.
- [17] P. Abbon et al., New. J. Phys. **9** (2007) 170.
- [18] M. Kuster et al., New. J. Phys. **9** (2007) 169.
- [19] S. Andriamonje et al. (CAST Collaboration), JCAP **0912** (2009) 002.
- [20] S. Andriamonje et al. (CAST Collaboration), JCAP **1003** (2010) 032.
- [21] R. Horvat, M. Krčmar and B. Lakić, Phys. Rev. D **69** (2004) 125011.
- [22] G. Cantatore et al. (CAST Collaboration), [arXiv:0809.4581(hep-ex)].

- [23] CAST Collaboration, SPSC-TDR-001, CERN-SPSC-2006-029.
- [24] S. Andriamonje *et al.*, JINST **5** (2010) P02001.
- [25] J. Galan *et al.*, JINST **5** (2010) P01009.
- [26] S. Aune *et al.* (CAST Collaboration), Nucl. Instrum. Meth. A **604** (2009) 15.
- [27] S. Hannestad, A. Mirizzi, G.G. Raffelt, and Y.Y.Y. Wong, JCAP **0804** (2008) 019.
- [28] S. Hannestad, A. Mirizzi, G.G. Raffelt and Y.Y.Y. Wong, JCAP **1008** (2010) 001.

t & *m*

Bits, Time, Carriers, and Matter

SALOMON S. MIZRAHI^{1*},

¹ *Departamento de Física-Universidade Federal de São Carlos
Rod. Washington Luis km 235, São Carlos, SP, 13565-905, Brazil*

Abstract: The formal structure of quantum information theory is based on the well founded concepts and postulates of quantum mechanics. In the present contribution I am inverting the usual approach, beginning with the realization of bit states (fundamental units of information). The condition of reversibility is imposed on an ordered sequence of actions operating on a bit states, making them unitary. It is also verified that the uniformity of time originates from a composition law for the actions. In the limit of infinitesimal intervals between actions, a reversible and linear equation arises for the superposition of bits. The admission that a bit of information is necessarily carried by a particle leads to the well known Schrödinger-Pauli equation, where the bit is associated to spin $1/2$. Within this approach the particle dynamics becomes “enslaved” by the spin dynamics. In other words, the bit (or spin) precedes in status the particle dynamical evolution, being at the root of the quantum character of the standard Schrödinger equation, even when spin and spatial degrees of freedom are uncoupled.

Introduction

In the last 15 years we have witnessed the amazing development of the quantum information theory going along with formidable and ingenious experiments involving single atoms, electrons and photons, and also the confirmation of many theoretical predictions as several kinds of Bell inequalities, GHZ criterion, etc. There is a belief [1] that quantum mechanics is a kind of information theory inserted in a class of reversible logic that borrowed concepts of classical information theory, such as bits, logic gates and protocols, supplemented with the concept of superposition of bit states in Hilbert space. The symbiosis between quantum mechanics and information theory permitted the blossom of theoretical, experimental and technological advances, resulting in significant achievements going

* salomon@df.ufscar.br

from the manipulation of a single electron to the current use of quantum cryptography.

Following a series of constructive arguments I will show that the wave-function of a particle $\psi(q)$ – which is the formal expression for its best description – is due to the existence of a bit (the fundamental unit of information, or physically the spin) that carries it. So the spin is at the base of the particle description by a wave-function. This argument was raised by David Hestenes [2]: “...the conventional interpretation of the Schrödinger theory as describing the electron without spin is logically inconsistent with Pauli and Dirac theories...”, still “...the Schrödinger equation must be regarded as identical to the Pauli equation in the absence of magnetic fields.”

Using the tools offered by the structure of the Hilbert space I will begin considering how the formalization of time arises from a discrete classical map of an arbitrary property. Since a bit of information must be transmitted, a physical carrier must be considered, for instance a massive particle. In the present approach I show that its wave-function is due to the existence of the spin, and the quantum dynamics arises as a consequence of properties of Hilbert space. Later on I will derive constructively the equation of motion of a bit and then the correlation with its carrier. Below I present a short discussion about time.

About Time

Despite the previous studies by Nicole Oresme (XIV century) and Galileo Galilei (XVI century) and the works of Torricelli (Galileo’s student) on the kinematical methods in geometry, Isaac Barrow can be considered as the first thinker to discuss its meaning more thoroughly. As he was interested in the relation between time and movement, he succeeded to present time in a solid physical basis. In his *Geometrical Lectures* (1670) [3], he asserted:

“Time denotes not an actual existence, but a certain capacity or possibility for a continuity of existence... Time does not imply motion, as far as its absolute and intrinsic nature is concerned; not far any more than it implies rest; whether things move or are still, whether we sleep or wake, Time pursues the ven tenor of its way. Time implies motion to be measurable; without motion we could not perceive the passage of Time.

...We must evidently regard Time as passing with a steady flow; therefore it must be compared with some handy steady motion, such as the motion of the stars, and especially of the Sun and the Moon [clocks]... But how do we... know that he is carried by an equal motion, and that one day, for example, or one year, is exactly equal to another, or of equal duration? I reply that, if the sun-dial is found to agree with motions of any kind of

time-measuring instrument, designed to be moved uniformly by successive repetition of its own peculiar motion, under suitable conditions, for whole periods or for proportional parts of them; then it is right to say that it registers an equal motion... It seems... the celestial bodies are not the first and original measures of Time..."

Isaac Newton adopted Barrows approach for time and expanded further his ideas by advocating its absoluteness and flow. He wrote in his *Principia* "Absolute, true and mathematical time, in and of itself and of its own nature, without reference to anything external, flows uniformly and by another name is called duration." For Newton time flows at the same rate for an observer in any reference frame.

Notwithstanding, another point of view was proposed by Gottfried Leibniz, opposing Newton idea of time flowing independently of matter. Leibniz defended the concept of time as a mean for ordering sequential events, writing "Time is the order of possibilities which cannot coexist and therefore must exist successively." For Leibniz time exists concomitantly with motion. Nevertheless in both approaches time is linear, uniform and continuous. Thus here I will show that a state evolving according to Schrödinger equation fits within Leibniz concept of time, however the object that changes in time need not be a particle or any massive object, it can be abstract as a bit state.

Linear map and causality

The simplest formal description of time consists in describing a discrete sequence of changes of a property X of some physical system. A discrete successive values of X in the field of real numbers can be broadly represented by the map $x_{n+1} = u(x_n, x_{n-1}, \dots, x_m)$, $n = 0, 1, 2, \dots$, and $0 < m$, where u is some function (regular or not) and $\{x_{n+1}, x_n, x_{n-1}, \dots, x_0\} \in \mathbb{R}$. This is a causal map because x_n is determined by its previous values. Many example can be found in the literature that lead to regular or chaotic motion depending on the choice of the function u [4]. I shall consider a Markovian map where x_{n+1} depends only on its previous value, $x_{n+1} = u(x_n)$. A one-dimensional inhomogeneous linear map is $u(x) = \ell x + a$, where ℓ and a are two real numbers. The causal deterministic linear map $x_{n+1} = \ell x_n + a$ admits the solution $x_n = \ell^n x_0 + a(1 - \ell)^{-1}(1 - \ell^n)$, where x_0 is the initial value. The linear map admits inversion, meaning that any previous value can be determined from the "last" one,

$$x_{n-m} = \ell^{-(m+1)}x_{n+1} - a \sum_{k=1}^{m+1} \ell^{-k}. \quad (1)$$

In particular, I consider the one-dimensional map

$$x_{n+1} = \bar{\alpha} + \alpha x_n \quad (2)$$

with parameters $\ell = \alpha$ and $a = \bar{\alpha} = 1 - \alpha$, and $\alpha \in (0, 1)$, which is invertible and for an initial value x_0 the solution is $x_n = \bar{\alpha}^n + \alpha^n x_0$, ($\bar{\alpha}^n = 1 - \alpha^n$).

The most general multidimensional linear transformation is $x'_\mu = U_{\mu\nu} x_\nu + a_\mu$, where x_ν , a_μ and x'_μ are components of vectors of arbitrary dimension, while $U_{\mu\nu}$ is an element of a square matrix. Defining the composition of two sequential transformations $(\mathbf{a}_1, \mathbf{U}_1)(\mathbf{a}_0, \mathbf{U}_0) = (\mathbf{a}_1 + \mathbf{U}_1 \mathbf{a}_0, \mathbf{U}_1 \mathbf{U}_0) = (\mathbf{a}_2, \mathbf{U}_2)$, for n sequential transformations we have

$$(\mathbf{a}_{n-1}, \mathbf{U}_{n-1}) \cdots (\mathbf{a}_0, \mathbf{U}_0) = \left(\sum_{q=0}^{n-1} \left(\prod_{s=q+1}^{n-1} \mathbf{U}_s \right) \mathbf{a}_q, \prod_{s=0}^{n-1} \mathbf{U}_s \right) = (\mathbf{a}_n, \mathbf{U}_n)$$

and $\mathbf{U}_s = \mathbf{1}$ if $s > n$. Writing the arrays of numbers in Dirac notation, $x_\mu \rightarrow (x_1 \cdots x_m)^\top \rightarrow |X\rangle$; $a_\mu \rightarrow (a_1 \cdots a_m)^\top \rightarrow |A\rangle$; so $U_{\mu\nu} x_\nu \rightarrow \mathbf{U} |X\rangle$, we have $|X_1\rangle = \mathbf{U} |X_0\rangle + |A_0\rangle$, and for n iterations

$$|X_n\rangle = \left(\prod_{s=1}^n \mathbf{U}_s \right) |X_0\rangle + \sum_{q=0}^{n-1} \left(\prod_{s=q+1}^{n-1} \mathbf{U}_s \right) |A_q\rangle. \quad (3)$$

Cbits

Instead of representing one bit of information by the digits 0 and 1, as usual in classical information theory, it is more convenient to consider a column matrix $|X\rangle$ representing the bit, called Cbit [5]. In two dimensions, the Cbit is represented by mutually exclusive states $|1\rangle = \begin{pmatrix} 1 \\ 0 \end{pmatrix}$ and $|0\rangle = \begin{pmatrix} 0 \\ 1 \end{pmatrix}$, for *on* and the *off* state, respectively. It can also be written as $|x\rangle$, $|\bar{x}\rangle$ ($\bar{x} = 1 - x$), $\{x, \bar{x}\} \in \mathbb{Z}_2 = \{0, 1\}$. The state space $\mathcal{B}_2 \equiv (|1\rangle, |0\rangle)$ is a subset of Hilbert space of the infinite countable basis state. The adjoint states $\langle 1| = (|1\rangle)^\top$, $\langle 0| = (|0\rangle)^\top$ are transposed, so $\mathcal{B}_2^\times \equiv (\langle 1|, \langle 0|)$ is the dual vector space of \mathcal{B}_2 , necessary to define two products: (1) *inner product* $\langle x|x'\rangle = \delta_{x,x'}$; (2) *outer product*, $|x\rangle \langle x'|$, which is a 2×2 matrix.

Maps and actions

Here I will consider homogeneous linear maps, putting $|A_0\rangle = 0$ in Eq. (3), and choose the action parameterized as $\mathbf{U}(\alpha, \mathbf{M}) = \bar{\alpha} \mathbf{I} + \alpha \mathbf{M}$, where \mathbf{M} is a square matrix of dimension m defined in \mathbb{R} . The action defines the map

$|x_1\rangle = \mathbf{U}(\alpha_0, \mathbf{M}) |x_0\rangle = \bar{\alpha}_0 |x_0\rangle + \alpha_0 (\mathbf{M} |x_0\rangle)$ and two sequential actions give

$$\mathbf{U}(\alpha_1, \mathbf{M}) \mathbf{U}(\alpha_0, \mathbf{M}) = \bar{\alpha}_1 \bar{\alpha}_0 \mathbf{I} + (\alpha_0 \bar{\alpha}_1 + \bar{\alpha}_0 \alpha_1) \mathbf{M} + \alpha_1 \alpha_0 \mathbf{M}^2.$$

Choosing \mathbf{M} as the generator of a cyclic group of order 2, $\mathbf{M}^2 = \mathbf{I}$, or $\mathbf{M}^{-1} = \mathbf{M}$, so $\mathbf{U}(\alpha_1, \mathbf{M}) \mathbf{U}(\alpha_0, \mathbf{M}) = \mathbf{U}(\alpha_2, \mathbf{M})$ with $\alpha_2 = \alpha_0 \bar{\alpha}_1 + \bar{\alpha}_0 \alpha_1$, $\alpha_2 \in (0, 1)$, therefore $\prod_{k=0}^{n-1} \mathbf{U}(\alpha_k, \mathbf{M}) = \mathbf{U}(\gamma_n, \mathbf{M})$ and the map of a sequence of actions is $|x_n\rangle = \mathbf{U}(\gamma_n, \mathbf{M}) |x_0\rangle$, where $\gamma_n = \gamma_n(\alpha_0, \dots, \alpha_{n-1})$. As $|\det \mathbf{M}| = 1$, the inverse element of $\mathbf{U}(\alpha_1, \mathbf{M})$ is $\mathbf{U}(\alpha_2, \mathbf{M})$, with $\alpha_2 = \alpha_1 / (2\alpha_1 - 1)$ and $\bar{\alpha}_2 = (\alpha_1 - 1) / (2\alpha_1 - 1)$. So, although

$$\mathbf{U}^{-1}(\alpha_1, \mathbf{M}) = \mathbf{U}\left(\frac{\alpha_1}{2\alpha_1 - 1}, \mathbf{M}\right),$$

for $\alpha_1 \in (0, 1)$, nevertheless $\alpha_2 \notin (0, 1)$ and α_2 is singular at $\alpha_1 = 1/2$. So the actions $\mathbf{U}(\alpha, \mathbf{M})$ define a semi-group. Since actions operate on Cbits, the natural choice is $\mathbf{M} = \mathbf{X}$ and $\mathbf{U}(\alpha, \mathbf{X}) \equiv \mathbf{U}_\alpha$, which maps a Cbit $|x_0\rangle$ into a superposition

$$\mathbf{U}_\alpha |x_0\rangle = |x_1\rangle = \alpha |x_0\rangle + \bar{\alpha} |\bar{x}_0\rangle, \quad (\bar{x}_0 = 1 - x_0). \quad (4)$$

Instead of the interval $(0, 1)$ for α , I shall admit only two values, $\{\alpha, \bar{\alpha}\} \in \mathbb{Z}_2 \equiv \{0, 1\}$, the RHS of Eq. (4) is not anymore a superposition, because α and $\bar{\alpha}$ are mutually exclusive, $\alpha \bar{\alpha} = 0$, and a Cbit is mapped into a Cbit. Now the actions $\{\mathbf{U}_0 = \mathbf{I}, \mathbf{U}_1 = \mathbf{X}\}$ form a group, with $\mathbf{U}_{\alpha_2} \mathbf{U}_{\alpha_1} = \mathbf{U}_\beta = \beta \mathbf{I} + \bar{\beta} \mathbf{X}$ and $\beta = \alpha_2 \alpha_1 + \bar{\alpha}_2 \bar{\alpha}_1$, $\bar{\beta} = \alpha_2 \bar{\alpha}_1 + \bar{\alpha}_2 \alpha_1$. So, n sequential actions $\mathbf{U}_{\bar{\alpha}} \equiv \mathbf{U}_{\alpha_n} \dots \mathbf{U}_{\alpha_2} \mathbf{U}_{\alpha_1}$ operating on $|x_0\rangle$ take it to $|x_n\rangle$, that can be $|1\rangle$ or $|0\rangle$. Each sequence of numbers $h_n = \{\alpha_n, \dots, \alpha_1\}$ defines one *history* or *trajectory*, h_n can be interpreted as a set of instructions for the sequential transformation from an initial Cbit $|x_0\rangle$ to $|x_n\rangle$. We can also write $\mathbf{U}_{\bar{\alpha}} |x_0\rangle = A_n(\bar{\alpha}) |x_0\rangle + B_n(\bar{\alpha}) |\bar{x}_0\rangle = |x_n\rangle$ where the coefficients $A_n(\bar{\alpha}), B_n(\bar{\alpha}) \in \mathbb{Z}_2$ will depend on all the α_j (and $\bar{\alpha}_j$), however the product $A_n(\bar{\alpha}) B_n(\bar{\alpha}) = 0$, or, again, $|x_n\rangle$ is either $|0\rangle$ or $|1\rangle$. By a trivial formal manipulation it is simple to show that the label of the state is associated to a classical map

$$|x_1\rangle = \mathbf{U}(\alpha_1) |x_0\rangle = (\alpha_1 \mathbf{I} + \bar{\alpha}_1 \mathbf{X}) |x_0\rangle = |\alpha_1 x_0 + \bar{\alpha}_1 \bar{x}_0\rangle,$$

with $x_1 \equiv \alpha_1 x_0 + \bar{\alpha}_1 \bar{x}_0$ and the label in $|x_n\rangle$ is $x_n = \alpha_n x_{n-1} + \bar{\alpha}_n \bar{x}_{n-1}$.

Actions with real parameters

I choose now the action $\mathbf{U}(\alpha, \beta) = \alpha \mathbf{I} + \beta \mathbf{X}$, with α and β real numbers and $\alpha \beta \neq 0$. Acting on the Cbit $|x_0\rangle$ the result is a superposition $\alpha |x_0\rangle + \beta |\bar{x}_0\rangle$,

(denominated Sbit, Qbit or qubit) which is a non-conventional result in classical information theory. As the normalization requires $\alpha^2 + \beta^2 = 1$, so $(\alpha, \beta) \in \tilde{\mathbb{R}}_2, \mathbb{R}_2$ standing for the set of all real numbers on a circle of radius 1. However, $(\alpha, \beta) \in \mathbb{R}_2$ leads to the following physical inconsistencies:

1. If the action $\mathbf{U}(\alpha, \beta)$ is an element of a group, then the composition of two sequential actions must be an element of the group $\mathbf{U}(\alpha_2, \beta_2) \mathbf{U}(\alpha_1, \beta_1) = \mathbf{U}(\alpha_3, \beta_3)$. However, with the required constraint $\alpha_1^2 + \beta_1^2 = 1$ and $\alpha_2^2 + \beta_2^2 = 1$, the resulting action gives $\alpha_3^2 + \beta_3^2 = 1 + 4\alpha_2\alpha_1\beta_2\beta_1 \neq 1$, thus $(\alpha_3, \beta_3) \notin \mathbb{R}_2$.
2. The inverse of the action is $\mathbf{U}^{-1}(\alpha, \beta) = \tilde{\alpha}\mathbf{I} + \tilde{\beta}\mathbf{X} = \mathbf{U}(\tilde{\alpha}, \tilde{\beta})$, where

$$\tilde{\alpha} = \frac{\alpha}{\alpha^2 - \beta^2} \quad \text{and} \quad \tilde{\beta} = -\frac{\beta}{\alpha^2 - \beta^2}$$

is also inconsistent because $\tilde{\alpha}$ and $\tilde{\beta}$ do not exist for $|\alpha| = |\beta|$ and for $|\alpha| \neq |\beta|$ one notes that $|\tilde{\alpha}|^2 + |\tilde{\beta}|^2 \neq 1$, so also $(\tilde{\alpha}, \tilde{\beta}) \notin \mathbb{R}_2$. It can be immediately verified that $\mathbf{U}^{-1}(\alpha, \beta) \mathbf{U}(\alpha, \beta) = \mathbf{I}$ only if $|\alpha| \neq |\beta|$. Due to the reality of α and β the transposed operator is $\mathbf{U}^T(\alpha, \beta) = \mathbf{U}(\alpha, \beta)$ thus since $\mathbf{U}^T(\alpha, \beta) \neq \mathbf{U}^{-1}(\alpha, \beta)$, therefore $\mathbf{U}(\alpha, \beta)$ is not unitary.

3. While the norm is conserved for the state $\mathbf{U}(\alpha, \beta)|x_0\rangle$, $\langle x_0|\mathbf{U}^T(\alpha, \beta)\mathbf{U}(\alpha, \beta)|x_0\rangle = 1$, it is not conserved for the state $\mathbf{U}^{-1}(\alpha, \beta)|x_0\rangle$, $\langle x_0|(\mathbf{U}^{-1})^T\mathbf{U}^{-1}|x_0\rangle = (\alpha^2 - \beta^2)^{-2}$.

Therefore, if one wants to construct a sequence of n actions $\mathbf{U}_n(\vec{\alpha}, \vec{\beta}) = \prod_{j=1}^n (\alpha_j\mathbf{I} + \beta_j\mathbf{X})$, with $\alpha_j^2 + \beta_j^2 = 1$, which complies with reversibility, the existence of the inverse of each action, $\tilde{\alpha}_j\mathbf{I} + \tilde{\beta}_j\mathbf{X}$ is a necessary condition for the existence of the full inverse sequence $\mathbf{U}_n^{-1}(\vec{\alpha}, \vec{\beta}) = \prod_{j=n}^1 (\tilde{\alpha}_j\mathbf{I} + \tilde{\beta}_j\mathbf{X})$. However, the parameters of the inverse action are not normalized, $\tilde{\alpha}_j^2 + \tilde{\beta}_j^2 = (\alpha_j^2 - \beta_j^2)^{-2} \neq 1$.

Restoring micro-reversibility and uniformity

In order to establish reversibility, the domain of coefficients α and β must be extended to the field complex numbers $(\alpha, \beta) \in \tilde{\mathbb{C}}$, with conditions $|\alpha|^2 + |\beta|^2 = 1$ and $\alpha^2 - \beta^2 = 1 \implies |\beta|^2 + \beta^2 = 0$, which are satisfied

for α real and β being pure imaginary, $\beta = -i|\beta|$. Since there is only one free parameter, a natural parameterization is $\alpha = \cos \zeta$ and $\beta = -i \sin \zeta$, (ζ real), thus the action $\mathbf{U}(\alpha, \beta) \equiv \mathbf{U}(\zeta) = \cos \zeta \mathbf{I} - i \sin \zeta \mathbf{X}$ is now a unitary operator and $\mathbf{U}(\zeta) |x_0\rangle = \cos \zeta |x_0\rangle - i \sin \zeta |\bar{x}_0\rangle$. The complex nature of $\mathbf{U}(\zeta)$ is therefore due to the requirement of reversibility. Acting on the Sbit ($a|x_0\rangle + b|\bar{x}_0\rangle$), one gets ($a_{\bar{\zeta}}|x_0\rangle + b_{\bar{\zeta}}|\bar{x}_0\rangle$), where the new coefficients $a_{\bar{\zeta}} = a \cos \zeta - ib \sin \zeta$ and $b_{\bar{\zeta}} = -i(a \sin \zeta + ib \cos \zeta)$ mix a, b and ζ . So, after one action the probabilities associated to the Cbits are $p_{x_0} = |a \cos \zeta - ib \sin \zeta|^2$, $p_{\bar{x}_0} = |a \sin \zeta + ib \cos \zeta|^2$, with $p_{x_0} + p_{\bar{x}_0} = 1$.

For the sequence of actions $\mathbf{U}_n(\bar{\zeta}) = \exp[-i\phi_n \mathbf{X}]$, where $\phi_n = \sum_{j=1}^n \zeta_j$, operating on $|x_0\rangle$, the result is $\cos \phi_n |x_0\rangle - i \sin \phi_n |\bar{x}_0\rangle = |\psi_n\rangle$. The parameter ϕ_n can be interpreted as a register, which establishes the ordering of the sequence of actions. Since nothing is said about the values of the ζ_j , the intervals between the actions are arbitrary; as shown in Fig. 1, each dot on the line represents one action. Uniformity is absent due to the indefiniteness of the ζ_j .

I will elaborate further on the basis of a reasonable hypothesis: the *composition* law of micro-causality, $\mathbf{U}(\phi_n) \mathbf{U}(\phi_m) = \mathbf{U}(\phi_{n+m})$, is assumed true, signifying that a sequence of m actions followed by another sequence of n actions is the equivalent to a single sequence of $n + m$ actions. The action $\mathbf{U}(\phi_n) = \exp[-i\phi_n \mathbf{X}]$ plus the composition law imply the equation $\phi_n + \phi_m = \phi_{n+m}$ so, necessarily and uniquely, ϕ_n must be linear in n , namely, $\phi_n = n\bar{\zeta}$, $\bar{\zeta}$ being a constant, thus $\mathbf{U}(\phi_n) = \mathbf{U}(n\bar{\zeta}) = \exp[-in\bar{\zeta} \mathbf{X}]$. A simple rule comes out, all the ζ_j are the same and all actions are identical, $\mathbf{U}(n\bar{\zeta}) = [\mathbf{U}(\bar{\zeta})]^n$. There is no iterative map, only a simple formula is sufficient to retrace back any sequence of actions, in the same form as we considered the dichotomic coefficient α_i in the previous section. Note the simple linear dependence on n and the uniformity of time arising as consequence of the composition law, see Fig. 2.

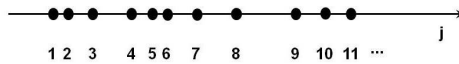


Figure 1: A sequence of arbitrarily spaced actions.

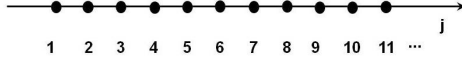


Figure 2: A sequence of uniformly distributed actions.

Evolution equation

Making the discrete intervals in Fig. 2 becoming quite small ($|\bar{\zeta}| \ll 1$), I write the difference between two consecutive actions $\mathbf{U}(n\bar{\zeta})$ and divide by $\bar{\zeta}$, getting $[\mathbf{U}((n+1)\bar{\zeta}) - \mathbf{U}(n\bar{\zeta})] / \bar{\zeta} = (e^{-i\bar{\zeta}\mathbf{X}} - 1) / \bar{\zeta} \exp[-in\bar{\zeta}\mathbf{X}]$. The limit to a continuous parameter is obtained for $n \gg 1$ and $|\bar{\zeta}| \ll 1$, however keeping the product $n\bar{\zeta} = \tau$ finite and $\tau \in (-\infty, \infty)$. A linear differential equation is established and the continuous parameter τ is the *time* in arbitrary units $ih_0 d\mathbf{U}(\tau) / d\tau = \mathbf{X}\mathbf{U}(\tau)$. The constant h_0 is introduced to adjust the dimensions of the equation. Thus the sequence of actions go to a single one, $\mathbf{U}(\tau) = e^{-i\tau\mathbf{X}/h_0}$. Writing $|x_\tau\rangle = \mathbf{U}(\tau)|x_0\rangle$, the linear differential equation for the qubit state

$$ih_0 \frac{d|x_\tau\rangle}{d\tau} = \mathbf{X}|x_\tau\rangle, \quad (5)$$

stands for its evolution and \mathbf{X} , the generator of the evolution, determines how the qubit $|x_\tau\rangle$ as time goes on. It is worth noting that (1) the factor i appears in Eq. (5) because the generator \mathbf{X} is hermitian, it would not exist for an anti-hermitian generator; (2) linearity in time is consequence of the composition law: $|x_0\rangle \rightarrow |x_m\rangle \rightarrow |x_{m+n}\rangle$ is equivalent to $|x_0\rangle \rightarrow |x_{m+n}\rangle$ ($m > n > 0$).

Qubit and its carrier

We can generalize Eq. (5) by writing the generator of the evolution as $\mathbf{G} = \mu\mathbf{I} + \nu\mathbf{X}$, where μ and ν are two real parameters whose dimensions depend on the physical property they represent, so the dynamical equation for the qubit is written as

$$ih_0 \frac{d|\psi_t\rangle}{dt} = \mathbf{G}|\psi_t\rangle, \quad (6)$$

and the evolution operator is $\mathbf{U}(t) = e^{-it(\mu\mathbf{I} + \nu\mathbf{X})/h_0}$, \mathbf{I} and \mathbf{X} commute. The addition of the term $\mu\mathbf{I}/h_0$ is apparently innocuous because the factor

$e^{-it\mu I/h_0}$ does not imply any change on a state vector¹ $|\psi_\tau\rangle$, but for a phase factor $e^{-it\mu I/h_0} |\psi_0\rangle = e^{-it\mu/h_0} |\psi_0\rangle$, whereas $e^{-it\nu X/h_0}$ do really affect the evolution of the state vector, $|\psi_t\rangle = e^{-it\mu/h_0} |\psi'_t\rangle$, $|\psi'_t\rangle = e^{-it\nu X/h_0} |\psi_0\rangle$.

The eigenvalues and eigenstates of the generator G are, $g_\pm = \mu \pm \nu$ and $|x_{\pm 1}\rangle = (|0\rangle \pm |1\rangle) / \sqrt{2}$. The general solution to Eq. (6) is $|\psi_t\rangle = \sum_{\sigma=\pm 1} e^{-ig_\sigma t/h_0} c_\sigma |x_\sigma\rangle$, expressing the oscillatory behavior of the evolution. In analogy to classical mechanics, one can identify the generator of the motion as the Hamiltonian of the qubit, so the parameter μ becomes associated to the *carrier* that transports one qubit of information. Hence the extension from X to $\mu I + \nu X$ is essential because it introduces the carrier of the qubit. For an arbitrary initial condition the mean $\langle \psi_t | G | \psi_t \rangle = \mu + \nu (|c_{+1}|^2 - |c_{-1}|^2)$ is time-independent. We can recognize in the second term the *internal energy*, associated to the flipping of the qubit due to an external field and μ stands as a reference energy associated to the carrier. Regarding the constant h_0 it should have dimensions *Time* \times *Energy*, but should not be identified, by anticipation, to \hbar , the Planck constant.

For an initial state $|\psi_0\rangle = a_0 |x_0\rangle + b_0 |\bar{x}_0\rangle$, the solution to Eq. (6) displays periodic amplitudes

$$\begin{pmatrix} a_t \\ b_t \end{pmatrix} = e^{-it\mu/h_0} \begin{pmatrix} \cos(\nu t/h_0) & -i \sin(\nu t/h_0) \\ -i \sin(\nu t/h_0) & \cos(\nu t/h_0) \end{pmatrix} \begin{pmatrix} a_0 \\ b_0 \end{pmatrix}, \quad (7)$$

The coefficient a_t is a register of events recorded uniformly in a sequential order.

Information is physical

Equation (6) can be interpreted as an equation of motion of a qubit in Hilbert space plus an unknown carrier, that does not have yet a representation and does not show any variation in time while the qubit oscillates [6]. Thus, it becomes necessary to make some physical considerations: the carrier is a structure-less massive particle carrying one qubit of information (in quantum physics it is identified as the *spin*) so the generator G should contain information regarding the motion of the particle with mean energy μ . The simplest logical attempt is to introduce in the formalism the spatial localization of the carrier; the coefficients a_0, b_0 and μ should depend on the particle position in some reference frame,

¹States in Hilbert space are rays and a ray is an equivalent class of vectors that differ by a multiplicative phase factor. $|\psi\rangle$ and $e^{i\phi} |\psi\rangle$ represent the same physical state.

$a_0 \longrightarrow a_0(q)$, $b_0 \longrightarrow b_0(q)$, $\mu \longrightarrow \mu(q)$ ($q \in \mathbb{R}$). Hence we can write $|\psi_0(q)\rangle = a_0(q)|x_0\rangle + b_0(q)|\bar{x}_0\rangle$, that has to satisfy the normalization condition $\int dq |a_0(q)|^2 + \int dq |b_0(q)|^2 = 1$, and still $|a_0(q)|^2$ and $|b_0(q)|^2$ are probabilities, associated to the kets $|x_0\rangle$ and $|\bar{x}_0\rangle$. One notes that the position of the particle should influence the outcomes of the measurements and the state $|\psi_0(q)\rangle$ entangles the qubit state with the position of the particle. Since I am not considering any interaction between both degrees of freedom the parameter ν is q -independent and $\mathbf{G}(q) = \mu(q)\mathbf{I} + \nu\mathbf{X}$.

The functions $a_0(q)$ and $b_0(q)$ should be determined from some law, for the particle, in the dynamical equation $i\hbar_0\partial|\psi(q,t)\rangle/\partial t = \mathbf{G}(q)|\psi(q,t)\rangle$. This equation merges the evolution of the qubit with the motion of its carrier, but still the dependence on position in $\mu(q)$ is irrelevant. In order to be important the parameter μ should also depend on derivatives of q and boundary conditions should be imposed, such that the solution of the appropriate differential equation could determine without ambiguity $a_0(q)$ and $b_0(q)$. Since there is no clue about the functional form of $\mu(q, \partial/\partial q, \dots)$, I am going to take advantage of Hamiltonian mechanics and set μ as the kinetic energy of a non-relativistic particle, $\mu \implies T(p) = p^2/2m$, where p is the linear momentum and m is the particle mass. The dynamical equation is

$$i\hbar_0 \frac{d|\tilde{\psi}_t(p)\rangle}{dt} = \mathbf{H}(p)|\tilde{\psi}_t(p)\rangle. \quad (8)$$

where $\mathbf{H}(p) = T(p)\mathbf{I} + \nu\mathbf{X}$. A general initial condition is that momentum and qubit state are correlated, with probability amplitudes depending on the particle momentum $|\tilde{\psi}_0(p)\rangle = \tilde{a}_0(p)|x_0\rangle + \tilde{b}_0(p)|\bar{x}_0\rangle$. Thus the particle continues to be described by classical mechanics, however our potential knowledge about it is contained in the coefficients $\tilde{a}_0(p)$, $\tilde{b}_0(p)$ and is being conveyed by $|\tilde{\psi}_t(p)\rangle$. The solution to Eq. (8) is $|\tilde{\psi}_t(p)\rangle = e^{-itT(p)/\hbar_0} [\tilde{a}_t(p)|x_0\rangle + \tilde{b}_t(p)|\bar{x}_0\rangle]$ and the carrier mean energy is $\langle \tilde{\psi}_t(p) | \mathbf{H}(p) | \tilde{\psi}_t(p) \rangle = T(p) + 2\varepsilon_0 \mathcal{R}e(\tilde{a}_0^*(p)\tilde{b}_0(p))$. If the initial qubit state depends on the carrier linear momentum the qubit-flip operation is affected by it.

According to classical mechanics, coordinate and momentum are conjugated variables, so one gets the state-vector in coordinate representation $|\psi_t(q)\rangle = \psi_{t,x_0}(q,t)|x_0\rangle + \psi_{t,\bar{x}_0}(q,t)|\bar{x}_0\rangle$ by the means of a Fourier transform of the amplitudes

$$\begin{pmatrix} \psi_{t,x_0}(q) \\ \psi_{t,\bar{x}_0}(q) \end{pmatrix} = \int dq' \left[\int \frac{dp}{2\pi} e^{ip(q-q')/\hbar_1} e^{-itT(p)/\hbar_0} \right] \begin{pmatrix} a_t(q') \\ b_t(q') \end{pmatrix}. \quad (9)$$

The constant \hbar_1 is introduced to set the correct dimensions, having the same units as \hbar_0 , but nothing is said about being the same constant. The

functions $|\psi_{t,x_0}(q)|^2$ and $|\psi_{t,\bar{x}_0}(q)|^2$ are the probabilities for the qubit being in the states $|x_0\rangle$ and $|\bar{x}_0\rangle$, respectively. So even not existing a direct interaction between the qubit and the carrier the probability to find the qubit in states $|x_0\rangle$ or $|\bar{x}_0\rangle$ is affected due to the entanglement between both. The time dependent matrix that evolves the coefficients $a_0(q')$ and $b_0(q')$ is the same as in Eq. (7), however having a q -dependence.

It is worth to stress again that if $T(p) = \mu$ is assumed momentum independent, from Eq. (9) we get $|\psi_{t,x_0}(q)|^2 = |a_t(q)|^2$ and $|\psi_{t,\bar{x}_0}(q)|^2 = |b_t(q)|^2$, and the coordinate q becomes an irrelevant parameter. So the introduction of $\mu = T(p)$ is an important physical ingredient. Additionally, we did an important assumption: the clock that measures the elapsed time of the evolution of the qubit is the same as the one that measures the evolution of the free particle, meaning that both degrees of freedom are measured by a *single clock*, thus partaking a single time t .

Returning to the formalism, as $pe^{ip(q-q')/h_1} = (-ih_1 d/dq) e^{ip(q-q')/h_1}$, in Eq. (9) we can substitute p by $-ih_1 d/dq$, so $|\psi(q,t)\rangle = e^{-it((-ih_1 \partial/\partial q)^2/(2mh_0))} \times [a_t(q)|x_0\rangle + b_t(q)|\bar{x}_0\rangle]$. Deriving with respect to t , and after some formal manipulations one gets

$$ih_0 \frac{\partial |\psi(q,t)\rangle}{\partial t} = \left[\frac{1}{2m} \left(-ih_1 \frac{\partial}{\partial q} \right)^2 I + \nu X \right] |\psi(q,t)\rangle, \quad (10)$$

obtaining the dependence of μ on the position coordinate. The generator of the motion for both degrees of freedom (qubit and particle position) is the Hamiltonian of the carrier. In the presence of an external force the potential energy $V(q)$ should be added to the expression in brackets in Eq. (10). Worth to observe that the constants, h_0 and h_1 , have the same dimensions but still they cannot be assumed being the same. Only comparison between predictions of Eq. (10) with experimental data could decide on the values of the constants and their universality. For $h_0 = h_1 = \hbar$, the Schrödinger equation follows, and we may recognize that the existence of a wave-function for the description of a particle is due the very existence of an internal degree of freedom, the particle spin.

Remarks and conclusions

Generalization of the generator in Eq. (10) to 3 dimensions is immediate, $\partial/\partial q \rightarrow \nabla$ and $X \rightarrow \vec{\sigma}$, with Hamiltonian $(-ih_1 \nabla)^2/2m + V(\vec{r}) + \vec{v} \cdot \vec{\sigma}$, where $\vec{\sigma}$ is the vector whose components are the Pauli matrices and \vec{v} is an external field vector that could also be time-dependent. Why the quantum equation persists, i.e., even when we set $\vec{v} = 0$? For $\nu = 0$ in Eq.

(10) qubit and particle position become uncorrelated due to the decoupling, but still the particle is described by a wave-function ruled by the equation $i\hbar_0\partial\psi_{t,x_0}(q)/\partial t = H_0(q, -i\hbar_1\partial/\partial q)\psi_{t,x_0}(q)$ (the same equation holds for $\psi_{t,\bar{x}_0}(q)$) and not by the classical dynamics. Thus if the initial conditions are the same then the wave-function $\psi_{t,x_0}(q)$ and $\psi_{t,\bar{x}_0}(q)$ are identical, therefore there is redundancy and the information is duplicated. Because we have introduced probabilities in the theory, we cannot retrieve the deterministic laws of classical mechanics although we used classical physics for its derivation. We should remember that the spin of electrons in atoms is never quiescent, there are correlations and interactions with the other degrees of freedom. However even if there was no interaction, the Schrödinger equation would be the most fitted to describe the particle dynamics because the spin is omnipresent.

Usually, foggy arguments are involved in the derivation of Schrödinger equation, where dynamical variable are transformed into operators *ad hoc* $E \rightarrow i\hbar\partial/\partial t$, $p \rightarrow -i\hbar\partial/\partial x$, minimization of the action, extension of the Hamilton-Jacobi formalism, etc. As a matter of fact, its discovery is based on many previously existing experimental data, and its success is due essentially to its capacity to circumvent the epistemological problems that were present in the matrix mechanics theory of Heisenberg, Born and Jordan and to also encompass de Broglie hypothesis of the wave character of a massive particle. Moreover, why a particle is represented by a wave-function is not clearly elucidated, although justified by the necessity of its description through a wave equation and probabilities.

Still a valid question is: as quantum mechanics is constituted by a set of rules for doing probabilistic predictions (in a very peculiar manner) about measurements that come out from prepared experiments involving macroscopic apparatuses and the properties of a microscopic systems (although the apparatus is made of atoms) what are the limits of dimensional size and energies (mass or/and kinetic energy) of the system to still display quantum effects? We know that these are present in subatomic physics (even for structure-less particles as the light leptons) up to buckyballs (a structure made of 60 carbon atoms) and SQUID rings at very low temperature, that could hardly be recognized as microscopic. It seems that although size as well as energies are important for the measurement of quantum effects, they are not too much determinant and there are no rules to establish sharp limits. In conclusion, the reasonings presented in this contribution go modestly and without wide generalization to other research in the field, relating quantum phenomena to the amount of information carried by a massive particle. Summarizing in one sentence, by setting a qubit as the fundamental unit of information, the need arises for physical carrier which

shows measurable quantum effects, otherwise material particles would behave classically.

Acknowledgments

The author thanks the financial support received by FAPESP and CNPq (Brazilian agencies), under the auspices of Instituto Nacional de Ciência e Tecnologia - Informação Quântica (INCT-IQ).

References

- [1] C.A. Fuchs, *Quantum Mechanics as Quantum Information (and only a little more)*, [arXiv:quant-ph/0205039].
- [2] R. Gurtler and D. Hestenes, 1975, *J. Math. Phys.* **16** (1975) 573-584; D. Hestenes, *Am. J. Phys.* **47** (1979) 399-415.
- [3] I. Barrow, *Geometrical lectures*, in <http://ia700300.us.archive.org/load.djvu.applet.php?file=19/items/geometricollectu00barruoft/geometricollectu00barruoft.djvu>.
- [4] D.W. Jordan and P. Smith, *Nonlinear Ordinary Differential Equations: An Introduction to Dynamical Systems*, (Oxford Applied and Engineering Mathematics).
- [5] N.D. Mermin, *Quantum Computer Science: An Introduction*, Cambridge University Press (2007).
- [6] R. Landauer, *Information is Physical*, *Physics Today* **44** (1991) 23-29.

t & *m*

CP Violation in B Meson Decays - Present and Future

P. KRIŽAN^{1,2*}

¹ Faculty of Mathematics and Physics, University of Ljubljana, Ljubljana, Slovenia

² J. Stefan Institute, Jamova 39, SI-1000 Ljubljana, Slovenia

Abstract: The paper briefly reviews measurements of CP violation in B meson decays, and then proceeds with discussing the future experiments at super B factories. It presents the physics motivation and the tools, accelerators and detectors, and reviews the status of the two projects, SuperKEKB/Belle-II in Japan and SuperB in Italy.

Introduction

The two B factories, PEP-II with BaBar and KEKB with Belle, have been a real success story. They were built with the primary goal of measuring CP violation in the B system. From the discovery of large CP violation in 2001 (Fig. 1), the B factory results evolved into a precision measurement of the CP violation parameter $\sin 2\phi_1 = \sin 2\beta = 0.655 \pm 0.024$ in $B \rightarrow J/\psi K^0$ decays [1, 2, 3]. As displayed in Fig. 2, the constraints from measurements of angles and sides of the unitarity triangle show a remarkable agreement, which significantly contributed to the 2008 Nobel prize awarded to M. Kobayashi and T. Maskawa. The two B factories also observed direct CP violation in B decays, measured rare decay modes of B mesons, and observed mixing of D^0 mesons. They measured CP violation in $b \rightarrow s$ transitions, thus probing new sources of CP violation. The study of forward-backward asymmetry in $b \rightarrow sl^+l^-$ has by now become a powerful tool in the search for physics beyond the Standard Model (SM). Both collaborations also searched for lepton flavor violating τ decays, and, last but not least, observed a long list of new hadrons, some of which do not seem to fit into the standard meson and baryon schemes. All this was only possible because of the fantastic performance of the accelerators, much beyond their design values. In the KEKB case, the peak luminosity reached

* peter.krizan@ijs.si

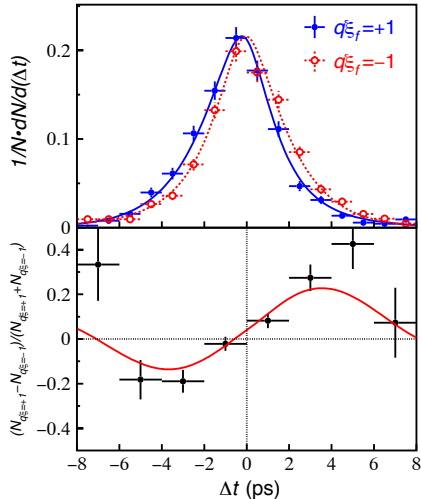


Figure 1: CP violation in $b \rightarrow c\bar{c}s$ transitions, one of the early measurements by the Belle Collaboration [4]. Top: time evolution for the decays of B^0 mesons (solid points) and their anti-particles, \bar{B}^0 mesons (open points). Bottom: the raw asymmetry (fractional difference) for the same data set.

a world record value of $2.1 \cdot 10^{34} \text{ cm}^{-2} \text{ s}^{-1}$, exceeding the design value by a factor of more than two. The two collaborations have accumulated data samples corresponding to integrated luminosities of 0.557 ab^{-1} (BaBar) and 1.041 ab^{-1} (Belle).

While B factories were built to check whether the SM with the CKM matrix is correct, the next generation of B factories (super B factories) will have to show in which way the SM is wrong. To search for departures from SM, a two orders of magnitude larger data sample of decays of B and D mesons and τ leptons is needed, corresponding to an integrated luminosity of $50\text{--}75 \text{ ab}^{-1}$. A substantial upgrade is therefore required both of the accelerator complex as well as of the detector [5, 6]. Note, however, that it will be a different world in four years, when the first super B factory starts to operate; there will be serious competition from the LHCb and BESIII experiments. Still, e^+e^- colliders operating at (or near) the $Y(4S)$ resonance will have considerable advantages in several classes of measurements, e.g., with final states involving neutral particles (γ, π^0) and neutrinos, and will be complementary in many more.

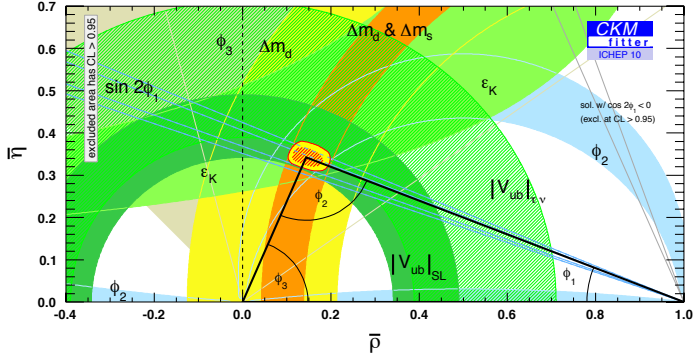


Figure 2: Constraints of the parameters of the unitarity triangle, shown in the $(\bar{\rho}, \bar{\eta})$ plane, as derived from CP violation measurements in the B and K meson systems, from measurements of $b \rightarrow u$ transitions, and from particle-antiparticle mixing of B_d and B_s mesons [7].

In what follows we shall first discuss the physics motivation, the accelerators and detectors, and then we shall review the status of the two projects, SuperKEKB/Belle-II in Japan and SuperB in Italy.

Physics motivation for super B factories

Examples of particularly challenging measurements which are only possible at a B factory are the studies of B meson decays with more than one neutrino in the final state. Such a process is the leptonic decay $B \rightarrow \tau \nu_\tau$ which is followed by the decay of the τ lepton with one or two additional neutrinos in the final state. In the SM, this transition proceeds via W annihilation, but in some new physics (NP) extensions it could also be mediated by a charged Higgs boson [8]. The measured branching fraction can therefore be used to set limits on the two parameters, the charged Higgs mass and the ratio of vacuum expectation values, $\tan \beta$. As shown in Fig. 3, with the present measurements (green) it is possible to exclude a sizable part of the parameter space; with a data sample corresponding to a luminosity of 50 ab^{-1} , the five standard deviations discovery region covers a substantial fraction of the parameter space (red). The sensitivity is comparable to direct searches with large data sets at the LHC.

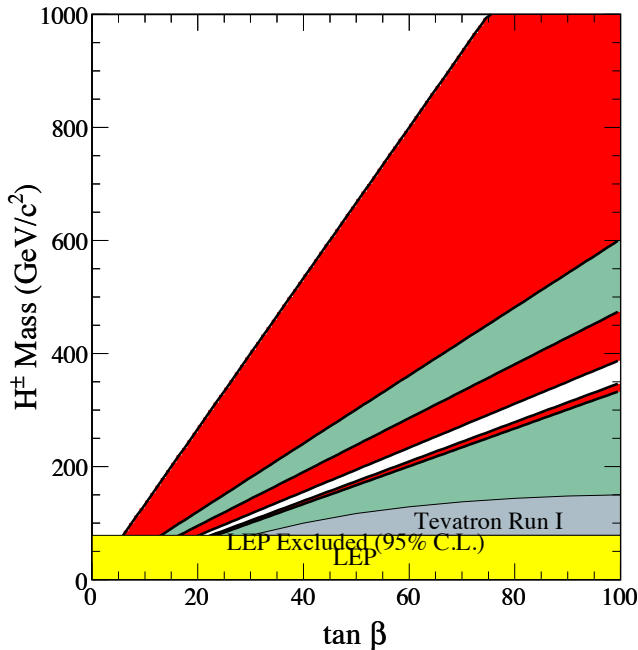


Figure 3: Five standard deviations discovery region (red) for the charged Higgs boson in the $(m_{H^\pm}, \tan \beta)$ plane, from the measurement of $\mathcal{B}(B^+ \rightarrow \tau^+ \nu)$ with 50 ab^{-1} [9]. Other shaded regions show the current 95% C.L. exclusion region.

Processes with just one neutrino in the final state can be searched for in the following way [10]. First, one of the B mesons is fully reconstructed in a number of exclusive decay channels like $B \rightarrow D^{(*)} \pi$. Because of the exclusive associated production of B meson pairs in a B factory, the remaining particles in the event must be the decay products of the associated B . In the $B^- \rightarrow \tau^- \bar{\nu}_\tau$, $\tau^- \rightarrow \mu^- \nu_\tau \bar{\nu}_\mu$, $e^- \nu_\tau \bar{\nu}_e$, $\pi^- \nu_\tau$, decay sequences, only one charged particle is detected. To exclude background events with additional neutral particles (π^0 or γ) in the final state, we use the remaining energy in the calorimeter which is not associated with reconstructed charged tracks. In this measurement we greatly profit from the excellent hermeticity of the spectrometers of the B factories.

A similar process, $B \rightarrow D\tau^-\bar{\nu}_\tau$ is sensitive to the charged Higgs boson as well [11]. Compared to $B \rightarrow \tau\nu_\tau$, it has a smaller theoretical uncertainty, a larger branching fraction [12, 13], and the differential distributions can be used to discriminate the contributions of W^+ and H^+ . It is worth noting that while LHC experiments are sensitive to $H - b - t$ coupling, in $B \rightarrow \tau\nu_\tau$ and $B \rightarrow D\tau\bar{\nu}_\tau$ we probe the $H - b - u$ and $H - b - c$ couplings. The decay $B \rightarrow K^{(*)}\nu\bar{\nu}$ has a similar event topology as $B^- \rightarrow \tau^-\bar{\nu}_\tau$, and a similar event analysis can be applied to it as well. By simultaneously measuring the branching fractions for the two decay types and comparing them to the SM predictions ($4 \cdot 10^{-6}$ for $K\nu\bar{\nu}$ and $6.8 \cdot 10^{-6}$ for $K^*\nu\bar{\nu}$, with contribution from penguin box diagrams) it is possible to determine the contributions of anomalous right-handed and left-handed couplings [14, 9, 15].

Another example of a decay which cannot be studied at LHCb is a measurement of CP violation in $B \rightarrow K_S\pi^0\gamma$ decays in a search for right-handed currents. The present uncertainty in the time-dependent CP violation parameter S is about 0.2, and should be reduced to a few percent level with 50 ab^{-1} of data. Super B factories will also be used to search for lepton flavour violating decays of τ leptons, in particular in the $\mu\gamma$ and $\ell\ell\ell$ final state. Theoretical predictions for branching fractions of these two decay modes are between 10^{-10} and 10^{-7} for various extensions of SM (mSUGRA+seesaw, SUSY+SO(10), SM+seesaw, non-universal Z^0 , SUSY+Higgs). The reach of super B factories (from 10^{-9} to 10^{-8} , depending on the decay mode) will allow probing of these predictions and discrimination between the different NP theories [16].

Two recent publications summarize the physics potential of a super B factory, one prepared by Belle-II authors and guests [9], and the other by SuperB collaborators and guests [15]. To summarize, there is a good chance to see new phenomena, such as CP violation in B decays from new physics sources, or lepton flavor violation in τ decays. The Super B factory results will help to diagnose or constrain new physics models. $B \rightarrow \tau\bar{\nu}_\tau$ and $B \rightarrow D^{(*)}\tau\bar{\nu}_\tau$ decays can probe the charged Higgs contribution in the large $\tan\beta$ region. The physics motivation for a super B factory is independent of LHC. If LHC experiments find new physics phenomena, precision flavour physics is compulsory to understand it; if no new physics is found at LHC, high statistics B and τ decays would be a unique way to search for new physics above the TeV scale (or at the TeV scale in case of the minimal flavour violation scenario). Needless to say that there are many more topics to explore, including for example CP violation searches for charmed hadrons, searches for new hadrons.

It is worthwhile to refer to a lesson from history: the top quark mass was first estimated through the observation of $B^0 - \bar{B}^0$ mixing at ARGUS,

and it took seven more years to directly observe it and measure its mass at the CDF and D0 experiments. Similarly, the prediction of the charm quark came from the observed absence of flavour changing neutral currents via the GIM mechanism. Its mass could be estimated from the observed K^0 mixing rate.

Accelerators

To search for departures from the SM, a data sample two orders of magnitude larger is needed. For such an increase in the data sample, a sizable upgrade of the B factory accelerator complex is required leading to a 40 times larger peak luminosity. These next generation accelerators are known as super B factories. There are two super B factory projects under way. The first one, SuperKEKB, foresees a substantial redesign of elements of the existing KEKB accelerator complex while retaining the same tunnel and related infrastructure. After 11 years of successful operation, the last KEKB beam was ceremonially aborted on June 30, 2010. This opened the way for the construction of SuperKEKB. To increase the luminosity by a factor of 40 the plan is to modestly increase the current (by a factor of 2) with respect to the KEKB values, and dramatically shrink the beam size at the collision point, while the beam beam parameter is kept at the KEKB value (Table 1). In this ‘nano-beam’ scheme which was invented by P. Raimondi for the Italian SuperB project [17], the beams collide at a rather large angle of 83 mrad (compared to 22 mrad in KEKB). In addition, a lower beam asymmetry of 7 GeV and 4 GeV instead of 8 GeV and 3.5 GeV is needed to reduce the beam losses due to Touschek scattering in the low energy beam.

The modifications of the KEKB accelerator complex include: improvements in electron injection, a new positron target and damping ring, redesign of the lattices of the low energy (LER) and high energy (HER) rings, replacing short dipoles with longer ones (LER), installing TiN-coated beam pipe with ante-chambers, modifications of the RF system, and a completely redesigned interaction region [18].

Another approach to the design a super B factory will be exploited in the Italian SuperB project [19]. Here it is foreseen that a new tunnel will be built (Fig. 4); the site will be chosen early in 2011. Parts of the beam elements of PEP-II will be reused in the accelerator construction. In addition to the nano-beam scheme, an essential feature of the SuperB accelerator is the crab waist collision of two beams in which special sextupoles will be used close to the interaction region to maximize the overlap of the two beams. This scheme was successfully tested at the DAΦNE ring [20]. The SuperB accelerator is designed in such a way that it can be modified

	LER	HER	
Energy	4.0	7.0	GeV
Half crossing angle	41.5		mrاد
Horizontal emittance	3.2	4.3	nm
Emittance ratio	0.27	0.25	%
Beta functions at IP	32 (x) / 0.27 (y)	25 / 0.31	mm
Beam currents	3.6	2.6	A
Beam-beam parameter	0.0886	0.0830	
Luminosity	$8 \cdot 10^{35}$		$\text{cm}^{-2} \text{s}^{-1}$

Table 1: SuperKEKB accelerator parameters for the low energy (LER) and high energy (HER) beams.

to run at the $\psi(3770)$ resonance close to charm threshold, where pairs of D^0 mesons are produced in a coherent $L = 1$ state. Data accumulated at charm threshold would allow precision charm mixing, CP violation and CPT violation studies. Another feature of the SuperB accelerator will be the polarization of the low energy (electron) beam. This will increase the sensitivity to lepton flavour violating τ decays and CP violation in τ decays through a reduction of backgrounds. It would also enable a precise $\sin^2 \Theta_W$ measurement.

Detectors

The planned substantial increase in luminosity requires a careful design of the detectors. To maintain the excellent performance of the spectrometers, the critical issues will be to mitigate the effects of higher backgrounds (by a factor of 10 to 20), leading to an increase in occupancy and radiation damage, as well as fake hits and pile-up noise in the electromagnetic calorimeter. Higher event rates will require substantial modifications in the trigger scheme, DAQ and computing relative to the current experiments. In addition, improved hadron identification is needed, and similarly good (or better) hermeticity is required [18].

For the Belle-II detector (Fig. 5), the following solutions will be adopted [18]. The inner layers of the vertex detector will be replaced with a pixel detector, the inner part of the main tracker (CDC, central drift chamber) will be replaced with a silicon strip detector, a better particle identification device will be used, the CsI(Tl) crystals of the end-cap calorimeter will be replaced by pure CsI, the resistive plate chambers of the end-cap muon



Figure 4: The new SuperB accelerator complex at one of the possible sites, the Frascati National Laboratory.

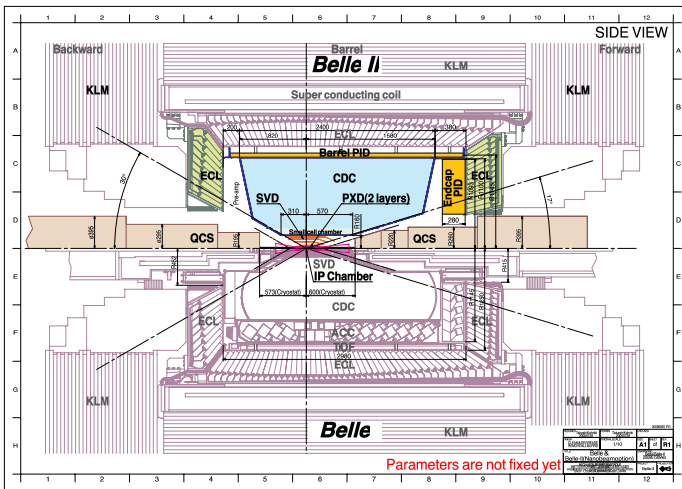


Figure 5: Upgraded Belle II spectrometer (top half) as compared to the present Belle detector (bottom half).

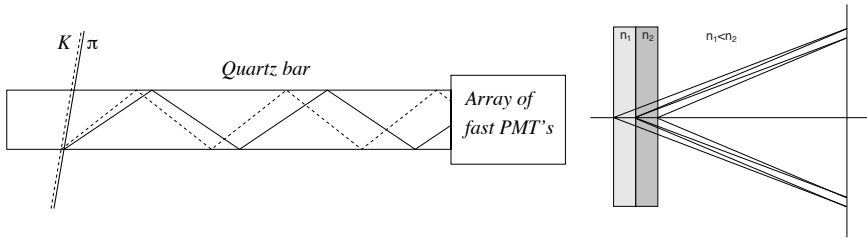


Figure 6: Belle-II particle identification systems: principle of operation of the TOP counter (left) and of the proximity focusing RICH with a non-homogeneous aerogel radiator in the focusing configuration (right).

and K_L^0 detection system will be replaced by scintillator strips read out by SiPMs, and all components will be read-out by fast readout electronics and an improved computing system.

The new vertex detector will have two pixel layers, at $r = 14$ mm and $r = 22$ mm around a 10 mm radius Be beam pipe, and four double-sided strip sensors at radii of 38 mm, 80 mm, 115 mm, and 140 mm. The pixel detector will be based on DEPFET sensors [21]. A significant improvement in vertex resolution is expected with respect to Belle, both for low momentum particles because of reduced Coulomb scattering, as well as for high momentum particles because the high resolution pixel detector is closer to the beam pipe and interaction point. Another important feature is a significant improvement in K_S^0 reconstruction efficiency and vertex resolution because of a larger volume covered by the vertex detector.

The hadron particle identification will be provided by a time-of-propagation (TOP) counter in the barrel part, and a RICH with a focusing aerogel radiator in the forward region of the spectrometer. The TOP counter [22] is a kind of DIRC counter with quartz radiator bars in which the two dimensional information from a Cherenkov ring image is represented by the time of arrival and impact position of the Cherenkov photons at the photon detector. At a given momentum, the slower kaons (dotted in Fig. 6) emit Cherenkov photons at a smaller angle than pions; as a result, also their Cherenkov photons propagate longer along the quartz bar. Compared to the DIRC, the TOP counter construction is more compact, since the large expansion volume is not needed as the photon detectors can be coupled directly to the quartz bar exit window. On the other hand, the TOP counter demands photon detectors with single photon time resolution below 100 ps. A 16-channel MCP PMT as developed by Hamamatsu has been investigated for this purpose [22]. For the end-cap region a proximity

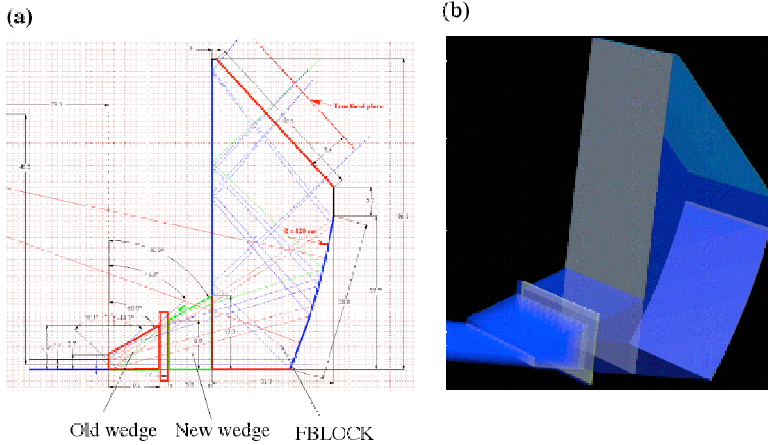


Figure 7: SuperB particle identification device: focusing DIRC counter.

focusing RICH with aerogel as radiator is being designed. The key issue in the performance of this type of RICH counter is to improve the Cherenkov angle resolution per track by increasing the number of detected photons. With a thicker radiator, the number of detected photons increases, but in a proximity focusing RICH the single photon resolution degrades because of the emission point uncertainty. However, this limitation can be overcome in a proximity focusing RICH with a non-homogeneous radiator [23], where one may achieve overlapping of the corresponding Cherenkov rings on the photon detector (Fig. 6). This represents a sort of focusing of the photons within the radiator, and eliminates or at least considerably reduces the spread due to emission point uncertainty. The SuperB detector [24] will reuse several components of the BaBar spectrometer. In the baseline version two major changes are foreseen, replacing CsI(Tl) crystals in the forward calorimeter with LSO crystals, and a modification of the particle identification device, the DIRC counter. Options include a pixel detector layer, a RICH as the forward particle identification device and a veto electromagnetic calorimeter in the backward region to improve the hermeticity of the spectrometer. In the new DIRC counter, the large stand-off box with single channel PMTs will be replaced by a compact focusing quartz block and multi-anode PMTs as photon sensors (Fig. 7). By measuring the time of arrival of Cherenkov photons, the fast photon detectors will allow to correct for the chromatic error, i.e., variation of Cherenkov angle with wavelength [25]. This focusing DIRC counter is expected to considerably extend

the π/K separation range. At the same time, the order-of-magnitude lower mass of the expansion volume will considerably reduce the level of beam induced backgrounds.

Status of the projects

The SuperKEKB/Belle-II project has received initial construction funding in 2010 for the positron damping ring, and with the Japanese 'Very Advanced Research Support Program' a sizable fraction of funds for the main ring upgrade (exceeding 100 MUSD) for the period 2010-2012. KEK plans to obtain additional funds to complete the construction as scheduled, i.e., start the SuperKEKB commissioning in the autumn of 2014, and start data taking in 2015. It is expected that by 2017 the first 5 ab^{-1} of data will be collected, and the full data sample of 50 ab^{-1} will be reached in 2020/2021.

The SuperB project is the first in the list of flagship projects of the new Italian national research plan over the next few years. The Italian government has delivered an initial funding for 2010 as a part of a multi-annual funding program. The aim of the project is to accumulate 75 ab^{-1} on a time scale similar to SuperKEKB/Belle-II.

Summary

B factories have proven to be an excellent tool for flavour physics, with reliable long term operation, constant improvement of operation, achieving and surpassing design performance. A major upgrade has started at KEK to construct the SuperKEKB accelerator and the Belle-II detector, and be ready for data taking by 2015. The SuperB project in Italy foresees building a new tunnel, reusing and upgrading the PEP-II accelerator and the BaBar detector. Its special features are a polarized electron beam and the ability to operate at the charm threshold. Analysis of the physics reach suggests that we can expect a new and exciting era of discoveries, complementary to the LHC.

References

- [1] K.F. Chen *et al.* [Belle Collaboration], Phys. Rev. Lett. **98** (2007) 031802.
- [2] B. Aubert *et al.* [BABAR Collaboration], Phys. Rev. D **79** (2009) 072009.
- [3] Heavy Flavor Averaging Group,
<http://www.slac.stanford.edu/xorg/hfag/triangle/summer2010/index.shtml#sin2b>
- [4] K. Abe *et al.* [Belle Collaboration], Phys. Rev. D **66** (2002) 071102.

- [5] K. Abe *et al.*, ed. S. Hashimoto, M. Hazumi, J. Haba, J.W. Flanagan, and Y. Ohnishi), *Letter of Intent for KEK Super B Factory*, KEK report 2004-04, <http://superb.kek.jp/documents/loi/>
- [6] M. Bona *et al.* [SuperB Collaboration], *SuperB: A High-Luminosity Asymmetric e^+e^- Super Flavor Factory. Conceptual Design Report*, [arXiv:0709.0451(hep-ex)].
- [7] CKMfitter, http://www.slac.stanford.edu/xorg/ckmfitter/ckm_results.html
- [8] W.S. Hou, *Phys. Rev. D* **48** (1993) 2342.
- [9] T. Aushev *et al.*, [arXiv:1002.5012(hep-ex)].
- [10] K. Ikado *et al.* [Belle Collaboration], *Phys. Rev. Lett.* **97** (2006) 251802; B. Aubert *et al.* [BABAR Collaboration], *Phys. Rev. Lett.* **95** (2005) 041804.
- [11] B. Grzadkowski and W.-S. Hou, *Phys. Lett. B* **283** (1992) 427; M. Tanaka, *Z. Phys. C* **67** (1995) 321; K. Kiers and A. Soni, *Phys. Rev. D* **56** (1997) 5786; H. Itoh, S. Komine, and Y. Okada, *Prog. Theor. Phys.* **114** (2005) 179; C.-H. Chen and C.-Q. Geng, *JHEP* **0610** (2006) 053; J.F. Kamenik and F. Mescia, *Phys. Rev. D* **78** (2008) 014003.
- [12] A. Matyja *et al.* [Belle Collaboration], *Phys. Rev. Lett.* **99** (2007) 191807; A. Bozek *et al.* [Belle Collaboration], *Phys. Rev. D* **82** (2010) 072005; B. Aubert *et al.* [BABAR Collaboration], *Phys. Rev. D* **79** (2009) 092002; B. Aubert *et al.* [BABAR Collaboration], *Phys. Rev. Lett.* **100** (2008) 021801; I. Adachi *et al.* [Belle Collaboration], [arXiv:0910.4301(hep-ex)].
- [13] A. Bozek, [arXiv:1101.2681v1(hep-ex)].
- [14] W. Altmannshofer, A.J. Buras, D.M. Straub, M. Wick, *JHEP* **0904** (2009) 022.
- [15] B. O’Leary *et al.* [SuperB Collaboration], [arXiv:1008.1541(hep-ex)].
- [16] T. Goto, Y. Okada, T. Shindou, and M. Tanaka, *Phys. Rev. D* **77** (2008) 095010.
- [17] P. Raimondi, *Status of the SuperB Effort*, presentation at the 2nd Workshop on Super B Factory, LNF-INFN, Frascati, March 2006, <http://www.lnf.infn.it/conference/superb06/talks/raimondi1.ppt> (2006).
- [18] T. Abe *et al.*, [arXiv:1011.0352(physics.ins-det)].
- [19] M. Biagini *et al.*, [arXiv:1009.6178(physics.acc-ph)].
- [20] Section 3 of [19]; M. Zdobov *et al.*, *Phys. Rev. Lett.* **104** (2010) 174801.
- [21] See for example J. Kemmer and G. Lutz, *Nucl. Instr. Meth. A* **253** (1987) 356; I. Peric, *Nucl. Instr. Meth. A* **579** (2007) 658.
- [22] K. Inami, *Nucl. Instr. Meth. A* **595** (2008) 96.
- [23] T. Iijima *et al.*, *Nucl. Instr. Meth. A* **548** (2005) 383.
- [24] E. Grauges *et al.*, [arXiv:1007.4241(physics.ins-det)].
- [25] J. Benitez *et al.*, *Nucl. Instrum. Meth. A* **595** (2008) 104.

t & *m*

Improved search for the neutron electric dipole moment at the Paul Scherrer Institut

P. SCHMIDT-WELLENBURG^{1*}

ON BEHALF OF THE NEDM COLLABORATION

¹ *Paul Scherrer Institut, 5232 Villigen PSI, Switzerland*

Abstract: One of the mysteries of our universe is the observed baryon asymmetry which can not be explained using the Standard Model of particle physics. According to Sacharov this implies further, yet unknown CP violation, which will be tested with a refined search for the neutron electric dipole moment. A collaboration of 15 European institutions has been preparing a sensitive experimental apparatus operated at the Paul Scherrer Institut, based on and exceeding the sensitivity of the former RAL/Sussex/ILL experiment. In the first step the sensitivity shall be improved to $d_n < 5 \times 10^{-27} \text{ ecm}$ to be compared with the present experimental limit of $d_n < 2.9 \times 10^{-26} \text{ ecm}$ (90% CL, Baker *et al.*, Phys. Rev. Lett. **97** (2006) 131801). This will be achieved by a significantly increased ultra-cold neutron (UCN) density and an according control of systematic effects. These include detailed studies of high voltage performance, leakage current control, removal and avoidance of magnetic impurities, enhancement of degaussing capabilities, improvement of the environmental magnetic field control, and multi-channel optical magnetometry including gradient control. For a detailed discussion of these issues please refer to previous conference proceedings: I. Altarev *et al.*, Nucl. Inst. Meth. A **611** (2009) 133 and C.A. Baker *et al.*, Physics Procedia (2010) accepted for publication. The planned 200 nights of data taking from 2011 to 2013 are expected to yield the required statistical sensitivity. Furthermore, a completely new experimental apparatus is being developed which will push the sensitivity well into the 10^{-28} ecm region.

* philipp.schmidt-wellenburg@psi.ch

t & *m*

Prospects for hunting non-perturbative physics at the Pierre Auger Observatory

LUIS A. ANCHORDOQUI¹, HAIM GOLDBERG², DARIUSZ GÓRA^{3,4}, THOMAS PAUL^{2*}, MARKUS ROTH³, SUBIR SARKAR⁵, AND LISA LEE WINDERS¹

¹ *Department of Physics, University of Wisconsin-Milwaukee, P.O. Box 413, Milwaukee, WI 53201, USA*

² *Northeastern University, 360 Huntington Ave., Boston, MA 02115, USA,*

³ *Karlsruhe Institute of Technology (KIT), D-76021 Karlsruhe, Germany*

⁴ *Institute of Nuclear Physics PAN, Krakow, Poland*

⁵ *Rudolf Peierls Centre for Theoretical Physics, University of Oxford, Oxford OX1 3NP, UK*

Abstract:

The Pierre Auger Observatory is designed for precise measurements of a large sample of air showers induced by the highest energy cosmic particles. In addition to detecting air showers induced by hadrons or photons, the observatory is capable of distinguishing showers which could be produced by ultrahigh energy neutrinos interacting in the atmosphere or in the Earth's crust. Interestingly, it may be possible to uncover non-perturbative physics by comparing the rate of nearly horizontal showers generated by deeply penetrating neutrinos to that of up-going showers produced by neutrinos skimming the Earth's surface. Such an observation, if realized, could have bearing on our picture of how the baryon asymmetry of the universe was created. Here we employ detailed Monte Carlo simulations to find out how large a neutrino sample would need to be gathered at the Auger observatory to make a compelling case for new non-perturbative physics. We find that the observation of 0 or 1 Earth-skimming and 10 nearly horizontal showers would be sufficient to exclude the standard model at the 99% confidence level.

* t.paul@neu.edu

Introduction

Cosmic rays have been observed with energies in the neighborhood of 10^{20} eV, or roughly $\sqrt{2}m_p 10^{20}$ eV $>$ 400 TeV in the center-of-mass frame, far in excess of energies currently accessible using man-made colliders. It is natural then to ask whether it might be possible to uncover hints of new physics beyond the reach of the LHC in cosmic ray events. It would be particularly interesting if non-perturbative physics were to become evident at these extreme energies, as this could have bearing on theories of the mechanism responsible for the baryon asymmetry of the universe.

Aside from the experimental challenges involved in studying properties of ultrahigh energy cosmic rays (UHECR), the flux at these extreme energies is minuscule, roughly corresponding to a “luminosity” $\mathcal{L} \approx 7 \cdot 10^{-10} (E/\text{PeV})^{-2} \text{ cm}^{-2} \text{ s}^{-1}$, around 50 orders of magnitude below the LHC luminosity. In spite of this, it may be possible to tease out evidence of new physics by studying the properties of air showers induced at the Earth by ultrahigh energy cosmic neutrinos (UHEC ν).

It is expected that UHEC ν are produced in association with the observed hadronic UHECR, either at the same sites where the charged cosmic rays are accelerated or by subsequent interactions during propagation through the cosmic microwave background radiation. Since neutrinos do not participate in the strong or electromagnetic interactions, any new physics effects should be more prominent for the case of neutrinos interacting at the Earth than for the case of hadrons interacting at the Earth. However, even if one can work out the expected enhancement of the νN cross-section corresponding to some hypothetical new physics, it is still difficult to project the corresponding event rate since the flux of UHEC ν is not known. Fortunately, it turns out that there are techniques to disentangle the effects of new physics and the unknown flux by exploiting multiple observables [1, 2, 3, 4, 5, 6].

It is possible to detect UHEC ν at the Pierre Auger Observatory [7] by searching for deeply-developing, large zenith angle ($>$ 75°) or “quasi-horizontal” (QH) air showers [8]. At these large angles, hadron-induced showers traverse the equivalent of several atmospheres before reaching detectors at the ground. Beyond about 2 atmospheres, most of the electromagnetic component of a shower is extinguished and only very high energy muons survive. Consequently, a hadron-induced shower front is relatively flat and the shower particles arrive within a narrow time window (Fig. 1 top panel). In contrast, a neutrino shower exhibits characteristics similar to those of a vertical shower, which has a more curved front and a wider distribution in particle arrival times due to the large num-

ber of lower energy electrons and photons. Furthermore, the “early” part of the shower will tend to be dominated by the electromagnetic component, while “late” portion will be enriched with tightly bunched muons (Fig. 1 middle panel). Using these characteristic features, it is possible to distinguish neutrino induced events from background hadronic showers. Moreover, because of full flavor mixing, tau neutrinos are expected to be as abundant as other species in the cosmic flux. Tau neutrinos can interact in the Earth’s crust, producing τ leptons which may decay above the Auger detectors; such events will be referred to as “Earth-skimming” (ES) events [9, 10] (Fig. 1 bottom panel). Details on how such events can be selected at the Auger Observatory are discussed in [11, 12].

Possible enhancements of the νN cross-section due to new non-perturbative physics in which the final state is hadron dominated can be uncovered by combining information from Earth-skimming and quasi-horizontal showers. In particular, if an anomalously large rate is found for deeply developing quasi-horizontal showers, it may be ascribed either to an enhancement of the incoming neutrino flux, or an enhancement in the νN cross-section. These two possibilities can be distinguished, however, by comparing the rates of Earth-skimming and quasi-horizontal events. For instance, an enhanced flux will increase both quasi-horizontal and Earth-skimming event rates, whereas an enhanced interaction cross-section will also increase the former but suppress the latter, because the hadrons dominating the interaction final state cannot escape the Earth’s crust.

The question we would like to answer is then how many Earth-skimming and quasi-horizontal events would we need to observe at the Auger Observatory to make a convincing case for the existence of non-perturbative physics in which the final state is dominated by hadrons. As discussed below, it is not necessary to collect a large number of events to rule out the Standard Model (SM), though current bounds on the neutrino flux [11, 12] do imply non-perturbative effects would still take years to find with the current Auger Observatory aperture. Nonetheless, it is not out of the question given the projected long time horizon of data taking at the observatory.

In the following sections we give an example of a of a non-perturbative physics scenario which is relevant in theories of baryogenesis and which is conceivably distinguishable via the technique outline above. We next give a brief description the Pierre Auger Observatory and indicate how neutrinos can be detected there. Next, we elaborate on the technique for distinguishing the effects of new physics from effects of the (unknown) flux. Then we discuss the computation of the acceptances for Earth-skimming and quasi-horizontal events. Finally we use this information to find out

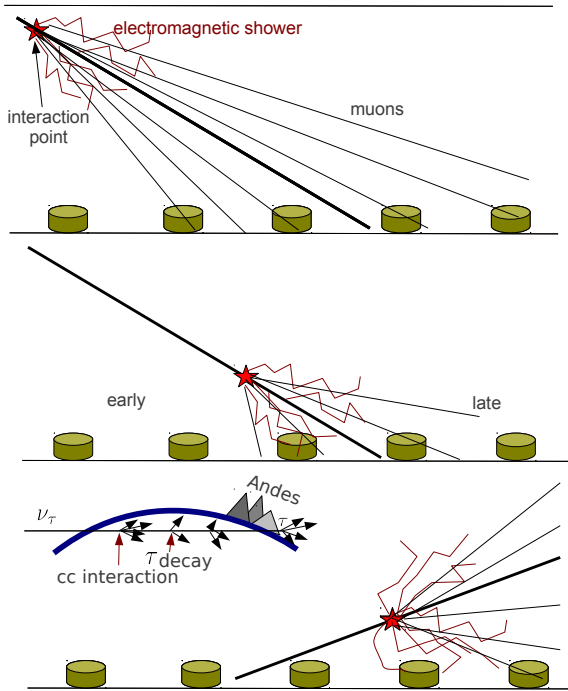


Figure 1: Schematic illustration of the properties of a hadron-induced shower (top), an ν -induced quasi-horizontal shower (middle) and a ν_τ -induced earth skimming shower. Note that only upgoing showers resulting from τ neutrino interactions in the Earth can be detected with any efficiency using the surface array. In contrast, all three neutrino species can be detected in down-going showers. Also note from the inset in the lower panel, that the incident τ can experience several CC interactions and decays and thereby undergo a regeneration process. The Andes mountain range lies to the west of the observatory, and provides roughly an additional 20% target volume for ν_τ interactions.

how large an event sample would be required to demonstrate the existence of new non-perturbative effects.

Non-perturbative physics

The technique described here provides a generic way to search for new non-perturbative physics in which the final state is dominated by hadrons, and does not depend on any particular hypothesis regarding the cause of the non-perturbative effect. Different theoretical scenarios have been proposed, however, which could in principle become experimentally evident via the techniques described here [13, 14]. We mention one such scenario which is of interest in the context of the TAM conference given its relevance to theories of the baryon asymmetry of the universe.

In 1976 't Hooft observed that the Standard Model does not strictly conserve baryon and lepton number [15]. Rather, non-trivial fluctuations in $SU(2)$ gauge fields generate an energy barrier interpolating between topologically distinct vacua, and an index theorem describing level crossings in the background of these fluctuations reveals that neither baryon nor lepton number is conserved during the transition, but only the combination $B - L$. Inclusion of the Higgs field in the calculation modifies the original instanton configuration [16], one aspect of which is prediction of an explicit energy scale for the height of the of the barrier (the “sphaleron” barrier) of around 10 TeV. More speculatively, it has been suggested that the topological transition could occur in two particle collisions at very high energies [17]. Of particular interest to cosmic ray physicists is whether such a phenomenon could manifest as an observable enhancement of the νN cross-section resulting in an increased rate of UHECR ν events. It has been argued in [14] that, optimistically, one could arrive at a cross-section 80 times larger than the vanilla SM cross-section in the energy range $9.5 < \log_{10}(E_\nu/\text{GeV}) < 10.5$.

Any observation of such a phenomenon could provide important input for theories of baryogenesis. In particular, it has been noted that the sphaleron barrier can be overcome through thermal transitions at high temperatures [18], and hence the associated B and L violation could have been important in the early universe. Some baryogenesis theories propose that the baryon asymmetry of the universe resulted from an initial asymmetry in lepton number produced during leptogenesis which was subsequently converted to a baryon asymmetry via sphaleron transitions [19]. In the remainder of this paper, we consider the potential to turn up evidence of the sphaleron or other non-perturbative effects at the Auger Observatory.

The Pierre Auger Observatory

The Pierre Auger Observatory [7] is designed to measure the extensive air showers produced by the highest energy cosmic rays ($> 10^{19}$ eV) with the goal of discovering their origins and shedding light on their composition. Two different techniques are used to detect air showers [20, 21]. First, a collection of telescopes is used to sense the fluorescence light produced by excited atmospheric nitrogen as the cascade of particles develops and deposits energy in the atmosphere. This method can be used only when the sky is moonless and dark, and thus has roughly a $10 \sim 15\%$ duty cycle. Second, an array of detectors on the ground is used to sample particle densities (or more accurately, energy densities) and arrival times as the air shower impinges upon the Earth's surface. Each surface detector consists of a tank containing 12 tons of purified water instrumented with three photomultiplier tubes which detect the Cherenkov light produced by passing particles. The signals from the photomultipliers are read out with flash analog to digital converters at a frequency of 40 MHz. This allows for detailed evaluation of the arrival time profile of the air shower particles, which, as discussed above, is crucial for distinguishing ν -induced showers from hadron-induced ones. The surface array has nearly a 100% duty cycle. A subsample of air showers detected by both the surface array and one or more fluorescence telescopes, so-called hybrid events, are very precisely measured and provide an invaluable tool for cross checks and energy calibration. Construction of the main observatory, located in Mendoza, Argentina, was completed in 2008, resulting in a total of 24 fluorescence telescopes overlooking 1600 surface detectors spaced 1.5 km apart on a triangular grid. More recently the observatory has been augmented with additional surface and fluorescence devices designed to detect showers down to 10^{17} eV [20]. Results from the Observatory are discussed elsewhere in these proceedings [22].

Using neutrinos to disentangle physics and flux

In this section we outline how a comparison of the rates of Earth-skimming and quasi-horizontal neutrino events can be exploited to disentangle possible effects of non-perturbative physics from the unknown neutrino flux. Consider first a flux of Earth-skimming τ neutrinos with energy in the range $10^{9.5} \text{ GeV} < E_\nu < 10^{10.5} \text{ GeV}$. The neutrinos can convert to τ leptons in the Earth via the charged current interaction $\nu_{\tau\pm} N \rightarrow \tau^\pm X$. In the SM,

the interaction path length for the neutrino is

$$L_{\text{CC}}^{\nu} = [N_A \rho_s \sigma_{\text{CC}}^{\nu}]^{-1}, \quad (1)$$

where σ_{CC}^{ν} is the charged current cross-section for a neutrino energy $E_{\nu} = E_0$. The density of the material through which the neutrinos pass, ρ_s , is about 2.65 g/cm^3 for the Earth's crust. N_A is Avogadro's number, $6.022 \cdot 10^{23} \text{ g}^{-1}$. Here we have neglected neutral current interactions, which at these energies only reduce the neutrino energy by approximately 20%, which is within the systematic uncertainty. For $E_0 \approx 10^{10} \text{ GeV}$, $L_{\text{CC}}^{\nu} \sim \mathcal{O}(100 \text{ km})$. Let us assume some hypothetical non-perturbative physics process enhances the νN cross-section. Then the interaction path length becomes

$$L_{\text{tot}}^{\nu} = [N_A \rho_s (\sigma_{\text{CC}}^{\nu} + \sigma_{\text{NP}}^{\nu})]^{-1}, \quad (2)$$

where σ_{NP}^{ν} is the non-perturbative contribution to the cross-section for $E_{\nu} = E_0$.

Once a τ is produced by a CC interaction, it can be absorbed in the Earth or escape and possibly decay, generating a detectable air shower. At these high energies, the τ propagation length in the Earth is dominated by energy loss rather than the finite τ lifetime. The energy loss can be expressed as

$$\frac{dE_{\tau}}{dz} = -(\alpha_{\tau} + \beta_{\tau} E_{\tau}) \rho_s, \quad (3)$$

where α characterizes energy loss due to ionization and β_{τ} characterizes losses through bremsstrahlung, pair production and hadronic interactions. At these energies, energy losses due to ionization turn out to be negligible, while $\beta_{\tau} \simeq 0.8 \cdot 10^{-6} \text{ cm}^2/\text{g}$ [23]. From Eqn. (3), we observe that the maximum path length for a detectable τ can be written

$$L^{\tau} = \frac{1}{\beta_{\tau} \rho_s} \ln(E_{\text{max}}/E_{\text{min}}), \quad (4)$$

where $E_{\text{max}} \approx E_0$ is the energy at which the τ is created, and E_{min} is the minimal energy at which a τ can produce a shower big enough to be detected. For $E_{\text{max}}/E_{\text{min}} = 10$, $L^{\tau} = 11 \text{ km}$.

The probability for a neutrino with incident nadir angle θ to emerge as a detectable τ is

$$P(\theta) = \int_0^{\ell} \frac{dz}{L_{\text{CC}}^{\nu}} \exp(-z/L_{\text{tot}}^{\nu}) \Theta[z - (\ell - L^{\tau})], \quad (5)$$

where $\ell = 2R_{\oplus} \cos \theta$ is the chord length of the intersection of the neutrino's trajectory with the Earth, with $R_{\oplus} \approx 6371 \text{ km}$ the Earth's radius. Note we

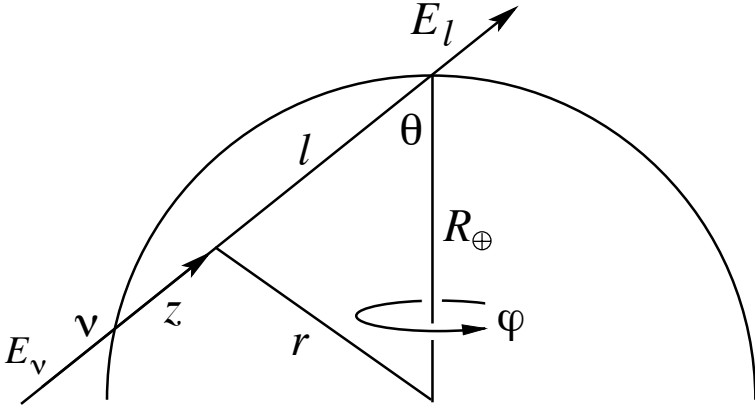


Figure 2: The chord length of the intersection of a neutrino with the Earth is $\ell = 2R_{\oplus} \cos \theta$. In the figure, the neutrino produces a lepton l after traveling some distance z inside the Earth's crust. If $z + L^{\tau} > \ell$, the lepton will escape the Earth and can generate an air shower.

have neglected the possibility that non-perturbative processes could lead to a detectable signal, since the hadrons which dominate the final state will be absorbed in the Earth. The step function in Eqn. (5) reflects the fact that a τ will only escape the Earth if $z + L^{\tau} > \ell$, as illustrated in Fig 2.

Assuming an isotropic tau neutrino flux, the number of taus that emerge from the Earth with sufficient energy to be detected is proportional to an “effective solid angle”

$$\Omega_{\text{eff}} \equiv \int P(\theta) \cos \theta \, d \cos \theta \, d\phi. \quad (6)$$

Evaluation of the integrals [1] yields the unfortunate expression

$$\begin{aligned} \Omega_{\text{eff}} &= 2\pi \frac{L_{\text{tot}}^{\nu}}{L_{\text{CC}}^{\nu}} [\exp(L^{\tau}/L_{\text{tot}}^{\nu}) - 1] \times \\ &\times \left[\left(\frac{L_{\text{tot}}^{\nu}}{2R_{\oplus}} \right)^2 - \left(\frac{L_{\text{tot}}^{\nu}}{2R_{\oplus}} + \left(\frac{L_{\text{tot}}^{\nu}}{2R_{\oplus}} \right)^2 \right) \exp(-2R_{\oplus}/L_{\text{tot}}^{\nu}) \right]. \quad (7) \end{aligned}$$

At the relevant energies, however, the neutrino interaction length satisfies $L_{\text{tot}}^{\nu} \ll R_{\oplus}$. In addition, if the hypothesized non-perturbative cross-section enhancement is less than typical hadronic cross-sections, we have $L_{\text{tot}}^{\nu} \gg$

L^τ . With these approximations, Eqn. (7) simplifies to [2]

$$\Omega_{\text{eff}} \approx 2\pi \frac{L_{\text{tot}}^{\nu 2} L^\tau}{4R_{\oplus}^2 L_{\text{CC}}^\nu}. \quad (8)$$

Eqn. (8) describes the functional dependence of the Earth-skimming event rate on the non-perturbative cross-section. This rate is, of course, also proportional to the neutrino flux $\Phi^{\nu\text{all}}$ at E_0 . Thus, the number of Earth-skimming neutrinos is given by

$$N_{\text{ES}} \approx C_{\text{ES}} \frac{\Phi^{\nu\text{all}}}{\Phi_0^{\nu\text{all}}} \frac{\sigma_{\text{CC}}^{\nu 2}}{(\sigma_{\text{CC}}^\nu + \sigma_{\text{NP}}^\nu)^2}, \quad (9)$$

where C_{ES} is the number of Earth-skimming events expected for some benchmark flux $\Phi_0^{\nu\text{all}}$ in the absence of new physics.

In contrast to Eqn.(9), the rate for quasi-horizontal showers has the form

$$N_{\text{QH}} = C_{\text{QH}} \frac{\Phi^{\nu\text{all}}}{\Phi_0^{\nu\text{all}}} \frac{\sigma_{\text{CC}}^\nu + \sigma_{\text{NP}}^\nu}{\sigma_{\text{CC}}^\nu}, \quad (10)$$

where C_{QH} is the number of quasi-horizontal events expected for flux $\Phi_0^{\nu\text{all}}$. Given a flux $\Phi^{\nu\text{all}}$ and new non-perturbative physics cross-section σ_{NP}^ν , both N_{ES} and N_{QH} are determined. On the other hand, given just a quasi-horizontal event rate N_{QH} , it is impossible to differentiate between an enhancement of the cross-section due to non-perturbative physics and an increase of the flux. However, in the region where significant event rates are expected, the contours of N_{QH} and N_{ES} , given by Eqns. (9) and (10), are more or less orthogonal and provide complementary information. This is illustrated in Fig. 3. With measurements of $N_{\text{QH}}^{\text{obs}}$ and $N_{\text{ES}}^{\text{obs}}$, both σ_{NP}^ν and $\Phi^{\nu\text{all}}$ may be determined independently, and neutrino interactions beyond the SM may be unambiguously identified, given sufficient statistics.

The remaining task is to compute the values of C_{ES} and C_{QH} which appear in Eqns. (9) and (10). To do this we need to know the detector acceptance for these two event categories. This is the topic of the next section.

Acceptance and systematic uncertainties

Detailed Monte Carlo simulations are used to compute the acceptance for ES and QH events. Neutrinos are propagated through the atmosphere, the Earth's crust, and the Andes mountains using an extended version [24] of

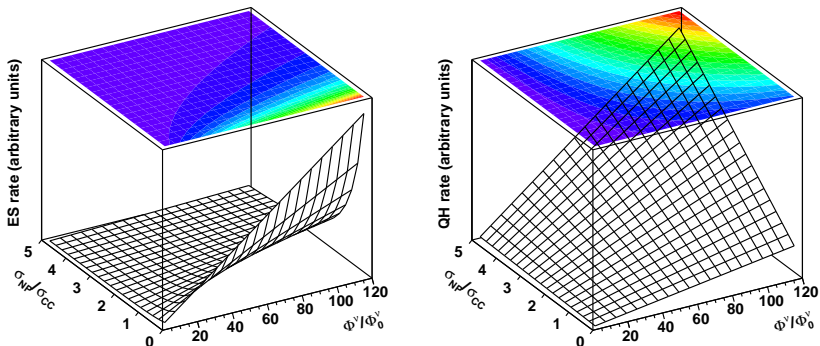


Figure 3: Event rates for Earth-skimming (left) and quasi-horizontal (right) events in the $\Phi^{\nu}/\Phi_0^{\nu} - \sigma_{NP}/\sigma_{CC}$ plane. Note that the contours are roughly orthogonal, and so the two types of event provide complementary information about flux and cross-section.

the code ANIS [25]. In the simulations, the νN cross-sections from reference [26] are employed. Particles resulting from νN interactions are fed to PYTHIA [27] and τ decays are simulated using TAUOLA [28].

The flux, energy and decay vertices of outgoing leptons are calculated inside an “active detector” volume of $3000 \times 10 \text{ km}^3$, including the real shape of the surface array. A relief map of the Andes mountains was constructed using digital elevation data from the Consortium for Spatial Information (CGIAR-CSI) [29]. The map of the area around the Auger site is depicted in Fig. 4.

To study the response of the detector, the outputs of PYTHIA and/or TAUOLA are used as input for the AIRES [30] air shower simulation package. The response of the surface detector array is simulated in detail using the Auger *Offline* simulation package [31]. Atmospheric background muons are also simulated in order to study the impact on neutrino identification, as such accidental muons can be wrongly classified as shower particles. The background from hadronic showers above 10^{17} eV is estimated to be $\mathcal{O}(1)$ in 20 years [11], so for the energy bin considered in this analysis, $9.5 < \log_{10}(E_{\nu}/\text{GeV})$, the background is negligible. Additional details on the simulation procedures can be found in [32].

To establish benchmark neutrino rates we use the Waxman-Bahcall bound [33] for the flux, $\Phi_0^{\nu\alpha} = 2.33 \cdot 10^{-8} E_{\nu}^{-2} \text{ GeV s}^{-1} \text{ cm}^{-2} \text{ sr}^{-1}$, and em-

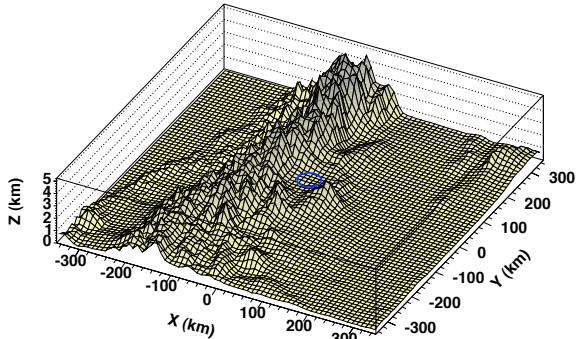


Figure 4: Topography in the vicinity of the Auger site. The surface array is centered at $X = Y = 0$.

ploy the acceptance computed by the simulations described above. In order to estimate the systematic uncertainty associated with our lack of knowledge of the dependence of the flux on energy, we consider several scenarios which plausibly bracket the range of possibilities:

1. $\Phi_0^{V\alpha}(E_\nu) = (C/E_0) E_\nu^{-1}$,
2. $\Phi_0^{V\alpha}(E_\nu) = C E_\nu^{-2}$,
3. $\Phi_0^{V\alpha}(E_\nu) = (C/E_0) E_\nu^{-3}$,
4. $\Phi_0^{V\alpha}(E_\nu) = C E_\nu^{-2} \exp[-\log_{10}(E_\nu/E_0)^2/(2\sigma^2)]$,

where $C = 2.33 \cdot 10^{-8} \text{ GeV s}^{-1} \text{ cm}^{-2} \text{ sr}^{-1}$, $E_0 = 10^{10} \text{ GeV}$, $\sigma = 0.5 \text{ GeV}$. Note that scenario 2 corresponds to our benchmark, the Waxmann-Bahcall flux. The expected rates for all 4 scenarios are summarized in Table 1. We use the expected rates for the benchmark flux to determine the values of C_{ES} and C_{QH} in Eqns. (9) and (10), ($C_{\text{ES}} = 0.15$ and $C_{\text{QH}} = 0.06$, as shown in Table 1).

Table 2 contains a summary of systematic uncertainties on the ratio of the number of ES to QH events. The uncertainty in spectrum shape is taken from Table 1. The uncertainty on the PDF is estimated by considering different parton distribution functions (GRV92NLO [34] and CTEQ66c [35]). Finally, the uncertainty on the energy loss, β_τ , of τ leptons as they propagate through the Earth's crust is derived from [36].

flux	Earth-skimming	quasi-horizontal				ratio
	$N_{\nu\tau}$	$N_{\nu e}$	$N_{\nu\tau}$	$N_{\nu\mu}$	$N_{\nu\text{all}}$	$N_{\nu\tau}/N_{\nu\text{all}}$
(1)	0.14	0.027	0.031	0.0056	0.06	2.14
(2)	0.15	0.026	0.029	0.0048	0.06	2.47
(3)	0.23	0.036	0.041	0.0062	0.08	2.75
(4)	0.12	0.021	0.024	0.0040	0.05	2.45

Table 1: Expected events per year (N_i) at the Auger Observatory in the energy range $9.5 < \log_{10}(E_\nu/\text{GeV}) < 10.5$, for various incident zenith angle (θ) ranges and the 4 flux models considered. Earth-skimming is taken in the zenith angle range between 90° and 95° and quasi-horizontal is calculated in the zenith angle range between 75° and 90° .

ratio	flux	PDF	β_τ	sum
	+11%	0%	+24%	+26%
2.47				2.47
	-13%	-21%	-25%	-35%

Table 2: Contributions to the systematic uncertainty on the Earth-skimming to quasi-horizontal event ratio. We have considered the energy range $9.5 < \log_{10}(E_\nu/\text{GeV}) < 10.5$ and the zenith angle range $75^\circ < \theta < 90^\circ$.

Discovery potential

Using the results from the previous sections we can project sensitivity of the Auger Observatory to νN cross-section enhancements for various assumptions about the flux. The quantities N_{ES} and N_{QH} as defined in Eqs. (9) and (10) can be regarded as the expected rates for these types of events, corresponding to different points in the $\Phi^{\nu\text{all}}/\Phi_0^{\nu\text{all}} - \sigma_{\text{NP}}/\sigma_{\text{CC}}$ parameter space. For a given pair of observed rates $N_{\text{ES}}^{\text{obs}}$ and $N_{\text{QH}}^{\text{obs}}$, two curves are obtained in the two-dimensional parameter space by setting $N_{\text{ES}}^{\text{obs}} = N_{\text{ES}}$ and $N_{\text{QH}}^{\text{obs}} = N_{\text{QH}}$. These curves intersect at a point, yielding the most probable values of flux and cross-section for the given observations. Fluctuations about this point define contours of constant χ^2 in an approximation to a multi-Poisson likelihood analysis. The contours are

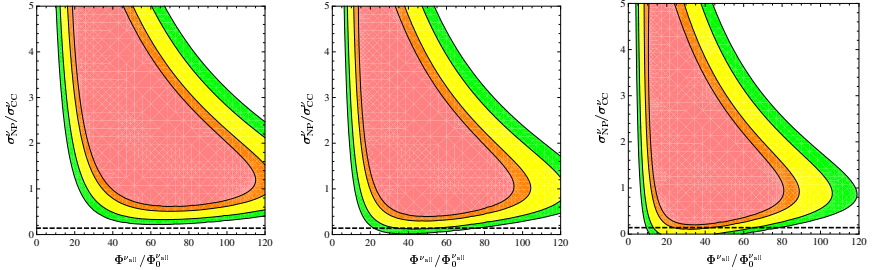


Figure 5: Illustrative bounds obtainable for fluxes and cross-sections at $\sqrt{s} \approx 250$ TeV for different numbers of QH and ES events detected at the Auger Observatory. The different shaded regions indicate the 90%, 95%, 99% and 3σ confidence level contours in the $\Phi^{V_{\text{all}}}/\Phi_0^{V_{\text{all}}} - \sigma_{\text{NP}}^{\nu}/\sigma_{\text{CC}}$ plane, for $N_{\text{ES}}^{\text{obs}} = 1, N_{\text{QH}}^{\text{obs}} = 10$ (left), $N_{\text{ES}}^{\text{obs}} = 1, N_{\text{QH}}^{\text{obs}} = 7$ (middle), and $N_{\text{ES}}^{\text{obs}} = 1, N_{\text{QH}}^{\text{obs}} = 5$ (right). The dashed line indicates the result of including the systematic uncertainty on the NLO QCD CC neutrino-nucleon cross-section [39].

defined by

$$\chi^2 = \sum_i 2 \left[N_i - N_i^{\text{obs}} \right] + 2 N_i^{\text{obs}} \ln \left[N_i^{\text{obs}} / N_i \right], \quad (11)$$

where $i = \text{ES, QH}$ [37]. In Fig. 5, we show results for three representative cases. Taking $(N_{\text{ES}}^{\text{obs}} = 1, N_{\text{QH}}^{\text{obs}} = 10)$, $(N_{\text{ES}}^{\text{obs}} = 1, N_{\text{QH}}^{\text{obs}} = 7)$, and $(N_{\text{ES}}^{\text{obs}} = 1, N_{\text{QH}}^{\text{obs}} = 5)$ we show the 90%, 95%, 99% and 3σ CL contours for 2 d.o.f. ($\chi^2 = 4.61, 5.99, 9.21, \text{ and } 11.83$, respectively). For $N_{\text{ES}}^{\text{obs}} = 1$ and $N_{\text{QH}}^{\text{obs}} = 10$, the possibility of a SM interpretation along the $\sigma_{\text{NP}}^{\nu} = 0$ axis (taking into account systematic uncertainties) would be excluded at greater than 99% CL for *any* assumed flux. The power of the Earth-skimming information is such that the best fit consistent with the SM would require a flux of about 50 times the Waxman-Bahcall flux, which is already excluded by present limits [38].

Summary

Though the Pierre Auger Observatory was not designed primarily as a neutrino detector, it is nonetheless possible to detect neutrino-induced air showers, either from down-going neutrinos interacting in the atmosphere,

or from τ neutrinos which interact in the Earth's crust producing a τ lepton which decays in the vicinity of the observatory. Here we have re-examined a technique to search for physics processes which could enhance the νN cross-section and be indicative of non-perturbative physics beyond the TeV scale (and beyond the reach of the LHC). The strategy involves comparing the rates of quasi-horizontal events and Earth-skimming events, which allows one to separate the effects of the (unknown) flux from effects of hypothesized non-perturbative physics. To assess the sensitivity of the Auger Observatory to such new physics we performed detailed Monte Carlo simulations of neutrino interactions in the Earth and atmosphere, as well as detailed simulation of the detector response to the resulting air showers. We find that the observation of 0 or 1 Earth-skimming neutrino and 10 quasi-horizontal neutrinos would be sufficient to exclude the Standard Model at the 99% confidence level. Given that neither Earth-skimming nor quasi-horizontal neutrino candidates have yet been recorded by the Auger Observatory [11, 12], we can project that if new non-perturbative physics exists it would require at least 10 years of additional data collection to find it, even in the most most optimistic case. Given the long time horizon of the Auger Observatory, however, such an observation is not entirely out of the question. A discovery of this type would be significant, as it could provide evidence of non-perturbative physics which is relevant to theories of baryogenesis.

Acknowledgements

I would like to extend a sizable *hvala lepa* to the organizers for an exceptionally well-arranged, interesting, and enjoyable conference. The work of T. Paul was supported in part by US National Science Foundation Grant PHY-0855388 and by the Slovene AD FUTURA foundation.

References

- [1] A. Kusenko and T.J. Weiler, Phys. Rev. Lett. **88** (2002) 161101, [arXiv:hep-ph/0106071].
- [2] L.A. Anchordoqui, J.L. Feng, H. Goldberg, and A.D. Shapere, Phys. Rev. D **65** (2002) 124027.
- [3] L.A. Anchordoqui, T. Han, D. Hooper, and S. Sarkar, Astropart. Phys. **25** (2006) 14, [arXiv:hep-ph/0508312].
- [4] S. Palomares-Ruiz, A. Irimia, and T.J. Weiler, Phys. Rev. D **73** (2006) 083003 [arXiv:astro-ph/0512231].
- [5] L.A. Anchordoqui, A.M. Cooper-Sarkar, D. Hooper, and S. Sarkar, Phys. Rev. D **74** (2006) 043008, [arXiv:hep-ph/0605086].

- [6] L.A. Anchordoqui, H. Goldberg, D. Gora, T. Paul, M. Roth, S. Sarkar, and L. L. Winders, *Phys. Rev. D* **82** (2010) 043001.
- [7] J. Abraham *et al.* [Pierre Auger Collaboration], *Nucl. Instrum. Meth. A* **523** (2004) 50-95 (2004).
- [8] K.S. Capelle, J.W. Cronin, G. Parente, and E. Zas, *Astropart. Phys.* **8** (1998) 321, [arXiv:astro-ph/9801313].
- [9] J.L. Feng, P. Fisher, F. Wilczek, and T. M. Yu, *Phys. Rev. Lett.* **88** (2002) 161102, [arXiv:hep-ph/0105067].
- [10] X. Bertou, P. Billoir, O. Deligny, C. Lachaud, and A. Letessier-Selvon, *Astropart. Phys.* **17** (2002) 183, [arXiv:astro-ph/0104452].
- [11] J. Abraham *et al.* [Pierre Auger Collaboration], [arXiv:0906.2347].
- [12] J. Abraham *et al.* [Pierre Auger Collaboration], *Phys. Rev. D* **79** (2009) 102001, [arXiv:0903.3385].
- [13] J.L. Feng and A. D. Shapere, *Phys. Rev. Lett.* **88** (2002) 021303, [arXiv:hep-ph/0109106]; L. Anchordoqui and H. Goldberg, *Phys. Rev. D* **65** (2002) 047502, [arXiv:hep-ph/0109242]; A. Ringwald and H. Tu, *Phys. Lett. B* **525** (2002) 135, [arXiv:hep-ph/0111042]; L.A. Anchordoqui, J.L. Feng, H. Goldberg, and A.D. Shapere, *Phys. Rev. D* **66** (2002) 103002, [arXiv:hep-ph/0207139]; E.J. Ahn, M. Ave, M. Cavaglia, and A.V. Olinto, *Phys. Rev. D* **68** (2003) 043004, [arXiv:hep-ph/0306008]; S. Dimopoulos and G. Landsberg, *Phys. Rev. Lett.* **87** (2001) 161602, [arXiv:hep-ph/0106295].
- [14] L.A. Anchordoqui, H. Goldberg, D. Gora, T. Paul, M. Roth, S. Sarkar, and L.L. Winders, [arXiv:hep-ph/1004.3190].
- [15] G. 't Hooft, *Phys. Rev. Lett.* **37** (1976) 8; G. 't Hooft, *Phys. Rev. D.* **14** (1976) 3432, Erratum *ibid.* **D 18** (1978) 2199.
- [16] F.R. Klinkhammer and N.S. Manton, *Phys. Rev. D* **30** (1984) 2212.
- [17] H. Aoyoma and H. Goldberg, *Phys. Lett. B* **188** (1987) 506; A. Ringwald, *Nucl. Phys. B* **330** (1990) 1; O. Espinosa, *Nucl. Phys. B* **343** (1990) 310; A. Ringwald, *JHEP* **0310** (2003) 008, [arXiv:hep-ph/0307034].
- [18] V.A. Kuzmin, V.A. Rubikov, and M.E. Shaposhnikov, *Phys. Lett. B* **155** (1985) 36; P.B. Arnold and L.D. McLerran, *Phys. Rev. D.* **36** (1987) 581.
- [19] M. Fukugita and T. Yanagida, *Phys. Lett. B* **174** (1986) 45.
- [20] J.A. Abraham *et al.* [Pierre Auger Collaboration], [arXiv:0906.2354].
- [21] J.A. Abraham *et al.* [Pierre Auger Collaboration], *Nucl. Instrum. Meth. A* **620** (2010) 227, [arXiv:0907.4282].
- [22] T. Paul, on behalf of the Pierre Auger Collaboration, these proceedings.
- [23] S.I. Dutta, M.H. Reno, I. Sarcevic, and D. Seckel, *Phys. Rev. D* **63** (2001) 094020, [arXiv:hep-ph/0012350].
- [24] D. Gora, M. Roth, and A. Tamburro, *Astropart. Phys.* **26** (2007) 402.
- [25] A. Gazizov and M. P. Kowalski, *Comput. Phys. Commun.* **172** (2005) 203, [arXiv:astro-ph/0406439].
- [26] A. Cooper-Sarkar and S. Sarkar, *JHEP* **0801** (2008) 075, [arXiv:0710.5303 (hep-ph)].
- [27] T. Sjostrand, S. Mrenna, and P.Z. Skands, *JHEP* **0605** (2006) 026, [arXiv:hep-ph/0603175].
- [28] S. Jadach, Z. Was, R. Decker, and J.H. Kuhn, *Comput. Phys. Commun.* **76** (1993) 361.
- [29] Consortium for Spatial Information (CGIAR-CSI). <http://srtm.csi.cgiar.org>
- [30] S.J. Sciutto, [arXiv:astro-ph/0106044].

- [31] S. Argiro *et al.*, Nucl. Instrum. Meth. A **580** (2007) 1485, [arXiv:0707.1652 (astro-ph)]; J. Allen *et al.*, J. Phys. Conf. Ser. **119** (2008) 032002.
- [32] D. Gora [Pierre Auger Collaboration], Nucl. Phys. Proc. Suppl. **196** (2009) 207-210.
- [33] E. Waxman and J. N. Bahcall, Phys. Rev. D **59** (1999) 023002, [arXiv:hep-ph/9807282].
- [34] M. Gluck, S. Kretzer, and E. Reya, Astropart. Phys. **11** (1999) 327, [arXiv:astro-ph/9809273].
- [35] P.M. Nadolsky *et al.*, Phys. Rev. D **78** (2008) 013004, [arXiv:0802.0007 (hep-ph)].
- [36] N. Armesto, C. Merino, G. Parente, and E. Zas, Phys. Rev. D **77** (2008) 013001, [arXiv:0709.4461 (hep-ph)]. See also, E.V. Bugaev and Yu.V. Shlepin, Phys. Rev. D **67** (2003) 034027, [arXiv:hep-ph/0203096]; H. Abramowicz and A. Levy, [arXiv:hep-ph/9712415]; A. Capella, A. Kaidalov, C. Merino, and J. Tran Thanh Van, Phys. Lett. B **337** (1994) 358, [arXiv:hep-ph/9405338].
- [37] S. Baker and R.D. Cousins, Nucl. Instrum. Meth. A **221** (1984) 437.
- [38] L.A. Anchordoqui and T. Montaruli, [arXiv:0912.1035 (astro-ph.HE)].
- [39] A.M. Cooper-Sarkar, private communication.

t & *m*

Results from the Pierre Auger Observatory

THOMAS PAUL^{1*}, FOR THE PIERRE AUGER COLLABORATION²

¹ *Northeastern University, 360 Huntington Ave., Boston, MA 02115, USA*

² *Observatorio Pierre Auger, Av. San Martin Norte 304, 5619 Malargüe, Argentina*

Full author list: http://www.auger.org/archive/authors_2010_12.html

Abstract: We review recent results from the Pierre Auger Observatory, including the measurement of the cosmic ray energy spectrum above 10^{18} eV, studies of cosmic ray composition, and searches for anisotropy in the cosmic ray arrival directions. The flux can be characterized by a broken power-law, with a hardening of the spectrum above $4 \cdot 10^{18}$ eV and a steepening of the spectrum beginning at about $3 \cdot 10^{19}$ eV, consistent with the 40-year old prediction of Greisen, Zatsepin and Kuzmin. Studies of the longitudinal development of cosmic ray air showers provide information on the average primary mass and indicate a trend to heavier composition with increasing energy when compared to model predictions. Searches for neutrinos and photons in the ultra-high energy cosmic ray flux have so far not turned up candidates, and competitive bounds have been established. Above about $5.5 \cdot 10^{19}$ eV, there is evidence for a correlation between the cosmic ray arrival directions and the distribution of nearby extragalactic matter.

Introduction

The Pierre Auger Observatory [1] is designed to measure properties of the extensive air showers produced by cosmic rays at the highest energies, above about 10^{18} eV. The Observatory features a large aperture to gather a significant sample of these rare events, as well as complementary detection techniques to mitigate some of the systematic uncertainties associated with deducing properties of cosmic rays from air shower observables.

The Auger Observatory is located in Mendoza Province, Argentina, and began collecting data in 2004, with construction of the baseline design completed by 2008. As of October 2010, the Observatory had collected

* t.paul@neu.edu

in excess of $20\,000\text{ km}^2\text{ sr yr}$ in exposure, significantly more exposure than other cosmic ray observatories combined. Two types of instruments are employed. Particle detectors on the ground sample air shower fronts as they arrive at the Earth's surface, while fluorescence telescopes measure the light produced as air shower particles excite atmospheric nitrogen.

The surface array [2] comprises 1600 surface detector (SD) stations, each consisting of a tank filled with 12 tons of water and instrumented with 3 photomultiplier tubes which detect the Cherenkov light produced as particles traverse the water. The signals from the photomultipliers are read out with flash analog to digital converters at 40 MHz and timestamped by a GPS unit, allowing for detailed study of the arrival time profile of shower particles. The tanks are arranged on a triangular grid with a 1.5 km spacing, covering about 3000 km^2 . The surface array operates with close to a 100% duty cycle, and the acceptance for events above $3\cdot 10^{18}\text{ eV}$ is nearly 100% [3].

The fluorescence detector (FD) system [4] consists of 4 buildings, each housing 6 telescopes which overlook the surface array. Each telescope employs an 11 m^2 segmented mirror to focus the fluorescence light entering through a 2.2 m diaphragm onto a camera which pixelizes the image using 440 photomultiplier tubes. The photomultiplier signals are digitized at 10 MHz, providing a time profile of the shower as it develops in the atmosphere. The FD can be operated only when the sky is dark and clear, and has a duty cycle of $10 \sim 15\%$. In contrast to the SD acceptance, the acceptance of FD events depends strongly on energy [5], extending down to about 10^{18} eV .

The two detector systems provide complementary information, as the SD measures the lateral distribution and time structure of shower particles arriving at the ground, and the FD measures the longitudinal development of the shower in the atmosphere. A subset of showers is observed simultaneously by the SD and FD. These "hybrid" events are very precisely measured and provide an invaluable calibration tool. In particular, the FD allows for a roughly colorimetric measurement of the shower energy since the amount of fluorescence light generated is proportional to the energy deposited along the shower path; in contrast, extracting the shower energy via analysis of particle densities at the ground relies on predictions from hadronic interaction models describing physics at energies beyond those accessible to current experiments. Hybrid events can therefore be exploited to set a model-independent energy scale for the SD array, which in turn has access to a greater data sample than the FD due to the greater live time.

In the following sections, we describe recent results from the Observatory, including the measurement of the cosmic ray energy spectrum, composition, and searches for anisotropy in the cosmic ray arrival directions.

Energy spectrum

Above 10^9 eV, the cosmic ray flux falls with energy, E , roughly as $E^{-\gamma}$ where the spectral index $\gamma \sim 3$. Several breaks in the spectral index have been observed, however, presumably reflecting some property of cosmic ray propagation or acceleration. Two of these spectral features appear in the energy region currently accessible to the Auger Observatory¹. The HiRes Collaboration reported a suppression of the flux above $E = 56 \pm 5(\text{stat}) \pm 9(\text{syst})$ EeV [10], with the spectral index γ of the flux steepening from 2.81 ± 0.03 to 5.1 ± 0.7 . This suppression was then confirmed by the Pierre Auger Collaboration, with $\gamma = 2.69 \pm 0.02(\text{stat}) \pm 0.06(\text{syst})$ and $\gamma = 4.2 \pm 0.4(\text{stat}) \pm 0.06(\text{syst})$ below and above $E = 40$ EeV, respectively (the systematic uncertainty in the energy determination is estimated as 22%) [11]. These observations are consistent with the predictions of Greisen, Zatsepin and Kuzmin [12, 13] (GZK), who noted that above $\sim 10^{20}$ eV, cosmic rays should interact strongly in the cosmic microwave background (CMB) radiation through photopion production (for protons) or photodisintegration (for heavier nuclei), leading to a degradation in the cosmic ray energy. One should note, however, that although the observations are consistent with the GZK predictions, they do not necessarily demonstrate that this is in fact the mechanism behind the suppression. It is also conceivable that the suppression signals the maximum energy achievable at nearby acceleration sites. Additional observations of the chemical composition and searches for photons or neutrinos produced via cosmic ray interactions in the CMB (GZK photons and neutrinos) might settle the issue. The second change in the spectral index, known as the “ankle” occurs at an energy of about $4 \cdot 10^{18}$ eV [14, 15, 16, 17]. This feature may be a result of a steep spectrum from galactic sources crossing over a flatter spectrum from extragalactic sources [18, 19]. An alternative explanation has been proposed [20, 21], however, in which the galactic to extragalactic transition happens at much lower energies, above which extragalactic protons dominate the flux. In this scenario, the ankle is carved out as a result of e^\pm pair production on the CMB photons.

¹Low energy extensions to the Observatory [2] are just reaching maturity and will extend acceptance into the region where an additional spectral feature, the “second knee,” has been reported [6, 7, 8, 9].

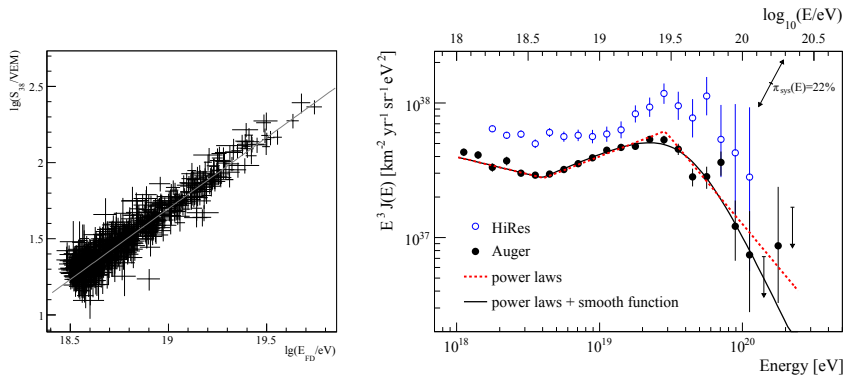


Figure 1: *Left*: S_{38° vs. Energy measured by the FD for a sample of 795 high quality hybrid events. These are used to calibrate the SD energy estimator. *Right*: Combined energy spectrum from hybrid and SD events. (Note the flux is scaled by E^3 in order to flatten the appearance of the spectrum.) HiRes results [27] are shown for comparison. The results of the two experiments are consistent within systematic uncertainties.

Last year, an updated Auger measurement of the energy spectrum was published [22], corresponding to a surface array exposure of 12 790 km² sr yr. This measurement uses both hybrid and SD-only events.

The first step in hybrid event reconstruction is determination of the shower geometry. This is found by combining information from the shower image and timing in one or more telescopes with the timing information from the surface array station with the largest signal. Once the geometry is determined, the energy deposition along the shower trajectory is reconstructed. This is then converted to the shower energy, taking account of the the fraction of the energy deposited out of the field of view of the telescope as well as effects of direct and scattered Cherenkov light and atmospheric conditions, which are monitored by a battery of instruments [23]. More details on the reconstruction procedure can be found in [24].

In the case of showers observed only by the surface array, the timing and signal sizes from hit stations are used to find a Lateral Distribution Function (LDF) characterizing the signal size perpendicular to the shower axis. From the LDF, the signal size at 1000 m from the core, called $S(1000)$ is extracted. This parameter has been shown to be relatively insensitive to assumptions about the functional form of the lateral distribution [25]. Due to attenuation in the atmosphere, a shower at a given energy will pro-

duce a smaller $S(1000)$ for a larger zenith angle than for a smaller one. This is accounted for with data by applying the constant intensity cut method [26], in which the assumption that UHECR flux is approximately isotropic in zenith allows one to determine a correction factor for $S(1000)$ at each zenith angle. The corrected $S(1000)$ is called S_{38° and corresponds to the $S(1000)$ which would have been observed had the shower arrived from 38° in zenith². Hybrid events are used to establish a relationship between S_{38° and the energy determined by the FD, as illustrated in Fig. 1 (left panel). This relation is then applied to the full SD data sample. More details on these reconstruction techniques can be found in [11, 22].

The combined energy spectrum using both hybrid and SD events is shown in Fig. 1 (right panel). The ankle feature and flux suppression are clearly visible. A broken power law fit to the spectrum shows that the break corresponding to the ankle is located at $\log_{10}(E/\text{eV}) = 18.61 \pm 0.01$ with $\gamma = 3.26 \pm 0.04$ before the break and $\gamma = 2.59 \pm 0.02$ after it. The break corresponding to the suppression is located at $\log_{10}(E/\text{eV}) = 19.46 \pm 0.03$. Compared to a power law extrapolation, the significance of the suppression is greater than 20σ .

Mass composition

Measurement of the cosmic ray mass composition provides crucial input for understanding sources and propagation of cosmic rays at ultra high energies. For instance, the variation of composition on energy may shed light on what mechanism is responsible for the ankle, and help to clarify whether the flux suppression is the GZK effect or a limitation of acceleration mechanisms [28].

The most readily-available composition-sensitive observable is X_{max} , the slant depth at which the longitudinal development of the shower reaches its maximum size in terms of number of particles. From a simple argument due to Heitler [29], it is easy to show that for a cascade of electrons and photons the X_{max} scales logarithmically with the energy of the primary particle. To understand how X_{max} is sensitive to composition it is helpful to invoke a superposition model³ in which a nucleus of mass A_0 and energy E is pictured as the superposition of A_0 nucleons, each possessing energy E/A_0 . Then, for some nuclear primaries of mass A , the average depth of shower maximum $\langle X_{\text{max}} \rangle$ for some energy E scales as

²The angle 38° is just the median zenith for the fiducial region use in this analysis.

³Note that this is not an implausible model, since for cosmic rays at these energies, the individual nucleon energies far exceed nuclear binding energies.

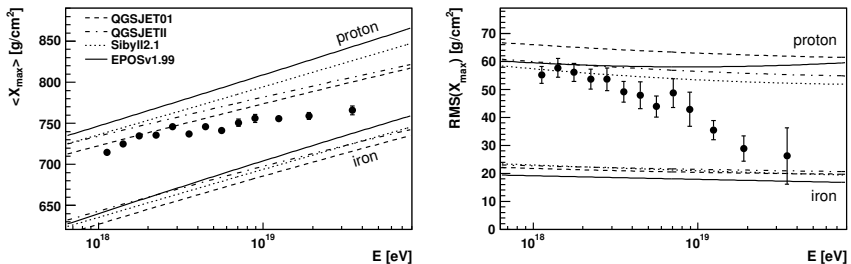


Figure 2: $\langle X_{\max} \rangle$ and $\text{RMS}(X_{\max})$ compared with air shower simulations [33] using different hadronic interaction models [34]. These results are based on data recorded between December 2004 and March 2009.

$\langle X_{\max} \rangle \propto \ln E - \langle \ln A \rangle$. Due to fluctuations in the position of the first interactions, one also expects that showers of a given primary energy and mass should exhibit shower-to-shower fluctuations in X_{\max} . Again from the superposition principle, one can interpret a shower induced by a nucleon of mass A_0 as a superposition A_0 subshowers, displaying an overall X_{\max} which is an average of all the subshower X_{\max} values. From this argument we expect greater shower-to-shower fluctuations for light primaries than for heavy primaries. The $\text{RMS}(X_{\max})$ for an ensemble of showers thus constitutes a complementary observable for discerning the primary mass. (See [30] for a more extensive discussion of these ideas.) An interesting quantity to study is the *elongation rate* [31], $dX_{\max}/d \log E$, the increase in X_{\max} per energy decade. This is sensitive to changes in composition with energy.

For UHECR, X_{\max} can be observed directly by the FD, or indirectly through surface array observables. Here we consider only the FD measurements. To ensure a high quality measurement, only well-reconstructed hybrid events are used and atmospheric measurements are required to be available to assess cloud contamination, aerosol and molecular conditions [23]. The X_{\max} resolution is about 20 g/cm^2 , which is established through simulation and also by observation of individual showers by more than one telescope. The $\text{RMS}(X_{\max})$ values are obtained by subtracting the detector resolution in quadrature from the width of the X_{\max} distribution. Details of the analysis techniques can be found in [32]. The results of the measurements of the variation of X_{\max} and $\text{RMS}(X_{\max})$ are shown in Fig. 2.

Interpreting the results of these measurements relies on comparisons to the predictions of models. As one can see in Fig. 2, there is considerable variation in predictions among different hadronic interaction models. Still,

if the model predictions are not wildly off, it appears there is an increase of average mass with energy. Alternatively, if one had reason to believe that protons should dominate up to high energies, these results in Fig. 2 would indicate significant changes in interaction physics at ultra-high energies [35]. Furthermore, assumption of a fixed elongation rate does not fit the measured $\langle X_{\max} \rangle$ values particularly well, yielding $\chi^2/\text{dof} = 34.9/11$. However, a broken line fit yields satisfactory agreement with the data ($\chi^2/\text{dof} = 9.7/9$) with the break at $\log_{10}(E/\text{eV}) = 18.24 \pm 0.05$ and a *change* in elongation rate of $\Delta = 82_{-21}^{+35}$ g/cm²/decade. Note that the location of this break is not far from the location of the ankle break in the energy spectrum ($\log_{10}(E_{\text{ankle}}/\text{eV}) = 18.61 \pm 0.01$). This appears to support to the hypothesis of a transition from galactic to extragalactic cosmic rays in the ankle region.

Searches for photons and neutrinos

The acceleration mechanism responsible for the UHECR is a long-standing puzzle. Generally acceleration models fall into either the “bottom-up” or the “top-down” category. In bottom-up models, some process such as first-order Fermi acceleration takes place at a site with sufficient extent and magnetic field to support acceleration of particles up to the highest energies observed (for reviews of the topic, see eg. [36, 37]). More speculative top-down models (see eg. [38, 39, 40]) postulate that the highest energy events result from decays of topological defects [41] super heavy dark matter (SHDM) [42, 43], or from neutrinos interacting in the cosmic relic neutrino background [46]. A common feature of top-down models is the prediction of a significant flux of photons and neutrinos at the highest energies, from $O(10\%)$ at 10^{19} eV to over 50% at 10^{20} eV, so it is interesting to hunt for these tell-tale signs in the cosmic flux.

On the other hand, even in the absence of exotic physics, some flux of photons [47] and neutrinos [49] should result via proton interactions in the CMB. Neutrinos are also expected to be produced at the same sources responsible for UHECR acceleration [48], and as they are unperturbed by intervening magnetic fields and matter, they could provide a direct window to otherwise inaccessible regions of the universe.

Searches for photon primaries have been conducted using both the surface and fluorescence instruments of the Auger Observatory. Photons penetrate quite deeply into the atmosphere due to decreased secondary multiplicities and suppression of cross-sections by the LPM effect [45]. Indeed it is rather easier to distinguish photons from protons and iron than protons and iron are to distinguish from one another. For example, at 10^{19} eV, the

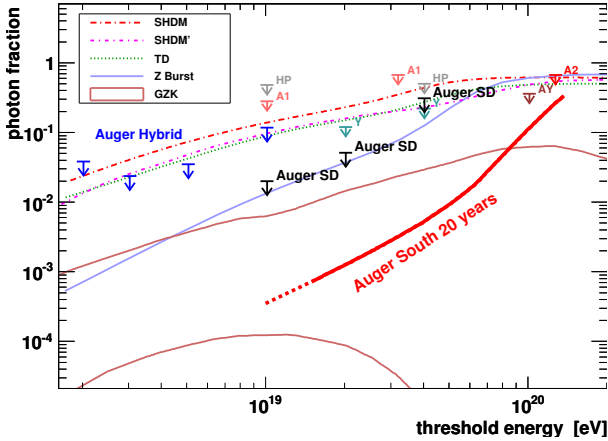


Figure 3: Upper limits on the photon fraction from different experiments. The limits from Auger operating in hybrid mode are labeled “Auger Hybrid”, while the SD only limits are labeled “Auger SD”. The banded region indicates the expected photon fraction from the GZK effect, as calculated in [47]. The thick red line shows the expected sensitivity of Auger to photon fractions after 20 years of operation. The lines indicate predictions from top-down models [47, 43, 44].

$\langle X_{\max} \rangle$ for a photon is about 1000 g/cm^2 while for protons and iron the numbers are 800 g/cm^2 and 700 g/cm^2 respectively.

While analysis of the fluorescence data exploits the direct view of shower development, analysis of data from the SD relies on measurement of quantities which are indirectly related to the X_{\max} , such as the signal risetime at 1000 m from the shower core and the curvature of the shower front. The resulting bound on photon flux are shown in Fig. 3. Further details on the analysis procedures can be found in [50, 51, 52].

It is possible to detect ultra-high energy cosmic neutrinos at the Pierre Auger Observatory by searching for deeply-developing, large zenith angle ($> 75^\circ$) showers [53]. At these large angles, hadron-induced showers traverse the equivalent of several atmospheres before reaching detectors at the ground. Beyond about 2 atmospheres, most of the electromagnetic component of a shower is extinguished and only very high energy muons survive. Consequently, a hadron-induced shower front is relatively flat and the shower particles arrive within a narrow time window (Fig. 4 top panel). In contrast, a neutrino shower exhibits characteristics similar to

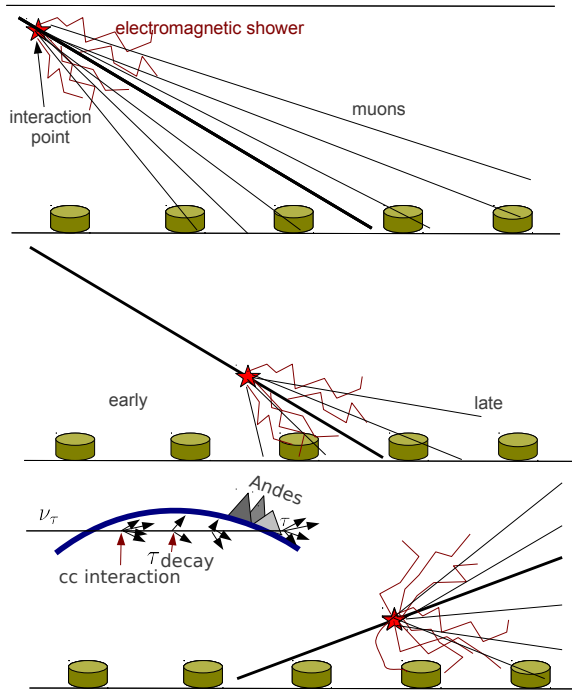


Figure 4: Schematic illustration of the properties of a hadron-induced shower (top), an ν -induced nearly horizontal shower (middle) and a ν_τ -induced earth skimming shower (bottom). Note that only up-going showers resulting from τ neutrino interactions in the Earth can be detected with any efficiency using the surface array. In contrast, all three neutrino species can be detected in down-going showers. Also note from the inset in the lower panel, that the incident τ can experience several CC interactions and decays and thereby undergo a regeneration process. The Andes mountain range lies to the west of the observatory, and provides roughly an additional 20% target volume for ν_τ interactions.

those of a vertical shower, which has a more curved front and a wider distribution in particle arrival times due to the large number of lower energy electrons and photons. Furthermore, the “early” part of the shower will tend to be dominated by the electromagnetic component, while “late” por-

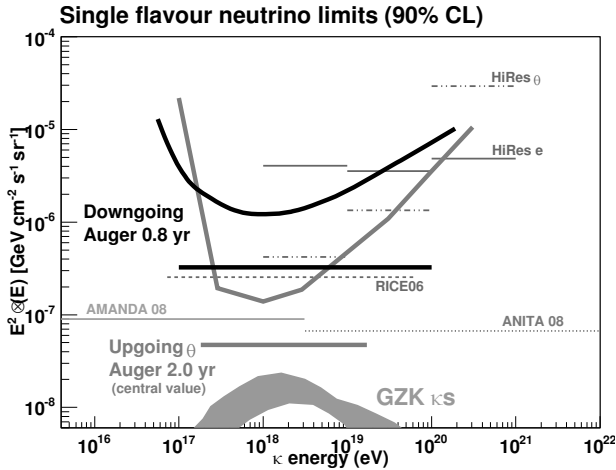


Figure 5: Differential and integral bounds for diffuse neutrinos as observed by several experiments. Note that the differential bounds indicate the the maximum sensitivity at the Auger Observatory occurs in the region where the GZK neutrino flux is expected to be greatest.

tion will be enriched with tightly bunched muons (Fig. 4 middle panel). Using these characteristic features, it is possible to distinguish neutrino induced events from background hadronic showers. Moreover, because of full flavor mixing, tau neutrinos are expected to be as abundant as other species in the cosmic flux. Tau neutrinos can interact in the Earth’s crust, producing τ leptons which may decay above the Auger detectors [54, 55] (Fig. 4 bottom panel). Details on how such events can be selected at the Auger Observatory are discussed in [56, 57].

So far no neutrino candidates have been observed, resulting in upper limits on the diffuse flux of neutrinos shown in Fig. 5. For the case of up-going τ neutrinos, the current bound is $E^2 \frac{dN}{dE} < 4.7_{-2.5}^{+2.2} \cdot 10^{-8} \text{ GeV cm}^{-2} \text{ s}^{-1} \text{ sr}^{-1}$. Though the Auger Observatory was not designed specifically as a neutrino detector, it is interesting to note that it exhibits good sensitivity in an energy regime complementary to those available to other dedicated instruments.

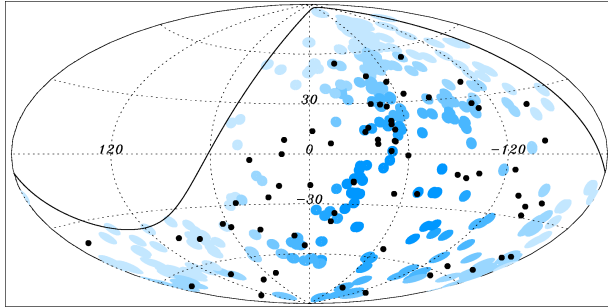


Figure 6: Sky map of 69 Auger events (black dots) with $E > 5.5 \cdot 10^{19}$ eV using data collected up to 31 December 2009, including the events used during the exploratory period. The blue circles have radius 3.1° and denote the 318 AGN from the VCV catalog which are within the field of view of the observatory and have $z < 0.018$.

Arrival Directions

Given that the highest energy cosmic rays observed should exhibit trajectories which are *relatively* unperturbed by galactic and intergalactic magnetic fields, it is natural to wonder whether isotropy begins to emerge at these high energies. Furthermore, if the observed flux suppression is the GZK effect, there is necessarily some distance, $O(100 \text{ Mpc})$, beyond which cosmic rays with energies near 10^{20} eV will not be seen. Since the matter density within about 100 Mpc is not isotropic, this compounds the potential for anisotropy to emerge in the UHECR sample. Using Auger data, both point source studies have been performed (outlined below) as well as harmonic analysis of arrival directions, which characterize anisotropy at various angular scales [59].

One way to increase the chance of success in finding out the sources of UHECR is to check for correlations between cosmic ray arrival directions and known candidate astrophysical objects. When following such an approach, however, care must be taken to ascertain how many statistical trials are made. In light of this, the Auger anisotropy analysis scheme followed a pre-defined process. First an exploratory data sample was employed for comparison with various source catalogs and for tests of various cut choices. The results of this exploratory period were then used to design prescriptions to be applied to subsequently gathered data.

One of these prescriptions was designed to test the correlation of events having energies $E > 5.6 \cdot 10^{19}$ eV with objects in the Veron-Cetty & Veron

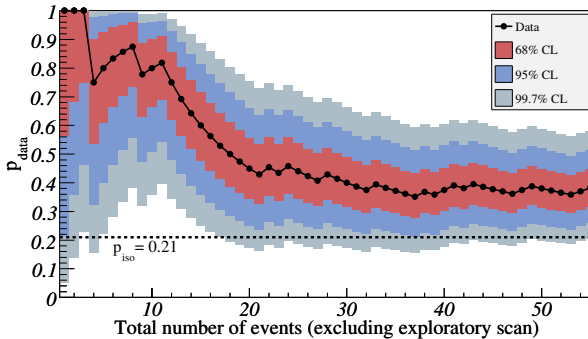


Figure 7: The most likely degree of correlation $p_{\text{data}} = k/N$ as a function of the total number of time ordered events, N , excluding events taken during the exploratory scan. k is the number of correlating events. The 68%, 95% and 99.7% confidence intervals are shown around the most likely value. The horizontal line shows the expectation for isotropy.

catalog of Active Galactic Nuclei. The prescription called for a search of 3.1° windows around catalog objects with redshifts $z < 0.0018$. The significance threshold set in the prescription was met in 2007 [60, 61] with 9 of the 13 events in the sample correlating, and an update was since published [62]. A skymap showing the locations of the events with $E > 5.5 \cdot 10^{19}$ eV is displayed in Fig. 6. The fraction of correlating events for the prescription period and for the period hence is shown in Fig. 7. The number of correlating events is now 21/55, or $0.38^{+0.07}_{-0.06}$ with 0.21 expected for isotropically distributed events. The strength of the correlation appears to be smaller than one would have expected given the initial results. However, evidence for anisotropy remains in the sense that there is a 0.3% chance to find 21 or more of 55 events from an isotropic distribution which correlate with a catalog object subject to the cuts on source opening angle and redshift.

A number of other interesting observations are described in [62], including comparisons with other catalogs as well as a specific search around the region of Centaurus A. It is important to keep in mind that these are all *a posteriori* studies, so one cannot use them to determine a confidence level for anisotropy as the number of trials is unknown.

A compelling concentration of events in the region around the direction of local active galaxy Centaurus A has been observed. The maximum departure from isotropy occurs for a ring of 18° around the object, in which

13 events are observed compared to an expectation of 3.2 from isotropy. One should note that, while these events could be coming from Centaurus A itself, which is only about 4 Mpc away, it is also possible they originate in the Centaurus galaxy cluster at a distance of about 45 Mpc. Details of other catalog searches can be found in [62].

Summary

The inaugural years of data taking at the Pierre Auger Observatory have yielded a large, high-quality data sample. The enormous area covered by the surface array together with an excellent fluorescence system and hybrid detection techniques have provided us with large statistics, good mass and energy resolution, and solid control of systematic uncertainties.

A number of important scientific results have thus far been obtained.

- A 20σ suppression of the energy spectrum has been observed in the region above $10^{19.6}$ eV. This is consistent with the predictions of Greisen, Zatsepin and Kuzmin, though it could also signify a cosmic acceleration endpoint.
- The measurements of $\langle X_{\max} \rangle$ and $\text{RMS}(X_{\max})$ show a trend to heavier composition with energy, or, more speculatively, some change in interaction physics at extreme energies if in fact the primary particles are mostly protons.
- There is evidence for a correlation between cosmic rays with energies above $5.5 \cdot 10^{19}$ eV and nearby extragalactic matter, though the case for the correlation is not as strong as it initially appeared. Correlations on such a small angular scale as those reported (3.1°) would seem to be at odds with the apparent trend to heavy composition at high energy, since heavier nuclei would be more deflected by intergalactic and galactic magnetic fields. Other anisotropy analyses have yielded potentially interesting targets for future study.
- Competitive bounds have been placed on the flux of diffuse neutrinos in an energy regime complementary to those covered by dedicated neutrino telescopes.
- Tight bounds have been placed on the flux of extremely high energy photons, ruling out some exotic models of cosmic acceleration.

Currently the Auger Observatory is collecting some $7000 \text{ km}^2 \text{ sr yr}$ of exposure each year, and is expected to run for 2 more decades. New detector systems [2] are being deployed which will lower the energy detection

threshold down to 10^{17} eV. An experimental radio detection program is also co-located with the observatory [63] and shows promising results. As always, the development of new analysis techniques is ongoing, and interesting new results can be expected.

Acknowledgements

The work of T. Paul was supported in part by US National Science Foundation Grant PHY-0855388 and by the Slovene AD FUTURA foundation. T. Paul would like to thank L. Anchordoqui, G. Alverson and R. Clay for proofreading the manuscript, and would like especially to extend a *hvala lepa* to the organizers for an exceptionally interesting and pleasant conference.

References

- [1] J. Abraham *et al.* [Pierre Auger Collaboration], Nucl. Instrum. Meth. A **523** (2004) 50-95.
- [2] J.A. Abraham *et al.* [Pierre Auger Collaboration], [arXiv:0906.2354].
- [3] J. Abraham *et al.* [Pierre Auger Collaboration], Nucl. Instrum. Meth. A **613** (2010) 29.
- [4] J.A. Abraham *et al.* [Pierre Auger Collaboration], Nucl. Instrum. Meth. A **620** (2010) 227, [arXiv:0907.4282].
- [5] P. Abreu *et al.* [Pierre Auger Collaboration], Astropart. Phys. **34** (2011) 368, [arXiv:1010.6162(astro-ph.HE)].
- [6] M. Nagano *et al.*, Nucl. J. Phys. G **10** (1984).
- [7] T. Abu-Zayyad *et al.* [HiRes-MIA Collaboration], Astrophys. J. **557** (2001) 686, [arXiv:astro-ph/0010652].
- [8] A.V. Glushkov *et al.*, *28th International Cosmic Ray Conferences (ICRC 2003), Tsukuba, Japan, 31 Jul - 7 Aug 2003*.
- [9] R.U. Abbasi *et al.* [High Resolution Fly's Eye Collaboration], Phys. Rev. Lett. **92** (2004) 151101, [arXiv:astro-ph/0208243].
- [10] R.U. Abbasi *et al.* [HiRes Collaboration], Phys. Rev. Lett. **100** (2008) 101101, [arXiv:astro-ph/0703099].
- [11] J. Abraham *et al.* [Pierre Auger Collaboration], Phys. Rev. Lett. **101** (2008) 061101, [arXiv:0806.4302(astro-ph)].
- [12] K. Greisen, Phys. Rev. Lett. **16** (1966) 748.
- [13] G.T. Zatsepin and V.A. Kuz'min, Pis'ma Zh. Eksp. Teor. Fiz. **4** (1966) 114.
- [14] J. Linsley, Proc. of 8th Int. Cosmic Ray Conf, Jaipur **4** (1963) 77.
- [15] M.A. Lawrence, R.J.O. Reid, and A.A. Watson, J. Phys. G **17** (1991) 733.
- [16] M. Nagano *et al.*, J. Phys. G **18** (1992) 423.
- [17] D.J. Bird *et al.* [HIRES Collaboration], Phys. Rev. Lett. **71** (1993) 3401.
- [18] A.M. Hillas, J. Phys. G **31** (2005) R95-R131.
- [19] T. Wibig and A.W. Wolfendale, J. Phys. G **31** (2005) 255-264, [arXiv:astro-ph/0410624].

- [20] V. Berezhinsky, A.Z. Gazizov, and S.I. Grigorieva, *Phys. Lett. B* **612** (2005) 147-153, [arXiv:astro-ph/0502550].
- [21] R. Aloisio, V. Berezhinsky, P. Blasi *et al.*, *Phys. Rev. D* **77** (2008) 025007, [arXiv:0706.2834(astro-ph)].
- [22] J. Abraham *et al.* [Pierre Auger Collaboration], *Phys. Lett. B* **685** (2010) 239, [arXiv:1002.1975(astro-ph.HE)].
- [23] J. Abraham *et al.* [Pierre Auger Collaboration], *Astropart. Phys.* **33** (2010) 108, [arXiv:1002.0366(astro-ph.IM)].
- [24] M. Unger, B.R. Dawson, R. Engel *et al.*, *Nucl. Instrum. Meth. A* **588** (2008) 433-441. [arXiv:0801.4309(astro-ph)].
- [25] D. Newton, J. Knapp, and A.A. Watson, *Astropart. Phys.* **26** (2007) 414-419, [arXiv:astro-ph/0608118].
- [26] J. Hersil, I. Escobar, D. Scott *et al.*, *Phys. Rev. Lett.* **6** (1961) 22-23.
- [27] R.U. Abbasi *et al.* [HiRes Collaboration], *Astropart. Phys.* **32** (2009) 53-60.
- [28] D. Allard, N.G. Busca, G. Decerprit *et al.*, *JCAP* **0810** (2008) 033, [arXiv:0805.4779(astro-ph)].
- [29] W. Heitler, Oxford University Press, 1954.
- [30] L. Anchordoqui, M.T. Doxa, A.G. Mariazzi *et al.*, *Annals Phys.* **314** (2004) 145-207.
- [31] J. Linsley, *Proc. 15th ICRC* **12** (1977) 89; T.K. Gaisser *et al.*, *Proc. 16th ICRC* **9** (1979) 258; J. Linsley and A.A. Watson, *Phys. Rev. Lett.* **46** (1981) 459.
- [32] J. Abraham *et al.* [Pierre Auger Collaboration], *Phys. Rev. Lett.* **104** (2010) 091101, [arXiv:1002.0699(astro-ph.HE)].
- [33] T. Bergmann *et al.*, *Astropart. Phys.* **26** (2007) 420.
- [34] N.N. Kalmykov and S.S. Ostapchenko, *Phys. Atom. Nucl.* **56** (1993) 346; S.S. Ostapchenko, *Nucl. Phys. Proc. Suppl.* **151** (2006), 143; T. Pierog and K. Werner, *Phys. Rev. Lett.* **101** (2008) 171101; E.J. Ahn *et al.*, *Phys. Rev. D* **80** (2009) 094003.
- [35] R. Ulrich, R. Engel, S. Muller *et al.*, [arXiv:0906.0418(astro-ph.HE)].
- [36] P.L. Biermann, *J. Phys. G* **23** (1997) 1-27.
- [37] M. Ostrowski, *Astropart. Phys.* **18** (2002) 229-236 [arXiv:astro-ph/0101053].
- [38] P. Bhattacharjee and G. Sigl, *Proc. of Physics and Astrophysics of Ultrahigh-energy Cosmic Rays, Meudon, France, 26-29 Jun 2000*.
- [39] S. Sarkar, *Acta Phys. Polon. B* **35** (2004) 351-364, [arXiv:hep-ph/0312223].
- [40] L. Anchordoqui, T.C. Paul, S. Reucroft *et al.*, *Int. J. Mod. Phys. A* **18** (2003) 2229-2366, [arXiv:hep-ph/0206072].
- [41] C.T. Hill, *Nucl. Phys. B* **224** (1983) 469; M.B. Hindmarsh and T.W.B. Kibble, *Rept. Prog. Phys.* **58** (1995) 477-562, [arXiv:hep-ph/9411342].
- [42] V. Berezhinsky, M. Kachelriess, and A. Vilenkin, *Phys. Rev. Lett.* **79** (1997) 4302-4305, [arXiv:astro-ph/9708217]; M. Birkel and S. Sarkar, *Astropart. Phys.* **9** (1998) 297-309, [arXiv:hep-ph/9804285]; S. Sarkar and R. Toldra, *Nucl. Phys. B* **621** (2002) 495-520, [arXiv:hep-ph/0108098]; C. Barbot and M. Drees, *Astropart. Phys.* **20** (2003) 5-44, [arXiv:hep-ph/0211406]; R. Aloisio, V. Berezhinsky, and M. Kachelriess, *Phys. Rev. D* **74** (2006) 023516, [arXiv:astro-ph/0604311]; R. Aloisio and V.S. Berezhinsky, *Astrophys. J.* **625** (2005) 249-255, [arXiv:astro-ph/0412578].
- [43] J.R. Ellis, V.E. Mayes, and D.V. Nanopoulos, *Phys. Rev. D* **74** (2006) 115003, [arXiv:astro-ph/0512303].
- [44] M. Risse and P. Homola, *Mod. Phys. Lett. A* **22** (2007) 749-766,

- [arXiv:astro-ph/0702632].
- [45] L.D. Landau and I. Pomeranchuk, Dokl. Akad. Nauk Ser. Fiz. **92** (1953) 735-738; L.D. Landau and I. Pomeranchuk, Dokl. Akad. Nauk Ser. Fiz. **92** (1953) 535-536; A.B. Migdal, Phys. Rev. **103** (1956) 1811-1820.
- [46] T.J. Weiler, Phys. Rev. Lett. **49** (1982) 234; T.J. Weiler, Astropart. Phys. **11** (1999) 303-316, [arXiv:hep-ph/9710431]; D. Fargion, B. Mele, and A. Salis, Astrophys. J. **517** (1999) 725-733, [arXiv:astro-ph/9710029].
- [47] G.B. Gelmini, O.E. Kalashev, and D.V. Semikoz, JCAP **0711** (2007) 002, [arXiv:0706.2181(astro-ph)].
- [48] E. Waxman and J. N. Bahcall, Phys. Rev. D **59** (1999) 023002, [arXiv:hep-ph/9807282].
- [49] F. Halzen and D. Hooper, Rept. Prog. Phys. **65** (2002) 1025-1078, [arXiv:astro-ph/0204527]; P. Bhattacharjee and G. Sigl, Phys. Rept. **327** (2000) 109-247, [arXiv:astro-ph/9811011]. J.K. Becker, Phys. Rept. **458** (2008) 173-246, [arXiv:0710.1557(astro-ph)].
- [50] J. Abraham *et al.* [Pierre Auger Collaboration], Astropart. Phys. **31** (2009) 399-406, [arXiv:0903.1127(astro-ph.HE)].
- [51] J. Abraham *et al.* [Pierre Auger Collaboration], Astropart. Phys. **29** (2008) 243-256, [arXiv:0712.1147(astro-ph)].
- [52] J. Abraham *et al.* [Pierre Auger Collaboration], Astropart. Phys. **27** (2007) 155-168, [arXiv:astro-ph/0606619].
- [53] K.S. Capelle, J.W. Cronin, G. Parente, and E. Zas, Astropart. Phys. **8** (1998) 321, [arXiv:astro-ph/9801313].
- [54] J.L. Feng, P. Fisher, F. Wilczek, and T.M. Yu, Phys. Rev. Lett. **88** (2002) 161102, [arXiv:hep-ph/0105067].
- [55] X. Bertou, P. Billoir, O. Deligny, C. Lachaud, and A. Letessier-Selvon, Astropart. Phys. **17** (2002) 183, [arXiv:astro-ph/0104452].
- [56] J. Abraham *et al.* [Pierre Auger Collaboration], [arXiv:0906.2347].
- [57] J. Abraham *et al.* [Pierre Auger Collaboration], Phys. Rev. D **79** (2009) 102001, [arXiv:0903.3385].
- [58] L.A. Anchordoqui, H. Goldberg, D. Gora, T. Paul, M. Roth, S. Sarkar, and L.L. Winders, Phys. Rev. D **82** (2010) 043001; T. Paul *et al.*, these Proceedings.
- [59] J. Abraham *et al.* [Pierre Auger Collaboration], Astropart. Phys. **43** (2011) 627.
- [60] J. Abraham *et al.* [Pierre Auger Collaboration], Astropart. Phys. **29** (2008) 188-204, [arXiv:0712.2843(astro-ph)].
- [61] J. Abraham *et al.* [Pierre Auger Collaboration], Science **318** (2007) 938-943, [arXiv:0711.2256(astro-ph)].
- [62] P. Abreu *et al.* [Pierre Auger Collaboration], Astropart. Phys. **34** (2010) 314-326, [arXiv:1009.1855].
- [63] B. Revenu [Pierre Auger and CODALEMA Collaboration], Nucl. Instrum. Meth. A **604** (2009) S37-S40.

t & *m*

LHCb Status and Prospects

R. LEFÈVRE^{1*} ON BEHALF OF THE LHCb COLLABORATION

¹ *Clermont Université, Université Blaise Pascal, CNRS/IN2P3,
Laboratoire de Physique Corpusculaire, BP 10448,
F-63000 Clermont-Ferrand, France*

Abstract: This contribution first discusses the main objectives of the LHCb experiment, the detector environment and its performances. The measurements of the J/ψ , open charm and beauty production cross-sections are then reported. The progresses and prospects for few selected key measurements are finally considered: ϕ_s in $B_s \rightarrow J/\psi \phi$, $B_s \rightarrow \mu\mu$ and the forward-backward asymmetry in $B^0 \rightarrow K^* \mu\mu$.

Introduction

The Cabibbo-Kobayashi-Maskawa (CKM) matrix [1] relates quarks mass eigenstates to flavour eigenstates. It describes quark flavour mixing within the Standard Model. The lesson of the CKM metrology up to now is that the Kobayashi-Maskawa mechanism is the dominant source of CP violation in the K^0 and B^0 systems. However, there is still room for sizeable contributions from New Physics.

The LHCb experiment [2] is dedicated to extensive, high precision studies of CP violation and rare decays in b -flavoured hadrons [3]. Concerning CP violation, the first key parameter for which LHCb should be able to significantly improve current results is the B_s oscillation phase ϕ_s . LHCb should also relatively quickly lead to major improvements of the measurements of the CKM angle γ , both from decays involving “tree” transitions and from decays involving “loop” transitions. Moreover LHCb will open new perspectives in the study of CP violation in the charm sector, both in the charm mixing and for what concerns direct CP violation in charm decays. For rare decays, LHCb should rapidly have the best sensitivity to the branching fraction of $B_s \rightarrow \mu\mu$ which is a very good probe of Flavour Changing Neutral Currents (FCNC) in loops. The other key element here

* regis.lefevre@cern.ch

is the helicity structure in the transition $b \rightarrow s\gamma$ which will be tested in LHCb with the modes $B^0 \rightarrow K^*\mu\mu$, $B_s \rightarrow \phi\gamma$ and $B^0 \rightarrow K^*ee$.

Performing precision measurements in a hadronic environment is a real challenge. The experiment has to cope with high multiplicity events, about 30 tracks per rapidity unit for single proton-proton collision events, and a high rate of background events, the proton-proton inelastic cross-section at $\sqrt{s} = 7$ TeV being about 60 mb. The reconstruction of B decays is even more difficult for events with pile-up so the nominal luminosity of LHCb will be limited to few $10^{32} \text{ cm}^{-2}\text{s}^{-1}$ to maximize the probability of single interaction per crossing. On the other hand, the $b\bar{b}$ cross-section is high at the LHC : about $300 \mu\text{b}$ at $\sqrt{s} = 7$ TeV ($\sim 500 \mu\text{b}$ at 14 TeV) to be compared to an e^+e^- cross-section of 1 nb at the $Y(4S)$. Of the order of 10^{12} $b\bar{b}$ pairs will be produced in LHCb for a nominal year of running, which corresponds to an integrated luminosity of 2 fb^{-1} (assuming 10^7 s at $2 \times 10^{32} \text{ cm}^{-2}\text{s}^{-1}$). In addition, LHCb has access to all the b species: B^0 , B^+ , B_s , B_c , Λ_b , Ξ_b ...

The LHCb detector

The $b\bar{b}$ pair production being predominantly forward peaked at the LHC, LHCb has been designed as a single-arm forward spectrometer to reduce the cost. The experiment covers polar angles from 10 to 300 mrad in the bending plane, 10 to 250 mrad in the non-bending plane. The vertex locator (VELO) and the tracking system provide very good vertexing and tracking capabilities. The VELO consists of two retractable detector halves and the sensors are only 8.2 mm away from the beam in stable beam condition. Excellent particle identification is achieved thanks to two ring imaging Cherenkov detectors, to the calorimeters and to five muon stations. The two Cherenkov detectors combine 3 radiators and provide $K - \pi$ separation for momenta between 2 and 100 GeV/c.

Another key element of the experiment is the trigger system: two levels reduce the rate from the 40 MHz input of the LHC clock to the 2 kHz output to the data acquisition. This is done exploiting fully the topology of B decays characterized by significant transverse momentum due to the high b quark mass and by long lifetime. The first level, called L0 (Level 0), is implemented in custom electronic boards working in a fully synchronous architecture with a fixed latency of 4 μs and a maximal output rate of 1 MHz. The calorimeters and the muon detectors are the main L0 contributors providing via dedicated electronics the highest momentum identified electron, photon, π^0 , hadron, muon and di-muon candidates. The second level, called HLT (High Level Trigger), uses a farm of about 2000 central processing units. The HLT first reduces the rate to something like 30 kHz

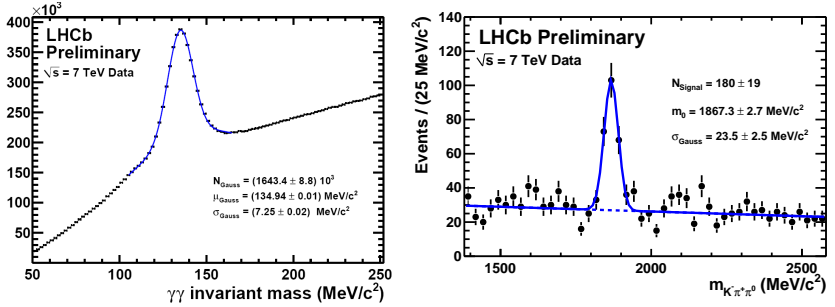


Figure 1: Invariant mass spectra of the $\pi^0 \rightarrow \gamma\gamma$ (left) and $D^0 \rightarrow K^- \pi^+ \pi^0$ (right) candidates in the first 3 nb^{-1} collected by LHCb at $\sqrt{s} = 7 \text{ TeV}$.

using the tracking information to confirm the L0 candidates, eventually adding an Impact Parameter (IP) cut. Only then inclusive and exclusive selections are built using the full event reconstruction.

Performances

The performance of the LHCb detector is very good, as it has been taking data efficiently throughout the year. At the end of September 2010, the integrated luminosity delivered by the LHC was 7.4 pb^{-1} and the one recorded by the experiment was 6.9 pb^{-1} , which corresponds to an average efficiency of 93%. A very important element required for tagging tracks from secondary vertices, and subsequently identification of B meson decays, is the IP resolution, which has also improved. For example, for tracks having a transverse momentum (p_T) of $1 \text{ GeV}/c$, the achieved IP resolution with the latest alignment is about $38 \mu\text{m}$, about 5% better than with previous alignment, and is expected to further improve in the future. The Monte Carlo (MC) based expectation for the IP resolution with perfect alignment is $30 \mu\text{m}$.

Figure 1 was obtained from the very first data collected at $\sqrt{s} = 7 \text{ TeV}$ and illustrates good performance of the calorimeters for photon identification and reconstruction. Making the invariant mass distribution of all pairs of photon clusters, the π^0 peak is clearly visible. The position of the peak and its width, only $7.25 \text{ MeV}/c^2$, show that the calorimeter cells were already properly calibrated. The $D^0 \rightarrow K^- \pi^+ \pi^0$ peak reported in figure 1 was the first heavy flavour resonance involving neutrals that was observed at LHCb. The resolution is excellent, given it is based on the very first data and involves both the tracking system and the calorimeters. At current

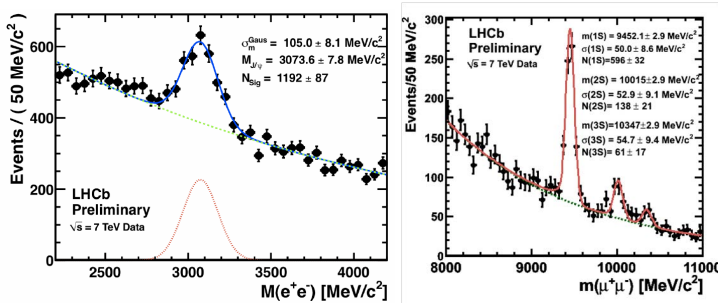


Figure 2: Invariant mass spectra of the $J/\psi \rightarrow e^+e^-$ (left) and $Y \rightarrow \mu^+\mu^-$ (right) candidates. The presented spectra correspond to integrated luminosities of about 0.15 pb^{-1} and 0.6 pb^{-1} respectively.

luminosity, this mode benefits of very high statistics. It is now used in particular as a calibration sample for the π^0 reconstruction. The calorimeters are also essential to identify and reconstruct electrons, where good performance has also already been achieved. As an example, the peak obtained for $J/\psi \rightarrow e^+e^-$ candidates is shown in figure 2.

The performances of the muon identification have also been tested on data. The efficiency is measured using a tag and probe method on $J/\psi \rightarrow \mu^+\mu^-$ candidates. Only one muon is identified by the muon system (“tag”), the other one (“probe”) is identified selecting a track associates to energy deposits in the calorimeters compatible with a minimum ionizing particle. The muon identification efficiency is then evaluated on the probe muon. The misidentifications of pions and kaons as muons have been measured using $K_S \rightarrow \pi\pi$ and $\phi \rightarrow KK$ decays, respectively. The results obtained on muon identification are compatible with the expectations based on the simulation. For tracks with a momentum higher than $10 \text{ GeV}/c$, the muon identification efficiency is above 90%, with misidentification rates lower than 2%. To illustrate how well LHCb performs on muons, figure 2 shows the di-muon invariant mass spectrum in the Y region. The $Y(1S)$, $Y(2S)$ and $Y(3S)$ are clearly visible. They are also very nicely separated thanks to the excellent mass resolution provided by the tracking system.

The identification of pions, kaons and protons with the Cherenkov detectors has been calibrated with $K_S \rightarrow \pi\pi$, $\phi \rightarrow KK$, and $\Lambda \rightarrow p\pi$ decays, respectively. Good separations are already obtained, not as good as in the simulation but still being improved. For tracks with a momentum lower than $50 \text{ GeV}/c$, the pion to kaon misidentification rate varies for instance

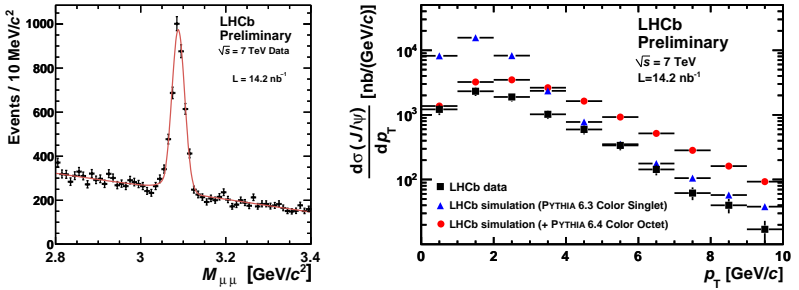


Figure 3: Invariant mass spectrum of the $J/\psi \rightarrow \mu^+\mu^-$ candidates (left) and measured differential inclusive J/ψ production cross-section as a function of p_T (right).

between 7 and 15% for a kaon identification efficiency varying between 95 and almost 100%.

J/ψ production cross-section

The J/ψ production has been studied on a sample of 14.2 nb^{-1} [4]. J/ψ of p_T up to $10 \text{ GeV}/c$ and rapidity in the range $y \in [2.5; 4]$ are considered. Figure 3 shows the invariant mass spectrum of the $J/\psi \rightarrow \mu^+\mu^-$ candidates. The distribution is fitted with a Crystal Ball function to describe the signal and a first order polynomial for the background. The inclusive J/ψ cross-section obtained from the fit is:

$$\sigma_{\text{inc } J/\psi}(p_T^{J/\psi} > 10 \text{ GeV}/c, 2.5 < y^{J/\psi} < 4) = (7.65 \pm 0.19 \pm 1.10^{+0.87}_{-1.27}) \mu\text{b},$$

where the first error is statistical, the second one corresponds to systematic uncertainties, and the third one indicates the acceptance uncertainty due to the unknown J/ψ polarization. The systematic uncertainties are dominated by the uncertainty on the integrated luminosity (10%), followed by the uncertainty on the tracking efficiency (4% per muon track, *i.e.* adding up to a global effect of 8%).

To measure the differential cross-section as a function of p_T , the J/ψ sample is divided in 10 sub-samples of $1 \text{ GeV}/c$ in p_T . The $\mu^+\mu^-$ invariant mass distribution is then fitted in each sub-sample using the same functions as for the whole sample. The measured p_T differential cross-section is reported in figure 3, assuming non polarized J/ψ . The data is compared to two Monte Carlo models but none of them reproduce the measurements. Comparisons to more complete theoretical predictions are expected soon.

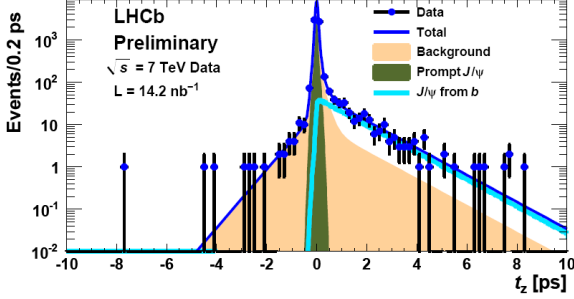


Figure 4: t_z distribution of the J/ψ candidates.

To statistically separate J/ψ from b , which tend to be produced away from the primary vertex, from prompt J/ψ , produced immediately at the primary vertex, the pseudo-proper time along the z -axis is used. It is defined as:

$$t_z = \frac{\Delta z \times M_{J/\psi}}{p_z},$$

where Δz is the distance along the z -axis between the J/ψ decay vertex and the closest primary vertex in the z direction, p_z is the measured J/ψ momentum in the z direction and $M_{J/\psi}$ the nominal J/ψ mass. Figure 4 shows the t_z distribution. The data is fitted with three contributions: prompt J/ψ , J/ψ from b and background. The J/ψ from b cross-section obtained from the fit is:

$$\sigma_{J/\psi \text{ from } b}(p_T^{J/\psi} > 10 \text{ GeV}/c, 2.5 < y^{J/\psi} < 4) = (0.81 \pm 0.06 \pm 0.13) \mu\text{b}.$$

Extrapolations with PYTHIA 6.4 give an average cross-section to produce b -flavoured or \bar{b} -flavoured hadrons (H_b) with a pseudo-rapidity between 2 and 6 of:

$$\sigma(pp \rightarrow H_b X, 2 < \eta(H_b) < 6) = (84.5 \pm 6.3 \pm 15.6) \mu\text{b},$$

and a $b\bar{b}$ production cross section in 4π of:

$$\sigma(pp \rightarrow b\bar{b} X) = (319 \pm 24 \pm 59) \mu\text{b}.$$

Beauty production from $b \rightarrow D^0 X \mu^- \bar{\nu}_\mu$ decays

Another way to measure the beauty production is to look at $b \rightarrow D^0 X \mu^- \bar{\nu}_\mu$ events [5]. This mode has a large branching fraction, $(6.84 \pm 0.35)\%$, and is

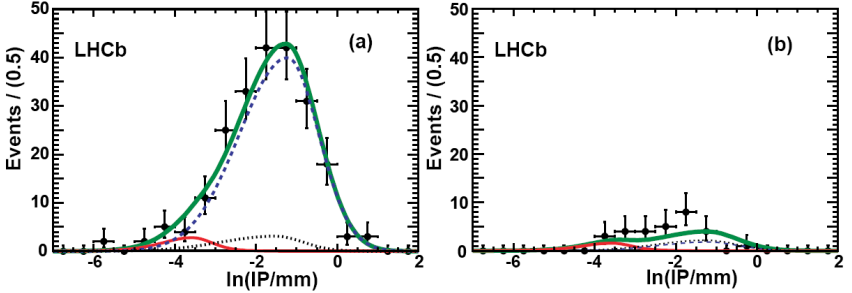


Figure 5: Natural logarithm of the D^0 IP for right-sign (left) and wrong-sign (right) D^0 -muon candidates. The dashed curves represent D^0 from b -flavoured hadron decays, the thin solid curves the prompt D^0 component, the dotted curves the non- D^0 background, and the thick solid curves the totals.

advantageous from the point of view of signal to background. The analysis uses two independent data sets: a micro-bias sample and a muon trigger sample. The first comes from the earliest period of data taking and was recorded using the micro-bias trigger which is just requiring one track to be reconstructed. It corresponds to an integrated luminosity of 2.9 nb^{-1} . The second sample was recorded later with a single muon trigger and corresponds to an integrated luminosity of 12.2 nb^{-1} . The analysis uses the $D^0 \rightarrow K^- \pi^-$ decay mode, which has a branching fraction of $(3.89 \pm 0.05)\%$ and is very clean.

The D^0 from b -flavoured hadron decays are statistically separated from the prompt D^0 component thanks to the IP of the D^0 candidate with respect to the closest primary vertex. Distributions of the natural logarithm of the D^0 IP are presented in figure 5. These distributions correspond to the muon trigger sample. They are presented separately for right-sign and wrong-sign candidates defined as the ones for which the charge of the muon and of the kaon from the D^0 are the same or opposite, respectively. The semi-leptonic b decays mostly lead to right-sign candidates. The wrong-sign sample is then important to make sure the backgrounds are well modeled. In figure 5, the shape associated to the signal D^0 from b -flavoured hadron decays has been taken from the Monte Carlo. The one for the prompt D^0 background has been extracted from the micro-bias sample by considering candidates for which the track which is supposed to be associated to the muon fails the muon identification criteria. The shape from the non- D^0 background is obtained from the D^0 side-bands. The fit presented in

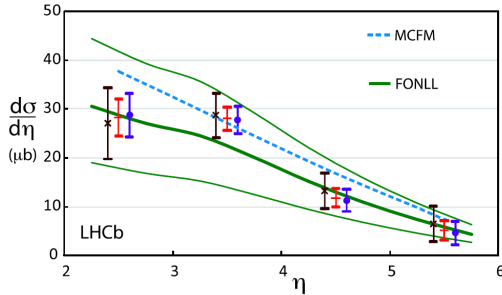


Figure 6: Measured differential b -flavoured hadron production cross-section as a function of η for the micro-bias sample (\times), the muon triggered sample (\bullet), and the average ($+$). The systematic uncertainties in the data are not included. The thin lines indicate the uncertainties on the FONLL prediction.

figure 5 well reproduce the data both for right-sign and wrong-sign candidates.

As shown in figure 6, the average cross-section to produce b -flavoured or \bar{b} -flavoured hadrons is measured in four pseudo-rapidity bins. The LEP b hadronization fractions are used for the central values. The results from the two independent data samples are compatible. Their combination is in good agreement with the theoretical predictions. Summing over the four pseudo-rapidity bins leads to the measurement:

$$\sigma(pp \rightarrow H_b X, 2 < \eta(H_b) < 6) = (75.3 \pm 5.4 \pm 13.0) \mu\text{b}.$$

Here also the systematic uncertainties are dominated by the uncertainty on the integrated luminosity (10%) and by the uncertainty on the tracking efficiency (3% for the kaon and the pion track, 4% for the muon track, *i.e.* adding up to a global effect of 10%). An extrapolation with PYTHIA 6.4 gives in 4π :

$$\sigma(pp \rightarrow b\bar{b}X) = (284 \pm 20 \pm 49) \mu\text{b}.$$

Those results are compatible with the one obtained from the J/ψ study. Combining them, using the LEP b hadronization fractions and extrapolating with PYTHIA 6.4, one obtains:

$$\sigma(pp \rightarrow H_b X, 2 < \eta(H_b) < 6) = (79.1 \pm 4.0 \pm 11.4) \mu\text{b},$$

and:

$$\sigma(pp \rightarrow b\bar{b}X) = (298 \pm 15 \pm 43) \mu\text{b}.$$

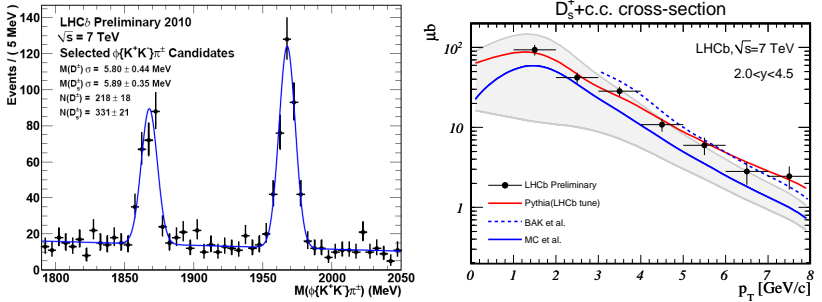


Figure 7: Invariant mass spectrum of the $\phi\pi^\pm$ candidates (left) and measured differential D_s^\pm production cross-section as a function of p_T (right). The shaded area indicates the uncertainties on the MC *et al.* prediction.

Open charm production

The open charm production has been studied on a data sample of 1.8 nb^{-1} collected with the micro-bias trigger. The production cross-sections of D^0/\bar{D}^0 , $D^{*\pm}$, D^\pm and D_s^\pm have been determined in bins of transverse momentum and rapidity in the region $p_T < 8 \text{ GeV}/c$ and $2 < y < 4.5$ [6].

The decay channels used are: $D^0 \rightarrow K^- \pi^+$, $D^{*+} \rightarrow D^0(K^- \pi^+) \pi^+$, $D^+ \rightarrow K^- \pi^+ \pi^+$, $D^+ \rightarrow \phi(K^- K^+) \pi^+$, $D_s^+ \rightarrow \phi(K^- K^+) \pi^+$, and their charge conjugates. For what concerns the D^+ , the production cross section is obtained from the $K^- \pi^+ \pi^+$ mode. The $\phi\pi^+$ mode is used to determine the cross-section ratio $\sigma(D^+)/\sigma(D_s^+)$. Just as in the previous section, the prompt D are statistically separated from the D from b -flavoured hadron decays using the IP of the D candidate with respect to the closest primary vertex.

As an illustration, figure 7 shows two plots related to the D_s^\pm . The D^\pm and D_s^\pm peaks are clearly visible in the $\phi\pi^\pm$ invariant mass spectrum. The corresponding mass resolutions are smaller than $6 \text{ GeV}/c^2$. This is another example of the excellent performances of the tracking system. The measured p_T differential D_s^\pm cross-section is compared with expectations from the LHCb tune of PYTHIA 6.4 and from QCD computations. Good agreements both in shape and in normalization are found. This statement is true for all the open charm cross-sections measured in this analysis. Extrapolating those measurements with PYTHIA 6.4 gives a $c\bar{c}$ production cross section in 4π about 20 times higher than what is measured for $b\bar{b}$:

$$\sigma(pp \rightarrow c\bar{c}X) = (6.10 \pm 0.93) \text{ mb.}$$

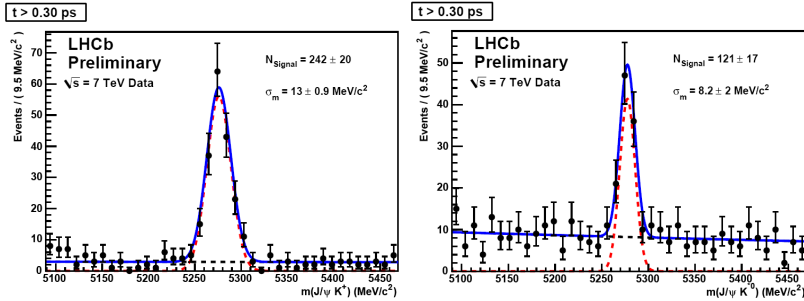


Figure 8: Invariant mass spectra of the $B^+ \rightarrow J/\psi K^+$ (left) and $B^0 \rightarrow J/\psi K^*$ (right) candidates with a proper time greater than 0.3 ps. The red dashed lines represent the signal contributions.

ϕ_s in $B_s \rightarrow J/\psi \phi$ decays

$B_s \rightarrow J/\psi \phi$ decays proceed via almost pure $\bar{b} \rightarrow c\bar{c}\bar{s}$ tree transition associated to a single weak phase Φ_D . Before decaying, a B_s meson may first oscillate to a \bar{B}_s meson with a mixing phase Φ_M . Interference between mixing and decay gives rise to a CP violation phase $\phi_s = \Phi_M - 2\Phi_D$.

In the Standard Model, $\Phi_D \approx \arg(V_{cs}V_{cb}^*)$ and $\Phi_M \approx 2\arg(V_{ts}V_{tb}^*)$. This gives $\phi_s^{SM} \approx -2\beta_s$ with $\beta_s = \arg(-V_{ts}V_{tb}^*/V_{cs}V_{cb}^*)$, which is very well determined from the CKM metrology: $\beta_s = 0.0182 \pm 0.0009$ (rad). ϕ_s is sensitive to New Physics in $\Delta F = 2$ transitions, where it becomes $\phi_s = \phi_s^{SM} + \phi_s^\Delta \approx -2\beta_s + \phi_s^\Delta$, which may lead to a large deviation from the Standard Model prediction.

The decay $B_s \rightarrow J/\psi \phi$ is a decay of a pseudo-scalar into two vectors. Angular momentum conservation implies that the final state is not a pure CP eigenstate but an admixture of CP-odd ($\ell = 1$) and CP-even ($\ell = 0, 2$) components, where ℓ is the relative angular momentum between the J/ψ and the ϕ . An angular analysis in the transversity base is then required to statistically separate the CP-odd and CP-even components.

In the expressions of those components, ϕ_s typically appears multiplied by terms such as $\sin(\Delta m_s t)$ where Δm_s is the mass difference of the B_s mass eigenstates. Since these terms have opposite sign between B_s and \bar{B}_s the analysis significantly benefits from flavour tagging. These terms also imply that the information on ϕ_s is mostly obtained from a time-dependent analysis in which the fast B_s oscillations are resolved thanks to an excellent proper time resolution.

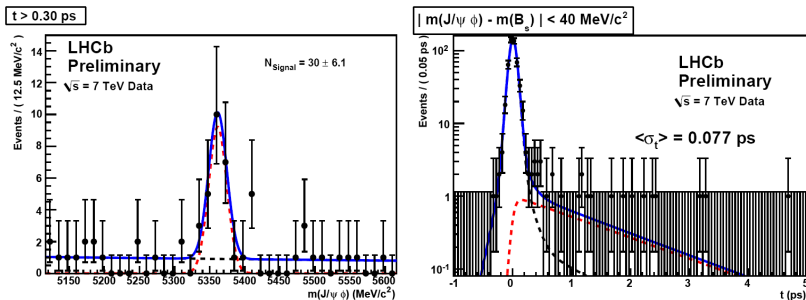


Figure 9: Invariant mass spectrum of the $B_s \rightarrow J/\psi \phi$ candidates with a proper time greater than 0.3 ps (left) and proper time distribution of the $B_s \rightarrow J/\psi \phi$ candidates within a 40 MeV/ c^2 mass window around the B_s (right). The red dashed lines represent the signal contribution.

The measurement of ϕ_s is far from simple as it requires a time-dependent angular analysis of the tagged $B_s \rightarrow J/\psi \phi$ decays.

Figure 8 shows the invariant mass peaks obtained for the $B^+ \rightarrow J/\psi K^+$ and $B^0 \rightarrow J/\psi K^*$ decay modes. Those modes are in fact studied using lifetime unbiased selections and the 0.3 ps proper time cut used in the figure is just for illustration purpose. They are very important for the measurement of the performances of the opposite side flavour taggers and to study the angular acceptance. The obtained yields are within expectations from Monte Carlo studies. One may notice the very good B mass resolutions, even if this is obtained with a J/ψ mass constraint. This is even further improved with the latest alignment for which the B mass resolution for the $B^+ \rightarrow J/\psi K^+$ sample is for example reduced from 13 MeV/ c^2 to 9 MeV/ c^2 .

As shown on figure 9, a clear signal from $B_s \rightarrow J/\psi \phi$ has already been seen. The average proper time resolution for B_s signal candidates is between 50 and 60 fs. This is a bit high with respect to the 36 fs expected from the simulation, but we expect the agreement to improve with further progresses in the alignment.

About the flavour tagging, a first signal of flavour oscillation from $B^0 \rightarrow D^{*-} \mu^+ \nu_\mu$ with $D^{*-} \rightarrow D^0 \pi^-$ and $D^0 \rightarrow K^+ \pi^-$ has been obtained with a data sample corresponding to an integrated luminosity of 1.9 pb $^{-1}$. This is reported in figure 10. The initial flavour at production is determined using the opposite side flavour taggers as tuned on the Monte Carlo. The flavour at decay is given by the charge of the muon. The flavour oscillation is clearly visible and in good agreement with the known B^0/\bar{B}^0 oscillation frequency Δm_d . The combination of the opposite side flavour taggers gives

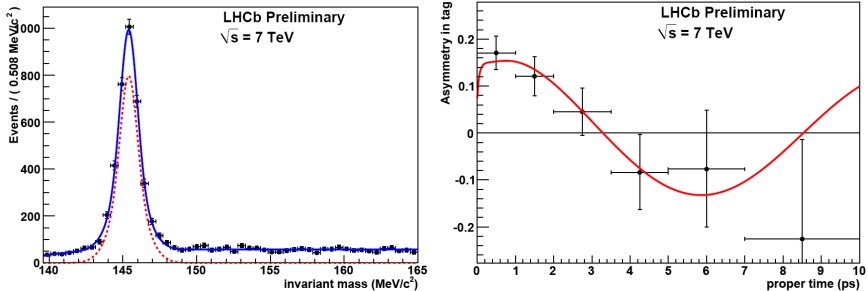


Figure 10: Distribution of $m_{D^*} - m_{D^0}$ for the $B^0 \rightarrow D^{*-} \mu^+ \nu_\mu$ candidates (left) and observed flavour asymmetry as a function of the B^0 proper time in $B^0 \rightarrow D^{*-} \mu^+ \nu_\mu$ decays (right).

a tagging power of 2%. This is 60% of the expected nominal performance when combining opposite side flavour taggers which is already quite good given that no tuning at all has yet been performed on data.

The expected sensitivity to ϕ_s is very good. Just with 50 pb^{-1} , LHCb should already supersede the results from the Tevatron experiments. With 500 pb^{-1} , the uncertainty on ϕ_s should be lower than 0.1 rad.

$B_s \rightarrow \mu\mu$ decays

In the Standard Model, the $B_s \rightarrow \mu\mu$ decay relies on a color-suppressed Z-penguin diagram. The Standard Model prediction for the $B_s \rightarrow \mu\mu$ branching fraction is $(3.35 \pm 0.32) \cdot 10^{-9}$. New Physics could affect this branching fraction. This is the case for instance for the two Higgs doublet models. For example in the MSSM, the $B_s \rightarrow \mu\mu$ branching fraction is proportional to $\tan^6 \beta$.

In LHCb, the search for $B_s \rightarrow \mu\mu$ will be done with a binned likelihood fit constructed on three independent variables: the di-muon invariant mass, the muon identification likelihood and the geometrical likelihood. The geometrical likelihood combines the discriminating variables from the VELO: distance of closest approach of the muons, IP of the muons, isolation of the muons (number of tracks that make a good vertex with one of the muon), B_s proper time and B_s IP.

Figure 11 shows two plots obtained checking the $B_s \rightarrow \mu\mu$ background distributions on the first data. They indicate that the Monte Carlo estimation is reasonable. On the right plot, the sensitive region corresponds to $m_{\mu^+\mu^-} - m_{B_s} \in [-60; 60] \text{ MeV}/c^2$ and geometrical likelihood > 0.5 . For

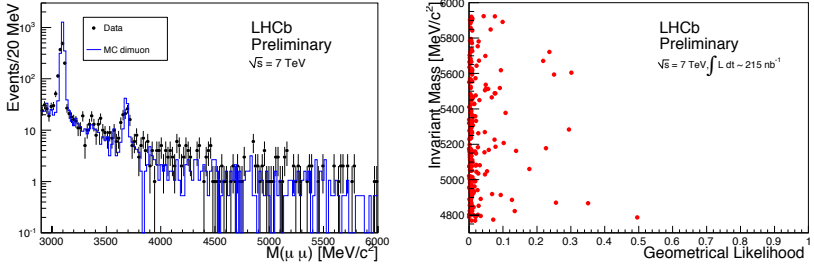


Figure 11: Di-muon invariant mass spectrum (left) and di-muon invariant mass vs. $B_s \rightarrow \mu\mu$ geometrical likelihood (right) for the first 0.2 pb^{-1} .

1 fb^{-1} , the expectation for the sensitive region is about 6 signal events and 30 background events.

LHCb should be very good at hunting $B_s \rightarrow \mu\mu$. It should have the world best limit when a data sample of 100 pb^{-1} would have been collected. For 1 fb^{-1} , five σ observations should be possible down to branching fractions of four times the Standard Model prediction.

Forward-backward asymmetry in $B^0 \rightarrow K^* \mu\mu$ decays

In the Standard Model, the $B^0 \rightarrow K^* \mu\mu$ decay proceeds via suppressed FCNC in $b \rightarrow s\gamma$ electroweak penguin transitions. Its branching fraction has already been measured: $(1.15 \pm 0.15) \cdot 10^{-6}$. It agrees to within 20% with the Standard Model.

The $b \rightarrow s\gamma$ transition is sensitive to magnetic, vector and axial semi-leptonic penguin operators. Many variables are sensitive to New Physics but for the first data (low statistics) LHCb will focus on the forward-backward asymmetry: A_{FB} . It is defined counting the number of positive (N_F) and negative (N_B) leptons going in the same direction as the K^* in the dilepton rest frame:

$$A_{FB} = \frac{N_F - N_B}{N_F + N_B}.$$

It is usually measured as a function of $q^2 = m_{\mu^+\mu^-}^2$. The most precise predictions are at zero crossing point, *i.e.* for q_0^2 such that $A_{FB}(q_0^2) = 0$, where the form factors cancelled out.

The prospects on A_{FB} are excellent in LHCb. The precisions of the current measurements from the B -factories should be reached for only 100 pb^{-1} .

Conclusion

The LHCb detector is fully operational. Its performance is already very promising and is still being improved. First measurements have been successfully carried out. LHCb has a great potential for what concerns CP violation and rare B decays. It will relatively quickly become the most sensitive experiment for many key measurements.

Acknowledgments

I would like to thank the organizing committee, and in particular Martin O'Loughlin and Samo Stanič for the nice organization of the conference and the pleasant stay in Budva.

References

- [1] M. Kobayashi and T. Maskawa, *Prog. Theor. Phys.* **49** (1973) 652.
- [2] A.A. Alves *et al.* [LHCb Collaboration], *JINST* **3** (2008) S08005.
- [3] B. Adeva *et al.* [LHCb Collaboration], LHCb-PUB-2009-029 (Dec 2009) arXiv:0912.4179.
- [4] [LHCb Collaboration], LHCb-CONF-2010-010 (Jul 2010).
- [5] R. Aaij *et al.* [LHCb Collaboration], *Phys. Lett. B* **694** (2010) 209.
- [6] [LHCb Collaboration], LHCb-CONF-2010-013 (Dec 2010).

t & *m*

Various Facets of Spacetime Foam

Y. JACK NG^{1,2*}

¹ *Department of Physics & Astronomy, University of North Carolina,
Chapel Hill, NC 27599-3255, USA*

² *European Southern Observatory, Karl-Schwarzschild-Str. 2,
85748 Garching, Germany*

Abstract: Spacetime foam manifests itself in a variety of ways. It has some attributes of a turbulent fluid. It is the source of the holographic principle. Cosmologically it may play a role in explaining why the energy density has the critical value, why dark energy/matter exists, and why the effective dynamical cosmological constant has the value as observed. Astrophysically the physics of spacetime foam helps to elucidate why the critical acceleration in modified Newtonian dynamics has the observed value; and it provides a possible connection between global physics and local galactic dynamics involving the phenomenon of flat rotation curves of galaxies and the observed Tully-Fisher relation. Spacetime foam physics also sheds light on nonlocal gravitational dynamics.

Introduction

Unity of physics dictates that various physical phenomena and the principles underlying them are related to one another. But some of the concepts, phenomena and structures found in physics are more fundamental than others. I believe spacetime foam (arising from quantum fluctuations of spacetime) belongs to the first (fundamental) category. In this talk I will show that spacetime foam has a multiplicity of sides and will argue ¹ that it is the origin of some of the various phenomena we see around us. Spacetime foam manifests itself in the holographic principle. Its physics calls for a critical cosmic energy density and the existence of dark energy/matter.

* yjng@physics.unc.edu

¹Some of the interpretation of the physics given here may deviate from the original works I did with my various collaborators. I alone am responsible for such a reinterpretation.

At least partly it explains the observed critical galactic acceleration and it provides an intriguing dark matter profile. It has some attributes of a turbulent fluid. And its physics may be related to the nonlocality of gravitational dynamics. Each of these various facets of spacetime foam will be discussed in a separate section below.

But first, let us examine how foamy spacetime is, or, in other words, how large quantum fluctuations of spacetime are. This can be done by using the following two methods.

- The Wigner-Salecker experiment [1, 2, 3, 4]

To quantify the problem, let us consider the fluctuations of a distance ℓ between a clock and a mirror. By sending a light signal from the clock to the mirror and back to the clock in a timing experiment, we can determine ℓ . The clock's and the mirror's positions jiggle according to Heisenberg's uncertainty principle, resulting in an uncertainty $\delta\ell$. From the jiggling of the clock's position alone, the uncertainty principle yields $(\delta\ell)^2 \geq \hbar\ell/mc$, where m is the mass of the clock. On the other hand, the clock must be large enough not to collapse into a black hole; this requires $\delta\ell \gtrsim 4Gm/c^2$, which combines with the requirement from quantum mechanics to yield $(\delta\ell)^3 \gtrsim 4\ell\ell_p^2$ (independent of the mass m of the clock), where $\ell_p = \sqrt{\hbar G/c^3} \approx 10^{-33}$ cm is the Planck length. We conclude that *the fluctuation of a distance scales as its cube root* [5]:

$$\delta\ell \gtrsim \ell^{1/3}\ell_p^{2/3},$$

where we have dropped multiplicative factors of order unity. Henceforth we will continue this practice of dropping such factors except in a couple of places.

- Mapping the geometry of spacetime[6, 7]

Let us consider mapping out the geometry of spacetime for a spherical volume of radius ℓ over the amount of time $T = 2\ell/c$ it takes light to cross the volume. One way to do this is to fill the space with clocks, exchanging signals with the other clocks and measuring the signals' times of arrival. This process of mapping the geometry of spacetime is a kind of computation, in which distances are gauged by transmitting and processing information. The total number of operations, including the ticks of the clocks and the measurements of signals, is bounded by the Margolus-Levitin theorem [8] in quantum computation, which stipulates that the rate of operations for any computer cannot exceed the amount of energy E that is available for computation divided by $\pi\hbar/2$. This theorem, combined with the bound on the

total mass of the clocks to prevent black hole formation, implies that the total number of operations that can occur in this spacetime volume is no greater than $2(\ell/\ell_p)^2/\pi$. To maximize spatial resolution (i.e., to minimize $\delta\ell$), each clock must tick only once during the entire time period. If we regard the operations partitioning the spacetime volume into "cells", then on the average each cell occupies a spatial volume no less than $(4\pi\ell^3/3)/(2\ell^2/\pi\ell_p^2) \sim \ell\ell_p^2$, yielding an average separation between neighboring cells no less than $\sim \ell^{1/3}\ell_p^{2/3}$. [9] This spatial separation is interpreted as the average minimum uncertainty in the measurement of a distance ℓ , that is, $\delta\ell \gtrsim \ell^{1/3}\ell_p^{2/3}$, the same result as found above in the Wigner-Salecker gedanken experiment. This result will be shown to be consistent with the holographic principle; hence the corresponding spacetime foam model is called the holographic model.

But there are many other models of spacetime foam [10]. We can characterize them with a parameter $\alpha \sim 1$ according to $\delta\ell \sim \ell^{1-\alpha}\ell_p^\alpha$. It is useful to introduce the following model as a foil to the ($\alpha = 2/3$) holographic model. Instead of maximizing spatial resolution in the mapping of spacetime geometry, let us consider spreading the spacetime cells uniformly in both space and time. In that case, each cell has the size of $(\ell^2\ell_p^2)^{1/4} = \ell^{1/2}\ell_p^{1/2}$ both spatially and temporally so that each clock ticks once in the time it takes to communicate with a neighboring clock. Since the dependence on $\ell^{1/2}$ has the hallmark of a random-walk fluctuation, the (quantum foam) model corresponding to $\delta\ell \gtrsim (\ell\ell_p)^{1/2}$ is called the random-walk model [11]. Compared to the holographic model, the random-walk model predicts a coarser spatial resolution, i.e., a larger distance fluctuation, in the mapping of spacetime geometry.² We will concentrate on the holographic model — the only correct model, in my opinion. But occasionally we will consider the general class of models parametrized by the different values of α (specifically only when we discuss the experimental/observational probing of spacetime foam). Unless clarity demands otherwise, we will put $c = 1$ and $\hbar = 1$ henceforth.

Spacetime foam and probing it with distant quasars/AGNs

How can we test the spacetime foam models? The Planck length $\ell_p \sim 10^{-33}$ cm is so short that we need an astronomical (even cosmological) dis-

²It also yields a smaller bound on the information content in a spatial region, viz., $(\ell/\ell_p)^2/(\ell/\ell_p)^{1/2} = (\ell^2/\ell_p^2)^{3/4} = (\ell/\ell_p)^{3/2}$ bits.

tance l for its fluctuation $\delta\ell$ to be detectable. Thus let us consider light (with wavelength λ) from distant quasars or bright active galactic nuclei [12, 13]. Due to the quantum fluctuations of spacetime, the wavefront, while planar, is itself “foamy”, having random fluctuations in phase [13] $\Delta\phi \sim 2\pi\delta\ell/\lambda$. When $\Delta\phi \sim \pi$, the cumulative uncertainty in the wave’s phase will have effectively scrambled the wave front sufficiently to prevent the observation of interferometric fringes. Consider the case of PKS1413+135 [14], an AGN for which the redshift is $z = 0.2467$. With $\ell \approx 1.2$ Gpc and $\lambda = 1.6\mu\text{m}$, we [13] find $\Delta\phi \sim 10 \times 2\pi$ and $10^{-9} \times 2\pi$ for the random-walk model and the holographic model of spacetime foam respectively. Thus the observation [14] by the Hubble Space Telescope of an Airy ring for this AGN *rules out the random-walk model* but fails to test the holographic model.

Furthermore we [15] note that, due to quantum foam-induced fluctuations in the phase, the wave vector can acquire a cumulative random fluctuation in direction with an angular spread of the order of $\Delta\phi/2\pi$. In effect, spacetime foam creates a “seeing disk” whose angular diameter is $\Delta\phi/(2\pi) \sim (\ell/\lambda)^{1-\alpha}(\ell_P/\lambda)^\alpha$ for the model parametrized by α .³

For a telescope or interferometer with baseline length D , this means that dispersion (on the order of $\Delta\phi/2\pi$ in the normal to the wave front) will be recorded as a spread in the angular size of a distant point source, causing a *reduction in the Strehl ratio, and/or the fringe visibility when $\Delta\phi/2\pi \sim \lambda/D$, i.e.,*

$$(\ell/\lambda)^{1-\alpha}(\ell_P/\lambda)^\alpha \sim \lambda/D$$

*for a diffraction limited telescope.*⁴ Thus, in principle, for arbitrarily large distances spacetime foam sets a lower limit on the observable angular size of a source at a given wavelength λ . Furthermore, the disappearance of “point sources” will be strongly wavelength dependent happening first at short wavelengths. Interferometer systems (like the Very Large Telescope Interferometers when it reaches its design performance) with multiple baselines may have sufficient signal to noise to allow for the detection of quantum

³This is partly based on the intuition (or reasonable assumption)[15] that spacetime foam fluctuations are isotropic such that the sizes of the wave-vector fluctuations perpendicular to and along the light of sight are comparable. But we should keep in mind that this intuition, though reasonable, could be wrong; after all, spatial isotropy is here “spontaneously” broken with the detected light being from a particular direction.

⁴For example, for a quasar of 1 Gpc away, at an infrared wavelength of the order of 2 microns, the holographic model of spacetime foam predicts a phase fluctuation $\Delta\phi \sim 2\pi \times 10^{-9}$ radians. On the other hand, an infrared interferometer with $D \sim 100$ meters has $\lambda/D \sim 5 \times 10^{-9}$. Such an interferometer has the potential to test the holographic model with a bright enough quasar that distance away.

foam fluctuations. For a discussion of the constraints recent astrophysical data put on spacetime foam models, see [16].⁵

Spacetime foam and turbulence

John Wheeler [18] was among the first to realize the connections between quantum gravity and the ubiquitous phenomenon of turbulence. Due to quantum fluctuations, spacetime, when probed at very small scales, will appear very complicated — something akin in complexity to a chaotic turbulent froth (which, as we all know, he dubbed spacetime foam, also known as quantum foam — the subject matter of this talk.) The connections between quantum gravity and turbulence are quite natural if we recall the role of the (volume preserving) diffeomorphism symmetry in classical (unimodular) gravity and the volume preserving diffeomorphisms of classical fluid dynamics. We may also recall that, in the case of irrotational fluids in three spatial dimensions, the equation for the fluctuations of the velocity potential can be written in a geometric form [19] with a metric having the canonical ADM form [19, 20]. The upshot is that the velocity of the fluid v^i plays the role of the shift vector in Einsteinian gravity; a fluctuation of v^i would imply a quantum fluctuation of the shift vector.

Furthermore, in fully developed turbulence in three spatial dimensions, the remarkable Kolmogorov scaling [21] implies that v scales with length scale l as $\sim l^{1/3}$, consistent with experimental observations. On the other hand, according to the holographic model of spacetime foam, a distance l fluctuates by an amount $\delta l \sim l^{1/3} \ell_P^{2/3}$. If one defines a velocity as $v \sim \frac{\delta l}{t_c}$, where the natural characteristic time scale is $t_c \sim \frac{\ell_P}{c}$, then it follows that $v \sim c(\ell/\ell_P)^{1/3}$.⁶ Thus we have obtained a *Kolmogorov-like scaling in turbulence, i.e., the velocity scales as*

$$v \sim \ell^{1/3}.$$

Since the velocities play the role of the shifts, they describe how the metric fluctuates at the Planck scale. The implication is that *at short distances, spacetime is a chaotic and stochastic fluid in a turbulent regime* with the Kolmogorov length ℓ . [22]

⁵See Ref. [11, 17] for a discussion of using gravitational-wave interferometers (like LIGO) or laser atom interferometers to detect spacetime foam.

⁶Here the speed of sound c and the Planck length ℓ_P for an induced gravitational constant are effective quantities.

Spacetime foam and the holographic principle

In essence, the holographic principle[23, 24, 25] says that although the world around us appears to have three spatial dimensions, its contents can actually be encoded on a two-dimensional surface, like a hologram. In other words, the maximum entropy, i.e., the maximum number of degrees of freedom, of a region of space is given by its surface area in Planck units. In this section, we will heuristically show that *the holographic principle has its origin in the quantum fluctuations of spacetime.*

Consider partitioning a spatial region measuring ℓ by ℓ by ℓ into many small cubes, with the small cubes being as small as physical laws allow, so that we can associate one degree of freedom with each small cube. [26] In other words, the number of degrees of freedom that the region can hold is given by the number of small cubes that can be put inside that region.

But how small can such cubes be? A moment's thought tells us that each side of a small cube cannot be smaller than the accuracy $\delta\ell$ with which we can measure each side ℓ of the big cube. Thus, the number of degrees of freedom (d.o.f.) in the region (measuring ℓ by ℓ by ℓ) is given by $\ell^3/\delta\ell^3$, which, since $\delta\ell \gtrsim \ell^{1/3}\ell_P^{2/3}$, is

$$\# \text{ d.o.f.} \lesssim (\ell/\ell_P)^2,$$

as stipulated by the holographic principle. Thus spacetime foam manifests itself holographically.

Spacetime foam and the critical cosmic energy density

Assuming that there is unity of physics connecting the Planck scale to the cosmic scale, we can now apply the holographic spacetime foam model to cosmology [6, 27, 28] and henceforth we call that cosmology the holographic foam cosmology (HFC).

Recall that the minimum $\delta\ell$ found for the holographic model corresponds to the case of maximum energy density $\rho = (3/8\pi)(\ell\ell_P)^{-2}$ for a sphere of radius ℓ not to collapse into a black hole. Hence the holographic model, unlike the other models, requires, for its consistency, the energy density to have the "critical" value.⁷ Hence, *according to HFC, the cosmic*

⁷By contrast, for instance, the corresponding energy density for the random-walk model takes on a range of values: $(\ell\ell_P)^{-2} \gtrsim \rho \gtrsim \ell^{-5/2}\ell_P^{-3/2}$. (The upper bound corresponds to the clocks ticking every $(\ell\ell_P)^{1/2}$ while the lower bound corresponds to the clocks ticking only once during the entire time $2\ell/c$.)

energy density is given by

$$\rho = (3/8\pi)(R_H \ell_P)^{-2},$$

where R_H is the Hubble radius.⁸ This is the critical cosmic energy density as observed.⁹ ¹⁰ Furthermore, since critical energy density is a hallmark of the inflationary universe scenario, HFC may be consistent with (warm) inflation [33].

Spacetime foam and dark energy/cosmological constant

In this section we will show that HFC "postdicts" the existence of dark energy and yields the correct magnitude of the effective cosmological constant. [6, 27, 28] The argument goes as follows: For the present cosmic era, the energy density is given by $\rho \sim H_0^2/G \sim (R_H \ell_P)^{-2}$ (about $(10^{-4} \text{ eV})^4$), where H_0 is the present Hubble parameter. Treating the whole universe as a computer, one can apply the Margolus-Levitin theorem to conclude that the universe computes at a rate ν up to $\rho R_H^3 \sim R_H \ell_P^{-2}$ ($\sim 10^{106}$ op/sec), for a total of $(R_H/\ell_P)^2$ ($\sim 10^{122}$) operations during its lifetime so far. If all the information of this huge computer is stored in ordinary matter, we can apply standard methods of statistical mechanics¹¹ to find that the total number I of bits is $[(R_H/\ell_P)^2]^{3/4} = (R_H/\ell_P)^{3/2}$ ($\sim 10^{92}$). It follows that each bit flips once in the amount of time given by $I/\nu \sim (R_H \ell_P)^{1/2}$ ($\sim 10^{-14}$ sec). However the average separation of neighboring bits is $(R_H^3/I)^{1/3} \sim (R_H \ell_P)^{1/2}$ ($\sim 10^{-3}$ cm). Hence, assuming only ordinary matter exists to store all the information we are led to conclude that the time to communicate with neighboring bits is equal to the time for each bit to flip once. It follows that the accuracy to which ordinary matter maps out the geometry of spacetime corresponds exactly to the case of events spread out uniformly in space and time as for the random-walk model of spacetime foam.

But, as argued in the introduction, the holographic model, not the random-walk model, is the correct model of spacetime foam. Furthermore,

⁸Instead of the Hubble radius, it has been suggested[29, 30] that one should perhaps use the Ricci's length.

⁹For an alternative explanation of the observed value for ρ , see [31, 32].

¹⁰Note that ρ depends on the geometric mean of R_H , the largest length scale, and ℓ_P , the smallest length scale. This indicates that there is an interplay or connection between ultraviolet and infrared dynamics in HFC and in spacetime foam physics.

¹¹Recall that energy (which determines the number of operations) and entropy (which determines the number of bits) depend on the 4th and 3rd power of temperature respectively.

the sharp images of PKS1413+135 observed at the Hubble Space Telescope have ruled out the latter model. From the theoretical as well as observational demise of the random-walk model and the fact that ordinary matter only contains an amount of information dense enough to map out spacetime at a level consistent with the random-walk model, one now infers that spacetime is mapped to a finer spatial accuracy than that which is possible with the use of ordinary matter. Therefore there must be another kind of substance with which spacetime can be mapped to the observed accuracy, as given by the holographic model. The natural conclusion is that *unconventional (dark) energy/matter exists!* Note that this argument does not make use of the evidence from recent cosmological (supernovae, cosmic microwave background, and galaxy clusters) observations.

Furthermore, the average energy carried by each constituent (particle/bit) of the unconventional energy/matter is $^{12} \sim \rho R_H^3 / I \sim R_H^{-1}$ ($\sim 10^{-31}$ eV). Such long-wavelength (hence “non-local”) constituents of dark energy act as a *dynamical cosmological constant with the observed magnitude* 13

$$\Lambda \sim 3H^2.$$

Thus HFC predicts an accelerating universe. In order to have an earlier decelerating universe and to have a cosmic transition from the decelerating expansion to a recent accelerating expansion, one needs dark matter and probably also an interaction between dark matter and dark energy [34]. 14

Spacetime foam and critical galactic acceleration/MoND

If holographic spacetime foam has provided the cosmos with an effective cosmological constant, one wonders if it may also affect local galactic dynamics. In particular, in view of Verlinde’s recent proposal [35] (see Appendix A) for the entropic [24], and thus holographic [23] reinterpretation of Newton’s law, it is natural to ask: can Newton’s second law be modified by holographic spacetime foam effects?

We first have to recognize that we live in an accelerating universe (in accordance with HFC). This suggests that we will need a generalization [36] of Verlinde’s proposal to de Sitter space with a positive cosmological constant which, according to HFC, is related to the Hubble parameter H by $\Lambda \sim 3H^2$. The Unruh-Hawking temperature [37] as measured by a

12 Recall that $I \sim (R_H / \ell_P)^2$ for holographic foam cosmology.

13 For an alternative explanation of the observed magnitude of Λ , see [31, 32].

14 As argued in [34], an appropriate interaction between the two components can even help to alleviate the cosmic coincidence problem.

non-inertial observer with acceleration a in the de Sitter space is given by $\sqrt{a^2 + a_0^2}/(2\pi k_B)$ [38], where $a_0 = \sqrt{\Lambda/3}$ [25]. Consequently, we can define the net temperature measured by the non-inertial observer (relative to the inertial observer) to be $\tilde{T} = [(a^2 + a_0^2)^{1/2} - a_0]/(2\pi k_B)$.

We can now follow Verlinde's approach [35].¹⁵ Then the entropic force, acting on the test mass m with acceleration a in de Sitter space, is given by $F_{\text{entropic}} = \tilde{T} \nabla_x S = m[(a^2 + a_0^2)^{1/2} - a_0]$. For $a \gg a_0$, the entropic force is given by $F_{\text{entropic}} \approx ma$. But for $a \ll a_0$, we have $F_{\text{entropic}} \approx ma^2/2a_0$; and so the terminal velocity v of the test mass m should be determined from $ma^2/2a_0 = mv^2/r$ [36]. The observed flat galactic rotation curves (i.e., at large r , v is independent of r) and the observed Tully-Fisher relation (the speed of stars being correlated with the galaxies' brightness, i.e., $v^4 \propto M$) [39] now require that $a \approx (4a_N a_0^3)^{1/4}$, where $a_N = GM/r^2$ is the magnitude of the usual Newtonian acceleration.¹⁶ But that means $F_{\text{entropic}} \approx ma^2/2a_0 \approx m\sqrt{a_N a_0}$ for the small acceleration $a \ll a_0$ regime. Thus we are led to the modified Newtonian dynamics, or MoND [40], due to Milgrom, which stipulates that the acceleration of a test mass m due to the source M is given by $a = a_N$ and $\sqrt{a_N a_c}$ for $a \gg a_c$ and $a \ll a_c$ respectively¹⁷ — provided we can identify a_0 as Milgrom's critical acceleration a_c . Milgrom has observed that a_c is numerically related to the speed of light c and the Hubble scale H as¹⁸ $a_c \sim cH \sim 10^{-8} \text{ cm/s}^2$. But $a_0 = (\Lambda/3)^{1/2}$, and $\Lambda \sim 3H^2$ as argued in the last section for HFC, it follows that a_0 is of the order of magnitude of

$$a_{\text{critical}} \sim \sqrt{\Lambda/3} \sim H.$$

In other words, we have successfully predicted the correct magnitude of the critical galactic acceleration, and furthermore have found that global physics (in the form of a dynamical cosmological constant with its origin in spacetime foam) can affect local galactic motion!

¹⁵We replace the T in Appendix A by \tilde{T} for the Unruh temperature.

¹⁶One can check this by carrying out a simple dimensional analysis and recalling that there are two accelerations in the problem: viz, a_N and a_0 . The factor of $4^{1/4}$ in a is included for convenience only.

¹⁷Our result is not surprising, since MoND has been designed to give the observed flat rotation curves and the Tully-Fisher relation in the first place. Let us also note that actually Milgrom suggested [41] that the generalized Unruh temperature \tilde{T} can give the correct behaviors of the interpolating function between the usual Newtonian acceleration and his suggested MoNDian deformation for very small accelerations. He was right, but he could not offer any justification.

¹⁸To be more precise, $a_c \sim cH/(2\pi)$.

Spacetime foam and cold dark matter with MoND scaling

With only a single parameter (a_c), MoND can explain easily and rather successfully (while the cold dark matter (CDM) paradigm cannot) the observed flat galactic rotation curves^{19 20} and the observed Tully-Fisher relation. But there are problems with MoND at the cluster and cosmological scales, where apparently CDM works much better [43]. This inspires us [36] to ask: Could there be some kind of dark matter that can behave like MoND at the galactic scale?

Let us continue to follow Verlinde’s holographic approach. Invoking the imaginary holographic screen of radius r , we can write²¹ $2\pi k_B \tilde{T} = \frac{G \tilde{M}}{r^2}$, where \tilde{M} represents the *total* mass enclosed within the volume $V = 4\pi r^3/3$. But, as we will show below, consistency with the discussion in the previous section (and with observational data) demands that $\tilde{M} = M + M'$ where M' is some unknown mass — that is, dark matter. Thus, *we need the concept of dark matter for consistency.*

First note that it is natural to write the entropic force $F_{\text{entropic}} = m[(a^2 + a_0^2)^{1/2} - a_0]$ as $F_{\text{entropic}} = m a_N [1 + 2(a_0/a)^2]$ since the latter expression is arguably the simplest interpolating formula²² for F_{entropic} that satisfies the two requirements: $a \approx (4a_N a_0^3)^{1/4}$ in the small acceleration $a \ll a_0$ regime, and $a = a_N$ in the $a \gg a_0$ regime. But we can also write F in another, yet equivalent, form: $F_{\text{entropic}} = mG(M + M')/r^2$. These two forms of F illustrate the idea of CDM-MoND duality.[36] The first form can be interpreted to mean that there is no dark matter, but that the law of gravity is modified, while the second form means that there is dark matter (which, by construction, is consistent with MoND) but that the law of gravity is not modified. The second form gives us this intriguing dark matter profile: $M' = 2(a_0/a)^2 M$. Dark matter of this kind can behave as if there is no dark matter but MoND. Therefore, we call it “MoNDian dark matter”. [36] One can solve for M' as a function of r in the two acceleration regimes: $M' \approx 0$ for $a \gg a_0$, and (with $a_0 \sim \sqrt{\Lambda}$)

$$M' \sim (\sqrt{\Lambda}/G)^{1/2} M^{1/2} r$$

¹⁹Since the galactic dynamics is very complex, it is not surprising that MoND *cannot explain all* of the observed galactic velocity curves.

²⁰For other attempts to explain the rotation curves of galaxies, see, e.g., [42]; but typically they all make use of more than one parameter.

²¹We replace the T and M in Appendix A by \tilde{T} and \tilde{M} respectively.

²²But it is not unique – actually, it may be wrong for the $a \sim a_0$ regime.

for $a \ll a_0$. Intriguingly the dark matter profile we have obtained relates, at the galactic scale,²³ dark matter (M'), dark energy (Λ) and ordinary matter (M) to one another.²⁴ As a side remark, this dark matter profile can be used to recover the observed flat rotation curves and the Tully-Fisher relation.

Spacetime foam and nonlocality

According to the holographic principle, the number of degrees of freedom in a region of space is bounded not by the volume but by the surrounding surface. This suggests that the physical degrees of freedom are not independent but, considered at the Planck scale, they must be infinitely correlated, with the result that the spacetime location of an event may lose its invariant significance. *If we take the point of view that holography has its origin in spacetime foam (as we have argued above), then we can argue that spacetime foam gives rise to nonlocality.* This argument is also supported by the following observation [28] that the long-wavelength (hence “non-local”) “particles” constituting dark energy in HFC obey an exotic statistics which has attributes of nonlocality.

Consider a perfect gas of N particles obeying Boltzmann statistics at temperature T in a volume V . For the problem at hand, as the lowest-order approximation, we can neglect the contributions from matter and radiation to the cosmic energy density for the recent and present eras. Then the Friedmann equations for $\rho \sim H^2/G$ can be solved by $H \propto 1/a$ and $a \propto t$, where $a(t)$ is the cosmic scale factor. Thus let us take $V \sim R_H^3$, $T \sim R_H^{-1}$, and $N \sim (R_H/\ell_P)^2$. A standard calculation (for the relativistic case) yields the partition function $Z_N = (N!)^{-1}(V/\lambda^3)^N$, where $\lambda = (\pi)^{2/3}/T$, and the entropy $S = N[\ln(V/N\lambda^3) + 5/2]$. The important point to note is that, since $V \sim \lambda^3$, the entropy S becomes nonsensically negative unless $N \sim 1$ which is equally nonsensical because $N \sim (R_H/\ell_P)^2 \gg 1$. The solution comes with the observation that the N inside the log term for S somehow must be absent. Then $S \sim N \sim (R_H/\ell_P)^2$ without N being

²³One may wonder why MoND works at the galactic scale, but not at the cluster or cosmic scale. One of reasons is that, for the larger scales, one has to use Einstein’s equations with non-negligible contributions from the pressure and explicitly the cosmological constant, which have not been taken into account in the MoND scheme. [36]

²⁴This requires all the three components to exist (an arguably welcome news to HFC) and it indicates possible interactions among them – something, as observed above, that we may need to alleviate the cosmic coincidence problem and to have a cosmic phase transition from a decelerating to an accelerating expansion at redshift $z \sim 1$. [34]

small (of order 1) and S is non-negative as physically required. That is the case if the “particles” are distinguishable and nonidentical! For in that case, the Gibbs $1/N!$ factor is absent from the partition function Z_N . Now the only known consistent statistics in greater than two space dimensions without the Gibbs factor is infinite statistics (sometimes called “quantum Boltzmann statistics”) [44, 45, 46]. (A short description of infinite statistics is given in Appendix B.) Thus we [28] have shown that the “particles” constituting dark energy obey infinite statistics, instead of the familiar Fermi or Bose statistics.²⁵

But it is known that a theory of particles obeying infinite statistics cannot be local [48, 45]. The expression for the number operator

$$n_i = a_i^\dagger a_i + \sum_k a_k^\dagger a_i^\dagger a_i a_k + \sum_\ell \sum_k a_\ell^\dagger a_k^\dagger a_i^\dagger a_i a_k a_\ell + \dots,$$

is both *nonlocal* and nonpolynomial in the field operators, and so is the Hamiltonian. Altogether, the indication is that nonlocality is yet another facet of spacetime foam.^{26 27}

Discussion

In the above sections, we have discussed several facets of spacetime foam. In this section we will mention one *non*-facet of spacetime foam.

Motivated by the interesting detection of a minimal spread in the arrival times of high energy photons from distant GRB reported by Abdo *et al.* [50] we can consider using the spread in arrival times of photons as a possible technique for detecting spacetime foam. Now, the spread of arrival times can be traced to fluctuations in the distance that the photons have travelled from the distant source to our telescopes. Hence, according to the spacetime foam model parametrized by α , we get

$$\delta t \sim t^{1-\alpha} t_p^\alpha \sim \delta \ell / c$$

for the spread in arrival time of the photons, [51] independent of energy E (or photon wavelength λ). Here $t_p \sim 10^{-44}$ sec is the minuscule Planck time.

²⁵Using the Matrix theory approach, Jejjala, Kavic and Minic [47] have also argued that dark energy quanta obey infinite statistics.

²⁶An interesting question presents itself: Though the nonlocality in holography is probably related to the nonlocality in theories of infinite statistics, how exactly are they related?

²⁷The nonlocal nature of the dynamics of gravitation has been pointed out in other contexts before, see, e.g., [49].

Thus the result is that the time-of-flight differences increase only with the $(1 - \alpha)$ -power of the average overall time of travel $t = \ell/c$ from the gamma ray bursts to our detector, *leading to a time spread too small to be detectable* (except for the uninteresting range of α close to 0.) The new Fermi Gamma-ray Space Telescope results [50] of $\delta t \lesssim 1$ sec for $t \sim 7$ billion years rule out only spacetime foam models with $\alpha \lesssim 0.3$. The holographic model predicts an energy independent dispersion of arrival times $\sim 2.5 \times 10^{-24}$ sec.

Thus we see that, while useful in putting a limit on the variation of the speed of light of a definite sign, this technique is far less useful than the measured angular size in constraining the degree of fuzziness of spacetime in the spacetime foam models. It is easy to understand why that is the case: spacetime foam models predict that the speed of light fluctuates with the fluctuations taking on \pm sign with equal probability; at one instant a particular photon is faster than the average of the other photons, but at the next instant it is slower. The end result is that the cumulative effect due to spacetime foam on the spread in arrival times of photons from distant GRBs is very small (except for spacetime foam models with small α).

Conclusion

Due to the unity of physics, various physical phenomena and structures are inter-related. In this talk I have taken the extreme position of arguing that spacetime foam is the origin of a host of phenomena. For example, the holographic principle finds its roots in spacetime foam physics which also sheds light in explaining why dark energy/dark matter exists. Spacetime foam may explain the observed sizes/magnitudes of the cosmic energy density, the dynamical cosmological constant and the critical galactic acceleration in MoND. It points to the need for cold dark matter with MoND scaling. Possibly spacetime foam is a cause of nonlocal gravitational dynamics. And it has attributes of a turbulent fluid. These are some of the various facets of spacetime foam. Collectively, these facets provide an interesting picture of (and perhaps even some indirect evidence for) it. For completeness, I should add that an *observable* spread in arrival times for (simultaneously emitted) energetic photons from gamma-ray bursts is *not* among the facets of holographic spacetime foam.

Acknowledgments

I owe much of my understanding of the works presented in this talk to many people. They include H. van Dam, M. Arzano, W. Christiansen,

D. Floyd, C.M. Ho, V. Jejjala, T. Kephart, S. Lloyd, D. Minic, D. Pavon, E. Perlman, and C.H. Tze. I thank them all. I thank A. Glindemann for the hospitality extended to me at the Headquarters of the European Southern Observatory where most of this talk was written while I was on research leave supported by Kenan Leave from the University of North Carolina in Fall 2010. I also thank L. Ng for his help in the preparation of this manuscript. This work was also supported in part by the US Department of Energy and by the Bahnson Fund of UNC.

Appendix A: Entropic interpretation of Newton's laws

In this Appendix we review the recent work of E. Verlinde [35] in which the canonical Newton's laws are derived from the point of view of holography. Using the first law of thermodynamics, Verlinde proposes the concept of entropic force $F_{\text{entropic}} = T \Delta S / \Delta x$, where Δx denotes an infinitesimal spatial displacement of a particle with mass m from the heat bath with temperature T . He then invokes Bekenstein's original arguments concerning the entropy S of black holes [24] by imposing $\Delta S = 2\pi k_B m c \Delta x / \hbar$. Using the famous formula for the Unruh temperature, $k_B T = \hbar a / 2\pi c$, associated with a uniformly accelerating (Rindler) observer [37], he obtains

$$F_{\text{entropic}} = T \nabla_x S = ma,$$

Newton's second law (with the vectorial form $\vec{F} = m\vec{a}$, being dictated by the gradient of the entropy).

Next, Verlinde considers an imaginary quasi-local (spherical) holographic screen of area $A = 4\pi r^2$ with temperature T . Then, he assumes the equipartition of energy $E = N k_B T / 2$ with N being the total number of degrees of freedom (bits) on the screen given by $N = A c^3 / G \hbar$. Using the Unruh temperature formula and the fact that $E = M c^2$, he obtains

$$2\pi k_B T = GM / r^2$$

and recovers exactly the non-relativistic Newton's law of gravity, namely $a = GM / r^2$. Note that this is precisely the fundamental relation that Milgrom is proposing to modify so as to fit the galactic rotation curves.

Appendix B: Infinite statistics

What is infinite statistics? Succinctly, a Fock realization of infinite statistics²⁸ is given by the average of the commutation relations of the bosonic and fermionic oscillators

$$a_k a_\ell^\dagger = \delta_{k\ell}.$$

Two states obtained by acting with the N oscillators in different orders are orthogonal. It follows that the states may be in any representation of the permutation group. The statistical mechanics of particles obeying infinite statistics can be obtained in a way similar to Boltzmann statistics, with the crucial difference that the Gibbs $1/N!$ factor is absent for the former. Infinite statistics can be thought of as corresponding to the statistics of identical particles with an infinite number of internal degrees of freedom, which is equivalent to the statistics of nonidentical particles since they are distinguishable by their internal states.

As mentioned in the text, a theory of particles obeying infinite statistics cannot be local [48, 45]. (That is, the fields associated with infinite statistics are not local, neither in the sense that their observables commute at spacelike separation nor in the sense that their observables are pointlike functionals of the fields.) The expression for the number operator is both nonlocal and nonpolynomial in the field operators, and so is the Hamiltonian. The lack of locality may make it difficult to formulate a relativistic version of the theory; but it appears that a non-relativistic theory can be developed. Lacking locality also means that the familiar spin-statistics relation is no longer valid for particles obeying infinite statistics; hence they can have any spin. Remarkably, the TCP theorem and cluster decomposition have been shown to hold despite the lack of locality [45].

References

- [1] E.P. Wigner, *Rev. Mod. Phys.* **29** (1957) 255.
- [2] H. Salecker and E.P. Wigner, *Phys. Rev.* **109** (1958) 571.
- [3] Y.J. Ng and H. van Dam, *Mod. Phys. Lett. A* **9** (1994) 335.
- [4] Y.J. Ng and H. van Dam, *Mod. Phys. Lett. A* **10** (1995) 2801.
- [5] See also F. Karolyhazy, *Il Nuovo Cimento A* **42** (1966) 390; N. Sasakura, *Prog. Theor. Phys.* **102** (1999) 169; A. Frenkel, *Found. Phys.* **20** (1990) 159.
- [6] S. Lloyd and Y.J. Ng, *Scientific American* **291** #5 (2004) 52.
- [7] V. Giovannetti, S. Lloyd, and L. Maccone, *Science* **306** (2004) 1330.
- [8] N. Margolus and L.B. Levitin, *Physica (Amsterdam)* **120** D (1998) 188.

²⁸More generally, infinite statistics is realized by a q deformation of the commutation relations of the oscillators: $a_k a_\ell^\dagger - q a_\ell^\dagger a_k = \delta_{k\ell}$ with q between -1 and 1 (the case $q = \pm 1$ corresponds to bosons or fermions) [45].

- [9] Note the qualification “average”. This result is consistent with X. Calmet, M. Graesser, and S.D. Hsu, *Phys. Rev. Lett.* **93** (2004) 211101.
- [10] For related effects of quantum fluctuations of spacetime geometry, see e.g. L.H. Ford, *Phys. Rev. D* **51** (1995) 1692; B.L. Hu and K. Shiokawa, *Phys. Rev. D* **57** (1998) 3474.
- [11] G. Amelino-Camelia, *Nature* **398** (1999) 216.
- [12] R. Lieu and L.W. Hillman, *Astrophys. J.* **585** (2003) L77.
- [13] Y.J. Ng, W. Christiansen, and H. van Dam, *Astrophys. J.* **591** (2003) L87.
- [14] E.S. Perlman *et al.*, *Astrophys. J.* **124** (2002) 2401.
- [15] W. Christiansen, Y.J. Ng, and H. van Dam, *Phys. Rev. Lett.* **96** (2006) 051301.
- [16] W.A. Christiansen, D. Floyd, Y.J. Ng, and E. Perlman, [arXiv:0912.0535].
- [17] Y.J. Ng, *Mod. Phys. Lett. A* **18** (2003) 1073; Y.J. Ng, *Int. J. Mod. Phys.* **11** (2002) 1585; E. Goklu and C. Lammerzahl, [arXiv:0908.3797].
- [18] J.A. Wheeler in *Relativity, Groups and Topology*, ed. B.S. DeWitt and C.M. DeWitt, (Gordon and Breach, New York, 1963) 315.
- [19] W. Unruh, *Phys. Rev. Lett.* **46** (1981) 1351; *Phys. Rev. D* **51** (1995) 282.
- [20] M. Novello, M. Visser, and G. Volovik, eds., *Artificial black holes*, (World Scientific, Singapore, 2002).
- [21] A.N. Kolmogorov, *Dokl. Akad. Nauk SSSR* **30** (1941) 299.
- [22] V. Jejjala, D. Minic, Y.J. Ng, and C.H. Tze, *Class. Quant. Grav.* **25** (2008) 225012; *Mod. Phys. Lett. A* **25** (2010) 2541; *Int. J. Mod. Phys. D* **19** (2010) 2311.
- [23] G. 't Hooft in *Salamfestschrift*, ed. A. Ali *et al.*, (World Scientific, Singapore, 1993) 284; L. Susskind, *J. Math. Phys. (N.Y.)* **36** (1995) 6377; S.B. Giddings, *Phys. Rev. D* **46** (1992) 1347; R. Bousso, *Rev. Mod. Phys.* **74** (2002) 825.
- [24] J.D. Bekenstein, *Phys. Rev. D* **7** (1973) 2333.
- [25] S.W. Hawking, *Comm. Math. Phys.* **43** (1975) 199.
- [26] Y.J. Ng and H. van Dam, *Found. Phys.* **30** (2000) 795.
- [27] M. Arzano, T.W. Kephart, and Y.J. Ng, *Phys. Lett. B* **649** (2007) 243.
- [28] Y.J. Ng, *Phys. Lett. B* **657** (2007) 10.
- [29] I. Duran and D. Pavon, [arXiv:1012.2986].
- [30] C. Gao, F. Wu, X. Chen, and Y.G. Shen, *Phys. Rev. D* **79** (2009) 043511.
- [31] R.D. Sorkin, *Int. J. Theo. Phys.* **36** (1997) 2759.
- [32] Y.J. Ng and H. van Dam, *Phys. Rev. Lett.* **65** (1990) 1972; J.J. van der Bij, H. van Dam, and Y.J. Ng, *Physica A* **116** (1982) 307; L. Smolin, [arXiv:0904.4841].
- [33] See e.g. A. Berera, I.G. Moss, and R.O. Ramos, [arXiv:0808.1855].
- [34] W. Zimdahl and D. Pavon, [arXiv:0606555(astro-ph)]; D. Pavon and B. Wang, [arXiv:0712.0565]. Also see C. Wetterich, *Nucl. Phys. B* **302** (1988) 668.
- [35] E. Verlinde, [arXiv:1001.0785]; also see T. Jacobson, *Phys. Rev. Lett.* **75** (1995) 1260; T. Padmanabhan, [arXiv:0912.3165]; L. Smolin, [arXiv:1001.3668].
- [36] C.M. Ho, D. Minic, and Y.J. Ng, *Phys. Lett. B* **693** (2010) 567, [arXiv:1005.3537].
- [37] P.C.W. Davies, *J. Phys. A* **8** (1975) 609; W.G. Unruh, *Phys. Rev. D* **14** (1976) 870.
- [38] S. Deser and O. Levin, *Class. Quant. Grav.* **14** (1997) L163; T. Jacobson, *Class. Quant. Grav.* **15** (1998) 251.
- [39] See e.g. M. Milgrom, *Astrophys. J.* **698** (2009) 1630.
- [40] M. Milgrom, *Astrophys. J.* **270** (1983) 365; *ibid.* 371; *ibid.* 384; J.D. Bekenstein, *Phys. Rev. D* **70** (2004) 083509.
- [41] M. Milgrom, *Phys. Lett. A* **253** (1999) 273.

- [42] P.D. Mannheim, [arXiv:1101.2186]; J.W. Moffat, [arXiv:1101.1935].
- [43] For a recent review, see G. Bertone, D. Hooper, and J. Silk, Phys. Rept. **405** (2005) 279, and references therein.
- [44] S. Doplicher, R. Haag, and J. Roberts, Commun. Math. Phys. **23** (1971) 199; *ibid.* **35** (1974) 49; A.B. Govorkov, Theor. Math. Phys. **54** (1983) 234.
- [45] O.W. Greenberg, Phys. Rev. Lett. **64** (1990) 705.
- [46] Also see C. Cao, Y.X. Chen, and J.L. Li, Phys. Rev. D **80** (2009) 125019.
- [47] V. Jejjala, M. Kavic, and D. Minic, [arXiv:0705.4581].
- [48] K. Fredenhagen, Commun. Math. Phys. **79** (1981) 141.
- [49] S.B. Giddings, [arXiv:0705.2197]; G.T. Horowitz, [arXiv:0708.3680].
- [50] A.A. Abdo *et al.*, Nature **462** (2009) 331.
- [51] Y.J. Ng, Entropy **10** (2008) 441, [arXiv:0801.2962].

t & *m*

A short introduction to Asymptotic Safety

ROBERTO PERCACCI^{1*}

¹ *SISSA, via Bonomea 265, I-34136 Trieste, and
 INFN, Sezione di Trieste, Italy*

Abstract: I discuss the notion of asymptotic safety and possible applications to quantum field theories of gravity and matter.

What is asymptotic safety?

We want to discuss the high energy behavior of a quantum field theory (QFT). Assume that a “theory space” has been defined by giving a set of fields, their symmetries and a class of action functionals depending on fields ϕ and couplings g_i . We will write $g_i = k^{d_i} \tilde{g}_i$, where k is a momentum cutoff and d_i is the mass dimension of g_i . The real numbers \tilde{g}_i are taken as coordinates in theory space. Ideally the couplings g_i should be defined in terms of physical observables such as cross sections and decay rates. In any case “redundant” couplings, *i.e.* couplings that can be eliminated by field redefinitions, should not be included. We also assume that a Renormalization Group (RG) flow has been defined on theory space; it describes the dependence of the action on an energy scale k (or perhaps a “RG time” $t = \log k$). The action is assumed to have the form

$$\Gamma_k(\phi, g_i) = \sum_i g_i(k) \mathcal{O}_i(\phi), \quad (1)$$

where \mathcal{O}_i are typically local operators constructed with the field ϕ and its derivatives, which are compatible with the symmetries of the theory. We identify theories with RG trajectories.

It can generically be expected that when k goes to infinity some couplings $g_i(k)$ also go to infinity. What we want to avoid is that the dimensionless couplings \tilde{g}_i diverge. In fact, there are famous examples such as QED and ϕ^4 theory where this happens even at some finite scale k_{\max} . Such

* percacci@sissa.it

divergences signal a breakdown of the theory, and any theory where they occur can only hold for a finite energy range, and is said to be an “effective field theory”. In contrast, suppose that the RG flow admits a fixed point (FP), which is defined as a point \tilde{g}_{i*} where the beta functions of the dimensionless couplings vanish. An RG trajectory which ends (for $k \rightarrow \infty$) at the FP is free of such divergences; it is called a “renormalizable” or “asymptotically safe” (AS) trajectory and represents a UV complete theory [1]. The existence of such a trajectory is therefore a sufficient condition for the theory to be well behaved in the UV.

Now, let us try to count how many such trajectories there are in theory space. We define the “UV critical surface” associated to our FP to be the subset in theory space which is attracted towards it in the UV. Assuming that this surface is a smooth manifold, its dimension is equal to the dimension of its tangent space at the FP. The latter can be computed in the following way. Let $y_i = g_i - g_{i*}$; then in the vicinity of the FP the flow can be linearized:

$$\frac{dy_i}{dt} = M_{ij}y_j, \quad (2)$$

where

$$M_{ij} = \left. \frac{\partial \beta_i}{\partial \tilde{g}_j} \right|_*. \quad (3)$$

By a linear transformation $z_i = S_{ij}y_j$ we pass to coordinates in which M is diagonal. Then the equation becomes

$$\frac{dz_i}{dt} = \lambda_i z_i, \quad (4)$$

where λ_i are the eigenvalues of M . The solutions of this equation are $z_i(t) = e^{\lambda_i t} z_i(0)$, so the coordinates z_i for which $\lambda_i < 0$ are attracted towards the FP; they are called the “relevant” couplings. The coordinates for which $\lambda_i > 0$ are repelled and are called “irrelevant”. If an eigenvalue vanishes the corresponding coordinate is said to be “marginal” and its behavior cannot be determined by the linearized analysis. We will not consider such cases in the following, because they are not generic. The conclusion then is that the dimension of the UV critical surface is equal to the number of negative eigenvalues of M .

The condition of asymptotic safety requires that the theory has to lie in the UV critical surface of the FP. This leaves a number of free parameters that is equal to the dimension of this surface. Thus, the theory is more predictive when the critical surface has lower dimension. The ideal situation would be a theory with a one dimensional critical surface. In this case there would be a single renormalizable trajectory and once we have

determined the initial position at some scale k , the theory is completely determined. At the opposite extreme, if the UV critical surface was infinite dimensional, the theory would not be predictive. The intermediate case is a theory space with finite dimensional critical surface. Such a theory space would have the same good properties of a perturbatively renormalizable and asymptotically free theory, because it would be well behaved in the UV and it would have only a finite number of undetermined parameters.

It is useful to consider the example of the Gaussian FP, which corresponds to a free theory. The beta functions have the form

$$\frac{d\tilde{g}_i}{dt} = -d_i\tilde{g}_i + k^{-d_i}\beta_i. \quad (5)$$

The functions $\beta_i = dg_i/dt$ represent the loop corrections, which vanish at the Gaussian FP. In this case the eigenvalues of the matrix M are given just by the canonical dimensions:

$$\lambda_i = -d_i. \quad (6)$$

The relevant couplings are the ones that are power counting renormalizable, and the critical surface consists of the power counting renormalizable actions. We see that the requirement of asymptotic safety is a generalization of the requirement of asymptotic freedom and renormalizability to the case when the FP does not correspond simply to a free theory. Of course the case of a non-Gaussian FP is harder to study. If it is not too far from the Gaussian FP, one may be able to study it using perturbation theory, but unlike asymptotically free theories, in this case perturbation theory does not get better and better as the energy increases.

Gravity

Gravity is the domain of fundamental physics where the problem of finding a UV completion is most acute, and so it is here that most work on asymptotic safety has concentrated, following the original suggestion of [2]. (For earlier reviews see [3].) I will now show that it is reasonable to expect that there exist asymptotically safe theories of gravity¹.

It is well known that general relativity can be treated as an effective quantum field theory [5, 6]. This means that it is possible to compute quantum effects due to graviton loops, as long as the momenta of the particles in

¹a complementary approach to the one discussed here consists in performing Monte Carlo simulations of discretized gravity. Significant advances have been made in recent years, also lending support to the general idea of nonperturbative renormalizability. See [4] and references therein.

the loops are cut off at some scale. For example, in this way it has been possible to unambiguously compute quantum corrections to the Newtonian potential [7]. The results are independent of the structure of any “ultraviolet completion”, and therefore constitute genuine low energy predictions of any quantum theory of gravity. When one tries to push this effective field theory to energy scales comparable to the Planck scale, or beyond, well-known difficulties appear. It is convenient to distinguish two orders of problems. The first is that the strength of the gravitational coupling grows without bound. For a particle with energy p the effective strength of the gravitational coupling is measured by the dimensionless number $\sqrt{\tilde{G}}$, with $\tilde{G} = Gp^2$. This is because the gravitational couplings involve derivatives of the metric. The consequence of this is that if we let $p \rightarrow \infty$, also \tilde{G} grows without bound. The second problem is the need of introducing new counterterms at each order of perturbation theory. Since each counterterm has to be fixed by an experiment, the ability of the theory to predict the outcome of experiments is severely limited.

As we have seen in the previous section, the first problem could be fixed if \tilde{G} had a FP. In order to see whether this is reasonable, imagine evaluating the beta function using perturbation theory at one loop. The coefficient² of the Hilbert action is the square of Planck’s mass, $M_{\text{pl}}^2 = 1/16\pi G$. In the quantum theory it is expected to diverge quadratically with the cutoff, leading to a beta function of the form

$$k \frac{d}{dk} M_{\text{pl}}^2 = ck^2, \quad (7)$$

where c is some constant. Then, the beta function of G has the form

$$k \frac{dG}{dk} = -16\pi c G^2 k^2$$

and the beta function of \tilde{G} is

$$k \frac{d\tilde{G}}{dk} = 2\tilde{G} - 16\pi c \tilde{G}^2. \quad (8)$$

This beta function has an IR attractive fixed point at $\tilde{G} = 0$ and also an UV attractive nontrivial fixed point at $\tilde{G}_* = 1/8\pi c$. In order to establish whether $c > 0$ one has to do a calculation. The dependence of G on distance has been computed at one loop in the low energy effective field theory [8], leading to

$$16\pi c = \frac{167}{15\pi}.$$

²we choose units such that $c = 1$ and $\hbar = 1$. Then everything has dimension of a power of mass.

This has the desired positive sign, but it is not a particularly memorable number: it depends on details of the way in which it is computed. Fortunately, one can show that for any reasonable cutoff it will always have the same sign, so if one loop perturbation theory is a good guide, \tilde{G} would indeed cease to grow at high energy and settle at some constant value of order one.

Of course such a value of \tilde{G} is quite large and it is not really clear that near this FP perturbation theory can be trusted. Furthermore, it is also known [9] that loop effects will induce terms with higher derivatives. So the next thing one could do is calculate the one loop beta functions in a theory containing four derivative terms, with an action of the general form

$$\int d^4x \sqrt{g} \left[2Z\Lambda - ZR + \frac{1}{2\lambda}C^2 + \frac{1}{\xi}R^2 + \frac{1}{\rho}E \right], \quad (9)$$

where C^2 is the square of the Weyl tensor, E the integrand of the Euler term,

$$Z = \frac{1}{16\pi G}; \quad \frac{1}{\xi} = -\frac{\omega}{3\lambda}; \quad \frac{1}{\rho} = \frac{\theta}{\lambda}.$$

Such calculations have a long history [10]. They were mostly based on dimensional regularization. More recently, we have repeated this calculation using a mass-dependent heat kernel regularization procedure [11]. The beta functions of the four-derivative terms are

$$\begin{aligned} \beta_\lambda &= -\frac{1}{(4\pi)^2} \frac{133}{10} \lambda^2; \\ \beta_\xi &= -\frac{1}{(4\pi)^2} \left(10\lambda^2 - 5\lambda\xi + \frac{5}{36} \right); \\ \beta_\rho &= \frac{1}{(4\pi)^2} \frac{196}{45} \rho^2 \lambda. \end{aligned}$$

We see that the overall coupling λ is asymptotically free:

$$\lambda(k) = \frac{\lambda_0}{1 + \lambda_0 \frac{1}{(4\pi)^2} \frac{133}{10} \log\left(\frac{k}{k_0}\right)}, \quad (10)$$

whereas the ω and θ , which define the ratio of ξ and ρ to λ tend to the asymptotic limits $\omega(k) \rightarrow \omega_* \approx -0.0228$ and $\theta(k) \rightarrow \theta_* \approx 0.327$. On the other hand, the cosmological constant and Newton's constant have the

beta functions

$$\beta_{\tilde{\Lambda}} = -2\tilde{\Lambda} + \frac{1}{(4\pi)^2} \left[\frac{1 + 20\omega^2}{256\pi\tilde{G}\omega^2} \lambda^2 + \frac{1 + 86\omega + 40\omega^2}{12\omega} \lambda \tilde{\Lambda} \right] - \frac{1 + 10\omega^2}{64\pi^2\omega} \lambda + \frac{2\tilde{G}}{\pi} - q(\omega)\tilde{G}\tilde{\Lambda}, \quad (11)$$

$$\beta_{\tilde{G}} = 2\tilde{G} - \frac{1}{(4\pi)^2} \frac{3 + 26\omega - 40\omega^2}{12\omega} \lambda \tilde{G} - q(\omega)\tilde{G}^2, \quad (12)$$

where $q(\omega) = (83 + 70\omega + 8\omega^2)/18\pi$. The first few terms in these expressions agree with [10], but the last three terms of $\beta_{\tilde{\Lambda}}$ and the last term of $\beta_{\tilde{G}}$ are new. The flow in the invariant subspace $\lambda = 0, \omega = \omega_*, \theta = \theta_*$ is

$$\beta_{\tilde{\Lambda}} = -2\tilde{\Lambda} + \frac{2\tilde{G}}{\pi} - q_*\tilde{G}\tilde{\Lambda}, \quad (13)$$

$$\beta_{\tilde{G}} = 2\tilde{G} - q_*\tilde{G}^2, \quad (14)$$

where $q_* = q(\omega_*) \approx 1.440$. This flow admits a FP with

$$\tilde{\Lambda}_* = \frac{1}{\pi q_*} \approx 0.221, \quad \tilde{G}_* = \frac{2}{q_*} \approx 1.389.$$

It is quite striking that in spite of the very different structure of the theory, the beta function of Newton's constant is very similar to the one we found in Einstein's theory. Again, the FP for \tilde{G} occurs at some value of order one. Nevertheless, it has been argued in [12] that since λ , the true coupling constant in this theory, is asymptotically free, this result is reliable.

These calculations highlight the importance of using a mass dependent cutoff scheme: had we used dimensional regularization, we would not see the nontrivial FP. This is because dimensional regularization misses information about the power divergences. It is therefore not a convenient method to study the beta functions of dimensionful couplings.

In fact, even with dimensional regularization there is a somewhat roundabout way to see the effect of power divergences: they appear as logarithmic divergences in other dimensions. One can therefore recover this information by performing a dimensional continuation. In two dimensions G is dimensionless and its beta function can be extracted at one loop from the pole of a counterterm. It is $-38G^2/3$ [13]. Then, one can perform the so-called ϵ expansion, by studying the beta function as a function of the dimension d . For $d = 2 + \epsilon$, G has dimension ϵ , so $\tilde{G} = Gk^\epsilon$. The first term in the ϵ expansion gives

$$\beta_{\tilde{G}} = \epsilon\tilde{G} - \frac{38}{3}\tilde{G}^2, \quad (15)$$

so we recover the existence of a nontrivial FP in dimension $d > 2$. If we let $\epsilon = 2$ the FP occurs again at some positive value \tilde{G} . This was historically the first hint of asymptotic safety [2].

Both the one loop and the ϵ expansion give a FP which occurs in a regime where the approximation is not clearly reliable. It is for this reason that much of the recent work has been done using (some approximation to) an Exact RG Equation (ERGE), which has been first applied to gravity in [14, 15]. Without entering into details, suffice it to say that one can define a k -dependent effective action Γ_k by introducing an IR cutoff k in the functional integral, and that this functional obeys the equation

$$k \frac{d\Gamma_k}{dk} = \frac{1}{2} \text{Tr} \left[\frac{\delta^2 \Gamma_k}{\delta \phi \delta \phi} + R_k \right]^{-1} k \frac{dR_k}{dk}. \quad (16)$$

If Γ_k has the form (1),

$$k \frac{d\Gamma_k}{dk} = \sum_i \beta_i \mathcal{O}_i(\phi). \quad (17)$$

Therefore, expanding the r.h.s. of (16) on the basis of operators \mathcal{O}_i one can read off the beta functions of the individual couplings g_i . This method has several advantages: (i) it works in any dimension, (ii) there is no need to introduce UV regulators, since the r.h.s. of (16) is finite, and (iii) it does not depend on the couplings being small. Of course, it is generally impossible to compute the beta functions of infinitely many couplings and so one has to truncate the sum to finitely many terms. For example, if we keep only the first two terms in (9) we find, for a cutoff of type ‘‘Ib’’ [20]:

$$\beta_{\tilde{\Lambda}} = \frac{-2(1 - 2\tilde{\Lambda})^2 \tilde{\Lambda} + \frac{36 - 41\tilde{\Lambda} + 42\tilde{\Lambda}^2 - 600\tilde{\Lambda}^3}{72\pi} \tilde{G} + \frac{467 - 572\tilde{\Lambda}}{288\pi^2} \tilde{G}^2}{(1 - 2\tilde{\Lambda})^2 - \frac{29 - 9\tilde{\Lambda}}{72\pi} \tilde{G}},$$

$$\beta_{\tilde{G}} = \frac{2(1 - 2\tilde{\Lambda})^2 \tilde{G} - \frac{373 - 654\tilde{\Lambda} + 600\tilde{\Lambda}^2}{72\pi} \tilde{G}^2}{(1 - 2\tilde{\Lambda})^2 - \frac{29 - 9\tilde{\Lambda}}{72\pi} \tilde{G}}.$$

One can still glean the one loop result, which is obtained by neglecting Λ and setting the denominators to one. There has been a number of independent calculations, using different cutoffs and different gauges, and treating the ghosts in different ways, which give slightly different numbers but agree on the qualitative structure of the result [16, 17, 18, 19, 20, 21]. This method has been applied also to four-derivative gravity in [22], where a nontrivial FP with nonzero values for all the couplings is found.

In another direction, it has been possible to work out the beta functions for truncations of the form

$$\Gamma_k = \sum_{i=0}^n g_i \int d^4x \sqrt{g} R^i. \quad (18)$$

The case $n = 2$ was first examined in [23], while in [24, 25] the calculation was pushed up to $n = 8$. The results of these calculations can be summarized by the following tables, which give the position of the FP and the eigenvalues λ_i as functions of n .

Position of Fixed Point ($\times 10^{-3}$)

n	\tilde{g}_{0*}	\tilde{g}_{1*}	\tilde{g}_{2*}	\tilde{g}_{3*}	\tilde{g}_{4*}	\tilde{g}_{5*}	\tilde{g}_{6*}	\tilde{g}_{7*}	\tilde{g}_{8*}
1	5.23	-20.1							
2	3.29	-12.7	1.51						
3	5.18	-19.6	0.70	-9.7					
4	5.06	-20.6	0.27	-11.0	-8.65				
5	5.07	-20.5	0.27	-9.7	-8.03	-3.35			
6	5.05	-20.8	0.14	-10.2	-9.57	-3.59	2.46		
7	5.04	-20.8	0.03	-9.78	-10.5	-6.05	3.42	5.91	
8	5.07	-20.7	0.09	-8.58	-8.93	-6.81	1.17	6.20	4.70

Eigenvalues of linearized flow

n	$\text{Re } \lambda_1$	$\text{Im } \lambda_1$	λ_2	λ_3	$\text{Re } \lambda_4$	$\text{Im } \lambda_4$	λ_6	λ_7	λ_8
1	-2.38	-2.17							
2	-1.38	-2.32	-26.9						
3	-2.71	-2.27	-2.07	4.23					
4	-2.86	-2.45	-1.55	3.91	5.22				
5	-2.53	-2.69	-1.78	4.36	3.76	4.88			
6	-2.41	-2.42	-1.50	4.11	4.42	5.98	8.58		
7	-2.51	-2.44	-1.24	3.97	4.57	4.93	7.57	11.1	
8	-2.41	-2.54	-1.40	4.17	3.52	5.15	7.46	10.2	12.3

From these numbers one can draw several conclusions. First of all the FP exists for all truncations and secondly is relatively stable, in the sense that adding new terms to the truncations generally does not change very much the results of the lower truncation. Third, there are three negative eigenvalues, showing that the critical surface is three dimensional. In fact, knowing the eigenvectors of the matrix M , one can write explicitly the linearized

equation of this surface. Using g_0 , g_1 and g_2 as independent parameters,

$$\begin{aligned}\tilde{g}_3 &= 0.00061243 + 0.06817374 \tilde{g}_0 + 0.46351960 \tilde{g}_1 + 0.89500872 \tilde{g}_2 \\ \tilde{g}_4 &= -0.00916502 - 0.83651466 \tilde{g}_0 - 0.20894019 \tilde{g}_1 + 1.62075130 \tilde{g}_2 \\ \tilde{g}_5 &= -0.01569175 - 1.23487788 \tilde{g}_0 - 0.72544946 \tilde{g}_1 + 1.01749695 \tilde{g}_2 \\ \tilde{g}_6 &= -0.01271954 - 0.62264827 \tilde{g}_0 - 0.82401181 \tilde{g}_1 - 0.64680416 \tilde{g}_2 \\ \tilde{g}_7 &= -0.00083040 + 0.81387198 \tilde{g}_0 - 0.14843134 \tilde{g}_1 - 2.01811163 \tilde{g}_2 \\ \tilde{g}_8 &= 0.00905830 + 1.25429854 \tilde{g}_0 + 0.50854002 \tilde{g}_1 - 1.90116584 \tilde{g}_2\end{aligned}$$

This illustrates the predictivity of asymptotically safe theories: once the three parameters g_0 , g_1 and g_2 have been measured at some scale by means of three experiments, everything else is determined and any further experiment is a test of the theory. Of course, the specific results of this calculation should not be taken too seriously: there are many important things that have been neglected here.

Matter

However hard it may be to prove the asymptotic safety of gravity, it would still not be enough: for applications to the real world one will have to show that a (possibly unified [26]) theory of all interactions is asymptotically safe. The strong interactions are already described by an asymptotically safe theory, and there are reasons to believe that this result is not ruined by the coupling to gravity [27]. The electroweak and Higgs sectors of the standard model are perturbatively renormalizable, but some of their beta functions are positive. This means that either new weakly coupled degrees of freedom manifest themselves at some scale, before the couplings blow up, or else the theory is consistent, but in a nonperturbative sense. The simplest realization of the latter behavior is AS. If the world is described by an AS theory, there are two main possibilities: one is that AS is an inherently gravitational phenomenon, in which case AS would manifest itself at the Planck scale³; the other is that each interaction reaches the FP at its characteristic energy scale.

In the first case, one has to compute the effect of gravity on matter couplings and the effect of matter on the gravitational couplings. The effect of gravity on scalar couplings has been considered in [29, 30, 31], on gauge couplings in [32] and on Yukawa couplings in [33]. One possibility is that

³this includes the possibility that due to the presence of large extra dimensions the effective Planck mass is much lower than 10^{19} GeV. I refer to [28] for an analysis of this scenario.

the coupling to gravity makes all matter interactions asymptotically free, as conjectured long ago by Fradkin and Tseytlin [34]. There is some evidence that this can happen in some cases, with gravity preventing the Landau pole of scalar theory and QED [30, 32]. In this case the second part of the job, namely computing the effect of matter on gravity couplings, would be much simplified, because in order to establish the existence of a FP it would be enough to consider minimally coupled matter fields. This problem has been studied in [35], where it was found that the existence of a FP with desirable properties puts restrictions on the number of matter fields of each spin. In fact, for a large number of matter fields, the task is even simplified, and to leading order in a $1/N$ expansion one can prove the existence of a gravitational FP to all orders of the derivative expansion [36]. Things are more complicated if matter remains interacting also in the UV limit. One particularly striking possibility has been pointed out recently [38]: QED coupled to gravity seems to have two nontrivial FPs, in addition to the Gaussian one: at one gravity is interacting but QED is free, at the other they are both interacting. The latter has a lower dimensional critical surface and is therefore more predictive: on a renormalizable trajectory ending at this FP, the low energy value of the fine structure constant can in principle be calculated.

In the second case, matter and gravity would be separately AS. Then, one would have to prove that electroweak theory somehow heals itself of its UV problems. At the moment, there are two approaches to this idea: the first, motivated by the formal analogies between gravity and the nonlinear sigma models, is that a Higgsless version of the standard model could be AS. Some partial calculations support this view [39]. It has been shown recently that this possibility is compatible with electroweak precision data [40]. See also [41] for comments. The other possibility is that a suitably balanced theory of coupled scalars and fermions with potential and Yukawa couplings exhibits AS [42]. In both cases the Higgs VEV, which is the source of the masses of all pointlike particles, would run linearly above some scale, restoring scale invariance. This would affect the physics of the Higgs, which is being explored at LHC, making this by far the most exciting possibility from the point of view of possible experimental signatures.

Cosmology and time

It is generally expected that a quantum theory of gravity should be able to solve the puzzles that remain open in classical general relativity, for example the fate of spacetime near a singularity. Furthermore, a scale dependence of couplings (such as Newton's constant or the cosmological

constant) may well have an effect on the cosmological evolution, even at relatively late stages. For these reasons, cosmology, and especially very early cosmology, is probably the most promising domain of application of asymptotically safe gravity.

The most popular way of applying the RG to cosmology consists in identifying the cutoff scale k with some characteristic cosmological parameter (usually the Hubble scale $H(t) = \dot{a}(t)/a(t)$) and then replacing the constant gravitational couplings ($G, \Lambda \dots$) by their scale-dependent counterparts, making the gravitational couplings effectively time-dependent [43]. This substitution can be done in a solution, in the equations of motion or directly in the action, with different results. Consider for example the effect of "RG-improving" Einstein's equations [44]:

$$G_{\mu\nu} = 8\pi G(k)T_{\mu\nu} - \Lambda(k)g_{\mu\nu} . \quad (19)$$

For simplicity we assume a spatially flat Friedmann-Robertson-Walker metric with scale factor $a(t)$ and an energy momentum tensor in the form of a perfect fluid $T^\mu_\nu = \text{diag}(-\rho, p, p, p)$ with equation of state $p(\rho) = w\rho$. Both $G_{\mu\nu}$ and $R_{\mu\nu}$ can be expressed in terms of the Hubble rate:

$$R_{tt} = -3(\dot{H} + H^2) , \quad R = R^\mu{}_\mu = 6(\dot{H} + 2H^2) , \quad G_{tt} = 3H^2 ,$$

so that the (tt) -component and the trace of Einstein's equations become

$$3H^2 = 8\pi G\rho + \Lambda , \quad (20)$$

$$6(\dot{H} + 2H^2) = 8\pi G\rho(1 - 3w) + 4\Lambda . \quad (21)$$

Choose the cutoff $k = \zeta H$, for some real number ζ of order one. Then Newton's constant and the cosmological constant become functions of time: $G = G(\zeta H)$, $\Lambda = \Lambda(\zeta H)$, whose form is fixed by the renormalization group equations. To simplify, let us assume that we are at sufficiently high k such that we may assume that the (dimensionless) couplings \tilde{G} and $\tilde{\Lambda}$ are at their fixed point values. Then $G = \tilde{G}_*/(\zeta^2 H^2)$ and $\Lambda = \tilde{\Lambda}_* \zeta^2 H^2$. One then looks for inflationary de Sitter solutions

$$a(t) = a_0 e^{Ht} ; \quad H = \text{constant} , \quad (22)$$

or power law solutions

$$a(t) = a_0 t^p ; \quad H = \frac{p}{t} . \quad (23)$$

The equations admit power law solutions with

$$p = \frac{2}{(3 - \tilde{\Lambda}_* \zeta^2)(1 + w)} . \quad (24)$$

Let us set $w = 1/3$, as appropriate for ultrarelativistic matter. We see that for $1/2 < \tilde{\Lambda}_* \tilde{\zeta}^2/3 < 1$ the solution has inflationary character ($p > 1$), with the acceleration becoming stronger as $\tilde{\Lambda}_* \tilde{\zeta}^2/3$ increases. For $\tilde{\Lambda}_* \tilde{\zeta}^2/3 = 1$ (and any $w > -1$) the exponent diverges. We observe that this condition is equivalent to the equation $R = 4\Lambda$ written in the FP regime; the corresponding solution is a de Sitter universe. Similar conclusions have been shown to hold also for the fixed point of $f(R)$ gravity [45], and first steps towards a calculation of the spectrum of fluctuations have been made in [46]. A general qualitative analysis of the cosmological dynamics in the presence of running couplings has been given recently in [47].

This approach raises several issues. One is that inflation is supposed to occur at energies considerably lower than the Planck scale, so that the approximation of being close to the fixed point may actually not be warranted [48]. Another issue is the exit from inflation. Presumably this would happen when the RG trajectory departs from the immediate neighborhood of the fixed point, but a detailed study has not been done so far. Perhaps more worrisome is the nonconservation of the matter energy-momentum tensor. From Friedmann's equations one obtains a modified conservation equation

$$\dot{\rho} + 3H(\rho + p) = -\frac{1}{8\pi G}(\dot{\Lambda} + 8\pi\rho\dot{G})$$

We see that the time variation of the couplings, which follows from the time dependence of the cutoff, gives rise to nonconservation of the energy. One may try to interpret this in terms of the energy and momentum of the field modes that have been removed from the system by coarse graining. Bonanno and Reuter actually turn this into a positive feature [44]: they show that, under reasonable assumptions, the energy transferred to the matter system through the decay of the cosmological constant over the age of the universe is of the correct order of magnitude to explain the entropy of the cosmic background radiation.

In order to avoid these issues, Weinberg follows a different approach [49]. He writes the Friedmann equations following from the most general effective action that is local in curvatures and covariant derivatives of curvatures, and looks for de Sitter solutions. He argues that a choice of cutoff of the order of H may be a reasonable compromise between the conflicting requirements of avoiding large radiative corrections to the field equations, and the Einstein-Hilbert truncation being a reasonable approximation. In this approach the exit from inflation should be signalled by an instability of the solution. Unfortunately explicit calculations based on known properties of the fixed point of pure gravity seem to show too much instability, leading to a number of e -foldings that is too small.

Aside from these attempts to apply asymptotic safety to inflationary cosmology, one may try to make connection also to other ideas. One important fact is that physics at a fixed point is scale invariant⁴. Even though the fixed point Lagrangian contains dimensionful couplings, these scale with energy according to their canonical dimension so that all observable quantities have power law dependences. Under these circumstances, defining a clock becomes impossible even in principle and the notion of time loses its operational meaning [50]. Although one may still be able to define separate points, time intervals and distances become meaningless. In this sense, one may argue that a fixed point leads to a notion of minimal distance [51]. This is also in line with the view that the metric geometry “melts down” near the big bang, but the conformal geometry remains well defined. In fact it is worth noting that if the infrared behavior of gravity was also governed by a fixed point, as conjectured in [52], then one would have scale invariance at both ends of the cosmological evolution. This would lend support to Penrose’s Conformal Cyclic Cosmology [53].

Discussion, summary and prospects

I have presented some evidence that a theory of gravity and perhaps of all interactions is AS. None of the calculations performed so far can be said to be a proof, but the qualitative agreement of the results in all the approximations makes this by now a rather plausible scenario. If this was true, we would have an UV complete theory remaining within the familiar domain of QFT. It is important to appreciate the differences between this and other popular approaches to quantum gravity.

AS is a “bottom up” approach to quantum gravity: the discussion starts within the theory space of an effective field theory, and goes on to note that if the world corresponds to a trajectory of a special type, then the effective description can be pushed to arbitrarily high energy. An AS theory is simply the continuation of an effective theory to higher energy scales. As a result, an AS theory has the great advantage that if it exists, it is almost automatically in agreement with our knowledge of the low energy world. This is in contrast to string theory and loop quantum gravity, which are “top down” approaches. For them, making a connection with known low energy phenomenology is proving a very hard issue.

There is obviously a price to pay for this. On one hand, in a nonperturbative context it is hard to obtain reliable results and hard proofs. Further-

⁴due to the complex critical exponents, one may only have invariance under a discrete subgroup of scale transformations.

more, the action of the FP theory seems to contain infinitely many terms with nonzero couplings, making it unwieldy at best. It is in principle possible that the description of the fixed point could be simplified by a suitable change of variables (perhaps along the lines of [54]). Then, the AS QFT may turn out to be equivalent to one of the top down theories. In that case it would be enough to establish the equivalence in the vicinity of the Planck scale. From there downwards, one would just follow the RG as in any effective field theory.

This remark applies also to the scenario of “emergent gravity”. According to a popular point of view, gravity is not a fundamental interaction but rather the effective description of some underlying microscopic dynamics that may have little to do with the geometry [55, 56, 57]. It is often said that in this case attempts at formulating a quantum theory of gravity in terms of metric degrees of freedom are misplaced. As discussed in [58], even if gravity at very high energies was described by some as yet unknown theory with non-metric degrees of freedom, from some energy scale downwards it can be described by an effective theory of the metric, and in this effective theory couplings will run according to the RG as discussed above. At sufficiently low energy we would therefore be again in the theory space discussed in section 2. If there is a FP in this theory space, then the RG trajectory that describes emergent gravity will approach its UV critical surface at low energies, so that even in this case the notion of AS would prove to be a useful tool.

References

- [1] K.G. Wilson and J.B. Kogut, Phys. Rept. **12** (1974) 75; K.G. Wilson, Rev. Mod. Phys. **47** (1975) 773; S. Weinberg, *Critical Phenomena For Field Theorists*, Lectures presented at Int. School of Subnuclear Physics, Ettore Majorana, Erice, Sicily, Jul 23 – Aug 8, 1976.
- [2] S. Weinberg, in *General Relativity: An Einstein centenary survey*, ed. S.W. Hawking and W. Israel, 790–831, Cambridge University Press (1979).
- [3] M. Niedermaier and M. Reuter, Living Rev. Relativity **9** (2006) 5; M. Niedermaier, Class. Quant. Grav. **24** (2007) R171, [arXiv:gr-qc/0610018]; R. Percacci, in *Approaches to Quantum Gravity*, ed. D. Oriti, Cambridge University Press (2009), [arXiv:0709.3851(hep-th)]; D.F. Litim, PoS (QG-Ph) 024, [arXiv:0810.3675(hep-th)].
- [4] J. Ambjorn, J. Jurkiewicz, and R. Loll, Phys. Rev. D **72** (2005) 064014, [arXiv:hep-th/0505154].
- [5] C.P. Burgess, Living Rev. in Rel. **7** (2004) 5.
- [6] D. Espriu and D. Puigdomenech, Acta Phys. Polon. B **40** (2009) 3409-3437, [arXiv:0910.4110(hep-th)].

- [7] J.F. Donoghue, Phys. Rev. Lett. **72** (1994) 2996, [arXiv:gr-qc/9310024]; Phys. Rev. D **50** (1994) 3874, [arXiv:gr-qc/9405057]; I.B. Khriplovich and G.G. Kirilin, J. Exp. Theor. Phys. **95** (2002) 981, [arXiv:gr-qc/0207118].
- [8] N.E.J. Bjerrum-Bohr, J.F. Donoghue, and B.R. Holstein, Phys. Rev. D **67** (2003) 084033; Erratum *ibid.* **71** (2005) 069903, [arXiv:hep-th/0211072].
- [9] G. 't Hooft and M.J.G. Veltman, Ann. Inst. Poincare Phys. Theor. A **20** (1974) 69.
- [10] I.G. Avramidi and A.O. Barvinski, Phys. Lett. B **159** (1985) 269.
- [11] A. Codello and R. Percacci, Phys. Rev. Lett. **97** (2006) 221301, [arXiv:hep-th/0607128].
- [12] M.R. Niedermaier, Phys. Rev. Lett. **103** (2009) 101303; Nucl. Phys. B **833** (2010) 226-270.
- [13] H. Kawai and M. Ninomiya, Nucl. Phys. B **336** (1990) 115.
- [14] M. Reuter, Phys. Rev. D **57** (1998) 971, [arXiv:hep-th/9605030].
- [15] D. Dou and R. Percacci, Class. Quant. Grav. **15** (1998) 3449, [arXiv:hep-th/9707239].
- [16] W. Souma, Prog. Theor. Phys. **102** (1999) 181, [arXiv:hep-th/9907027].
- [17] O. Lauscher and M. Reuter, Phys. Rev. D **65** (2002) 025013, [arXiv:hep-th/0108040]; Phys. Rev. D **66** (2002) 025026, [arXiv:hep-th/0205062]; Class. Quant. Grav. **19** (2002) 483, [arXiv:hep-th/0110021]; Int. J. Mod. Phys. A **17** (2002) 993, [arXiv:hep-th/0112089].
- [18] M. Reuter and F. Saueressig, Phys. Rev. D **65** (2002) 065016, [arXiv:hep-th/0110054].
- [19] D. Litim, Phys. Rev. D **64** (2001) 105007, [arXiv:hep-th/0103195]; Phys. Rev. Lett. **92** (2004) 201301, [arXiv:hep-th/0312114]. P. Fischer and D.F. Litim, Phys. Lett. B **638** (2006) 497, [arXiv:hep-th/0602203].
- [20] A. Codello, R. Percacci, and C. Rahmede, Ann. Phys. **324** (2009) 44, [arXiv:0805.2909(hep-th)].
- [21] A. Eichhorn, H. Gies, and M. Scherer, Phys. Rev. D **80** (2009) 104003, [arXiv:0907.1828(hep-th)].
- [22] D. Benedetti, P.F. Machado, and F. Saueressig, Mod. Phys. Lett. A **24** (2009) 2233, [arXiv:0901.2984(hep-th)].
- [23] O. Lauscher and M. Reuter, Phys. Rev. D **65** (2002) 025013, [arXiv:hep-th/0108040].
- [24] A. Codello, R. Percacci, and C. Rahmede, Int. J. Mod. Phys. A **23** (2008) 143, [arXiv:0705.1769(hep-th)].
- [25] P.F. Machado and F. Saueressig, Phys. Rev. D **77** (2008) 124045, [arXiv:0712.0445(hep-th)].
- [26] R. Percacci, Phys. Lett. B **144** (1984) 37-40; Nucl. Phys. B **353** (1991) 271-290; F. Nesti and R. Percacci, J. Phys. A **41** (2008) 075405; Phys. Rev. D **81** (2010) 025010.
- [27] S. Folkerts, D. Litim, and J. Pawłowski, [arXiv:1101.5552(hep-th)].
- [28] J.A. Hewett, T. Rizzo, JHEP **0712** 009, [arXiv:0707.3182(hep-ph)]; D. Litim and T. Plehn, Phys. Rev. Lett. **100** (2008) 131301, [arXiv:0707.3983(hep-ph)]; [arXiv:1101.5548(hep-ph)].
- [29] L. Griguolo and R. Percacci, Phys. Rev. D **52** (1995) 5787, [arXiv:hep-th/9504092].
- [30] R. Percacci and D. Perini, Phys. Rev. D **68** (2003) 044018,

- [arXiv:hep-th/0304222].
- [31] G. Narain and R. Percacci, *Class. Quant. Grav.* **27** (2010) 075001, [arXiv:0911.0386(hep-th)]; G. Narain and C. Rahmede, *Class. Quant. Grav.* **27** (2010) 075002, [arXiv:0911.0394(hep-th)].
- [32] S.P. Robinson and F. Wilczek *Phys. Rev. Lett.* **96** (2006) 231601, [arXiv:hep-th/0509050]; A.R. Pietrykowski, *Phys. Rev. Lett.* **98** (2007) 061801, [arXiv:hep-th/0606208]; D.J. Toms *Phys. Rev. D* **76** (2007) 045015, [arXiv:0708.2990(hep-th)]; D. Ebert, J. Plefka, and A. Rodigast, *Phys. Lett. B* **660** (2008) 579; D.J. Toms, *Phys. Rev. Lett.* **101** (2008) 131301. J.E. Daum, U. Harst, and M. Reuter, *JHEP* **1001** (2010) 084, [arXiv:0910.4938(hep-th)].
- [33] O. Zanusso, L. Zambelli, G.P. Vacca, and R. Percacci, *Phys. Lett. B* **689** (2010) 90-94, [arXiv:0904.0938(hep-th)]; G.P. Vacca and O. Zanusso, *Phys. Rev. Lett.* **105** (2010) 231601, [arXiv:1009.1735(hep-th)].
- [34] E.S. Fradkin and A.A. Tseytlin, *Nucl. Phys. B* **201** (1982) 469.
- [35] R. Percacci and D. Perini, *Phys. Rev. D* **67** (2003) 081503, [arXiv:hep-th/0207033].
- [36] R. Percacci, *Phys. Rev. D* **73** (2006) 041501, [arXiv:hep-th/0511177].
- [37] D. Benedetti, P.F. Machado, and F. Saueressig, *Nucl. Phys. B* **824** (2010) 168, [arXiv:0902.4630(hep-th)].
- [38] U. Harst and M. Reuter, [arXiv:1101.6007(hep-th)].
- [39] A. Codello and R. Percacci, *Phys. Lett. B* **672** (2009) 280-283, [arXiv:0810.0715(hep-th)]; R. Percacci and O. Zanusso, *Phys. Rev. D* **81** (2010) 065012, [arXiv:0910.0851(hep-th)]; M. Fabbrichesi, R. Percacci, A. Tonero, and O. Zanusso *Phys. Rev. D* **83** (2011) 025016, [arXiv:1010.0912(hep-ph)].
- [40] M. Fabbrichesi, R. Percacci, A. Tonero, and L. Vecchi, [arXiv:1102.2113(hep-ph)].
- [41] R. Percacci, PoS (CLAQG08) 002, [arXiv:0910.4951(hep-th)]; X. Calmet, [arXiv:1008.3780(hep-ph)]; [arXiv:1012.5529(hep-ph)].
- [42] H. Gies and M.M. Scherer, *Eur. Phys. J. C* **66** (2010) 387-402, [arXiv:0901.2459(hep-th)]; H. Gies, S. Rechenberger, and M.M. Scherer, *Eur. Phys. J. C* **66** (2010) 403-418, [arXiv:0907.0327(hep-th)].
- [43] R. Floreanini and R. Percacci, *Phys. Lett. B* **356** (1995) 205; A. Babic, B. Guberina, R. Horvat, and H. Štefančić, *Phys. Rev. D* **65** (2002) 085002; F. Bauer, J. Solà, H. Štefančić, *Phys. Lett. B* **678** (2009) 427; F. Bauer, *Class. Quant. Grav.* **27** (2010) 055001.
- [44] A. Bonanno and M. Reuter, *JCAP* **0708** 024, [arXiv:0706.0174(hep-th)].
- [45] A. Bonanno, A. Contillo, and R. Percacci, [arXiv:1006.0192(gr-qc)].
- [46] A. Bonanno and M. Reuter, *Int. J. Mod. Phys. D* **13** (2004) 107-122, [arXiv:astro-ph/0210472]; A. Contillo, [arXiv:1011.4618(gr-qc)].
- [47] M. Hindmarsh, D. Litim, and C. Rahmede, [arXiv:1101.5401(gr-qc)].
- [48] S.H. Tye and J. Xu, *Phys. Rev. D* **82** (2010) 127302, [arXiv:1008.4787(hep-th)].
- [49] S. Weinberg, *Phys. Rev. D* **81** (2010) 083535, [arXiv:0911.3165(hep-th)].
- [50] S.E. Rugh and H. Zinkernagel, [arXiv:0805.1947(gr-qc)].
- [51] R. Percacci and D. Perini, *Class. and Quantum Grav.* **21** (2004) 5035, [arXiv:hep-th/0401071]; R. Percacci, *J. Phys. A* **40** (2007) 4895-4914, [arXiv:hep-th/0409199]; M. Reuter and J.M. Schwindt, *JHEP* **0601** (2006) 070, [arXiv:hep-th/0511021]; X. Calmet, S. Hossenfelder, and R. Percacci, *Phys. Rev. D* **82** (2010) 124024, [arXiv:1008.3345(gr-qc)].
- [52] E. Bentivegna, A. Bonanno, and M. Reuter, *JCAP* **0401** (2004) 001,

- [arXiv:astro-ph/0303150].
- [53] R. Penrose, Proceedings of EPAC 2006, 2759-2767.
- [54] K. Krasnov, Phys. Rev. **D 81** (2010) 084026, [arXiv:0911.4903(hep-th)].
- [55] A.D. Sakharov, Sov. Phys. Dokl. **12** (1968) 1040-1041; Dokl. Akad. Nauk Ser. Fiz. **177** (1967) 70-71; Sov. Phys. Usp. **34** (1991) 394;
S.L. Adler, Rev. Mod. Phys. **54** (1982) 729, Erratum *ibid.* **55** (1983) 837.
- [56] K. Akama, Lect. Notes Phys. **176** (1982) 267-271, [arXiv:hep-th/0001113].
- [57] T. Jacobson, Phys. Rev. Lett. **75** (1995) 1260; T. Padmanabhan, Class. Quantum Grav. **19** (2002) 5387; E. Verlinde, [arXiv:1001.0785(hep-th)]; C. Barcelo, S. Liberati, and M. Visser, Living Rev. Rel. **8** (2005) 12, [arXiv:gr-qc/0505065].
- [58] R. Percacci and G.P. Vacca, Class. and Quantum Grav. **27** (2010) 245026, [arXiv:1008.3621(hep-th)].

t & *m*

Singular Homogeneous Plane-Waves, Matrix Big-Bangs and their non-Abelian Theories

LORENZO SERI¹

¹ S.I.S.S.A. Scuola Internazionale Superiore di Studi Avanzati,
Via Bonomea 265, I-34134 Trieste, Italy

Abstract: The Hawking-Penrose theorems tell us that any reasonable cosmological model has to be singular. A theory of gravity that accounted for quantum effects in principle should be able to explain the physics of such singularities; in this spirit we discuss a generalisation of the so called Matrix Big-Bang, where our “string theory” is built over some special non-trivially singular backgrounds, the Singular Homogeneous Plane-Waves.

More precisely we will present what the Infinite Momentum Frame is, in order to sketch how the Matrix Theory is obtained from the general M-theory. Then we will discuss the concept of Penrose Limit and we will explain how the Singular Homogeneous Plane-Waves are related to a very large class of backgrounds. Having introduced in this way all the fundamental ingredients, we will write down the action of our theory and we will discuss its behaviour both near the singularity and for time growing infinitely large, when the ordinary flat-space physics is expected to be recovered. What we are to study is a non-Abelian theory with time-dependent coupling and it will be shown that near the singularity the quartic interaction becomes negligible (both at classical and quantum mechanical level) while for late times the emergence of the flat-space physics needs to be understood better.

Introduction

Hawking and Penrose [1] proved that under some general assumptions any cosmological solution of the Einstein equations shows a singularity. We do not spell out the formulation of these theorems; instead we are interested in explaining precisely what a singularity is. For doing this we give the following definition:

Definition A space-time is said to be *geodesically complete* if every geodesic can be extended to arbitrary values of its affine parameter.

By *singular* space-time, we mean a space-time that is not geodesically complete (taking into account only time-like and light-like geodesics). Intuitively, one would like to define a singularity as a point in which some fundamental observable (like the scalar curvature, the energy-momentum tensor, etc..) diverges or cannot be defined: this is impossible, though, because the space-time itself is defined as a solution of the Einstein equation and includes only the points where such equations make sense. Loosely speaking, the singularity is then defined as a “hole” in the space-time manifold: we become aware of its presence because a free-falling object describing the incomplete geodesics will end its existence within a finite proper time. In order to be rigorous we have to restrict our discussion to *inextendible* manifolds, as we do not want to include amongst physical singularities the ones obtained by simply removing a point; moreover we should appeal to some more general kind of completeness, as there are physical trajectories that are not geodesics (see [2]) and that can as well be used for detecting some “hole” in the structure of the space-time.

Now that we have overviewed what a singularity is we come back to the question raised by Hawking and Penrose. Any cosmological solution that General Relativity can provide us with is singular, so what? One simple-minded (and highly unsatisfactory for a physicist) answer would be to look at the cosmological singularity as at an impenetrable wall, the true origin of time, beyond which no physical evolution can be defined. On the other hand, it seems by far more reasonable to assume that General Relativity fails to describe the physics of singularities, and that some new theory is needed: in particular, if String Theory is really a good theory for quantum gravity, it should also provide us with some insights on cosmological singularities. One of the first attempts in this direction was made in [3, 4, 5]: the authors tried to generalize some well-known result about String Theory on time-independent singular spaces to similar spaces with a cosmological singularity. Besides other technical problems, this approach has the drawback that the background is almost everywhere flat and so not very well suited for serving as a realistic cosmological model. Later on Craps, Sethi and Verlinde [6] proposed their “Matrix Big Bang”: technically it consists in the generalization of the Seiberg-Sen formulation of Matrix Theory ([7], [8]) to a IIA background given by a flat space-time and a dilaton field linear in time. Even this solution is essentially flat, but Blau and O’Loughlin proved that the CSV procedure can be further generalized [9], using as background a class of non-trivially curved space-times, the Singular Homogeneous Plane-Waves (SHPWs). All in all, such a generalization of the Seiberg-Sen procedure to the SHPWs bring us to the study of a non-Abelian gauge theory with time-dependent coupling: this model

should retain the basic features of the evolution from the singularity to late times, where one expects to recover the usual flat space-time physics (see [10]).

A thorough presentation of this model would require a large amount of technical detail: it would be necessary to introduce several concepts of String and M-theory, we would need to describe the many properties of SHPWs, and we should eventually spell out in detail how matrix theory is built on these very special backgrounds. As this talk is intended for a wide audience and we do not want to take anything for granted, we are going to focus on the following three aspects:

- we will explain simply what the Discrete Light-Cone Quantization is, in order to motivate the Seiberg-Sen procedure;
- we will discuss in what sense we claim that the SHPWs represent a general class of singularities;
- finally we will present our non-Abelian model, exploiting its most relevant features.

The interested reader can find all the missing details in the references that we provide.

Infinite Momentum Frame and Discrete Light-Cone Quantization

The main point of this section is to explain how in a certain limit the DLCQ manages to select from a complicated theory a single sector, providing its exact description. In order to do so we first present the Infinite Momentum Frame, a useful tool of parton physics, that actually inspired the DLCQ procedure.

Let us assume that we have a bunch of particles with a very large collective momentum in a certain direction, as they are observed in the lab frame: performing the proper boost we will observe a perfectly random distribution of momenta amongst the particles, but in the lab frame these differences are totally negligible with respect to the collective momentum. Labelling the particles with a we define the collective longitudinal momentum as¹

$$P_{\parallel} = \sum_a |(p_a)_{\parallel}| \quad (1)$$

¹What we call P_{\parallel} is not exactly the total momentum along the longitudinal direction, but with our assumptions the difference is negligible.

and compactifying that longitudinal direction as a circle of radius R_s we will have a discretized $P_{\parallel} = N/R_s$. Now if we send N to infinity we will have $m_a \ll |(p_a)_{\parallel}|$, so that we can expand the energy,

$$E = \sum_a \sqrt{(p_a)_{\parallel}^2 + (p_a)_{\perp}^2 + m_a^2} = P_{\parallel} + \sum_a \frac{(p_a)_{\perp}^2 + m_a^2}{2|(p_a)_{\parallel}|}. \quad (2)$$

In the limit $N \rightarrow \infty$ the system become Galilean, with $|(p_a)_{\parallel}|$ playing the rôle of masses. In [11] it is explained how in this frame a set of Feynman rules can be defined, making use of the fact that some sectors of the theory decouple in this limit.

Choosing a light-like time we can define a similar procedure: say that x^+ is our time and we compactify x^- , so that $P_- = \sum_a (p_a)_- = N/R_s^2$. In this case the energy is *exactly* of the form

$$H_{lc} = P_+ = \sum_a \frac{(p_a)_{\perp}^2 + m_a^2}{2(p_a)_-} \quad (3)$$

so for every fixed N we have a system with Galilean symmetry. As P_- is conserved the Hilbert space decomposes into superselection sectors labeled by N ; moreover in order to have a non-negative Hamiltonian it is necessary that $(p_a)_- > 0$, so modes with negative p_- are automatically decoupled. Obviously the other sectors are not necessarily decoupled from each other: this depends on the particular theory under discussion and its interactions.

Seiberg [7] and Sen [8] applied this formalism to Matrix Theory in the case of a flat background. In String Theory (and Matrix Theory as well) in addition to strings there are present other $p + 1$ -dimensional objects, called Dp -branes: they may be thought of as p -dimensional surfaces that under evolution describe a $p + 1$ -dimensional “world-volume”. Taking N coincident D-branes, one obtains a non-Abelian gauge theory on the “world-volume”, while the transverse directions become $N \times N$ matrices: only when these matrices are commuting, one recovers the usual description of the space-time.

Seiberg and Sen proved using DLCQ that *in the limit* $N \rightarrow \infty$ a sector given by N $D0$ -branes is singled out from the complete Matrix Theory; as mentioned before, Craps, Sethi and Verlinde [6] and Blau and O’Loughlin [9] generalized such result to particular time-dependent backgrounds. We are now going to focus on the background chosen in [9] and then we will discuss the non-Abelian time-dependent theory so obtained.

²We notice that this is exactly the total momentum along the x^- direction, so it is conserved.

Singular Homogeneous Plane-Waves and Szekeres-Iyer metrics

The background to which we will apply our DLCQ procedure is

$$\begin{cases} ds^2 = -dx^+ dx^- + A_{ab}(x^+) x^a x^b (dx^+)^2 + \delta_{ab} dx^a dx^b, \\ e^{2\phi} = (x^+)^{\frac{3b}{b+1}}, \quad b \neq -1, \end{cases} \quad (4)$$

where

$$A_{ab}(x^+) = \frac{m_a(m_a - 1)}{x^{+2}} \delta_{ab} \quad (5)$$

and $\sum_a m_a(m_a - 1) = -3b/(b + 1)$. This is a solution to type IIA supergravity in ten dimensions and ϕ is the dilaton field.

We are mainly concerned with explaining the way in which the metric in (4) (Singular Homogeneous Plane-Wave) is related to a very large class of singular space-times. This relation implies that the results found for the SHPWs have some implications for the case of more general singularities, even though the state of the art is such that it is too early to formulate any precise conjecture in this sense.

Let us to point out some properties of the metric in (4). This plane-wave possesses two important features:

- it is singular in $x^+ = 0$;
- it is invariant under the scaling $(x^+, x^-, x^a) \rightarrow (\gamma x^+, \gamma^{-1} x^-, x^a)$; this isometry, together with the ones possessed by any plane-wave, makes the metric homogeneous³.

In particular, it is this very isometry that enables one to implement the Seiberg-Sen procedure on these backgrounds [9].

We need now to present the concept of *Penrose limit*, as introduced by Roger Penrose in [13]. This limiting procedure can be carried out by following three steps:

1. Given a metric $g_{\mu\nu}$, choose a null geodesic $\gamma(U)$ and embed it in a twist-free congruence of null geodesics: basically one sees the space-time as foliated in copies of the chosen geodesic and defines a coordinate system where V is light-like and the Y^i 's are space-like,

$$\begin{aligned} ds^2 = dUdV + a(U, V, Y^k) dV^2 + 2b_i(U, V, Y^k) dY^i dV + \\ + g_{ij}(U, V, Y^k) dY^i dY^j, \end{aligned} \quad (6)$$

³This is obviously intended away from eventual fixed points of the isometries

and any curve identified by fixing V and the Y^i 's is a geodesic of the congruence.

2. Redefine again the coordinates as

$$(U, V, Y^k) = (u, \lambda^2 v, \lambda y^k). \quad (7)$$

This corresponds to operate a boost $(U, V, Y^k) \rightarrow (\lambda^{-1}U, \lambda V, Y^k)$ followed by the rescaling $(U, V, Y^k) \rightarrow (\lambda U, \lambda V, \lambda Y^k)$. We will call ds_γ^2 the metric written in these new coordinates.

3. Compute the “limit metric”

$$d\bar{s}^2 = \lim_{\lambda \rightarrow 0} \lambda^{-2} ds_\gamma^2 = 2 dudv + \bar{g}_{ij}(u) dy^i dy^j \quad (8)$$

that turns out to be a plane wave.

In order to give some physical meaning to this procedure, we quote here Penrose himself [13]:

“We envisage a succession of observers travelling in the space-time whose world lines approach the null geodesic $\gamma(U)$ more and more closely; so we picture these observers as travelling with greater and greater speeds, approaching that of light. As their speeds increase they must correspondingly recalibrate their clocks to run faster and faster (assuming that all space-time measurements are referred to clock measurements in the standard way), so that in the limit the clocks measure the affine parameter U along γ . (Without clock recalibration a degenerate space-time metric would result.) In the limit the observers measure the space-time to have the plane wave structure.”

Let us focus on a particular class of singularities, the Szekeres and Iyer metrics:

$$ds^2 = -[x(U, V)]^r dUdV + [x(U, V)]^s d\Omega_d^2 \quad (9)$$

where $x(U, V) = 0$ identifies the singularity surface. In this class are included many relevant singular solutions for General Relativity, as the Friedmann-Robertson-Walker cosmological model and the Schwarzschild back hole; this can be easily seen by choosing the appropriate values for s and r and making explicit what $x(U, V)$ is in these special cases (see [12] for examples).

Applying the Penrose limit to the space-like singularities of the Szekeres-Iyer family one finds that if $s < r + 2$ the plane-wave obtained is a singular homogeneous one; this is represented in the left plot of the figure below, where the light shaded region corresponds to SHPWs. Nevertheless, the condition $s < r + 2$ does not sound physically meaningful:

why should we restrict ourselves to that particular half of the rs -plane? The answer to this question has been given in [12]: if we require the *Dominant Energy Condition* to be fulfilled, the only region allowed in the rs -plane is the blue triangle drawn in the right plot.

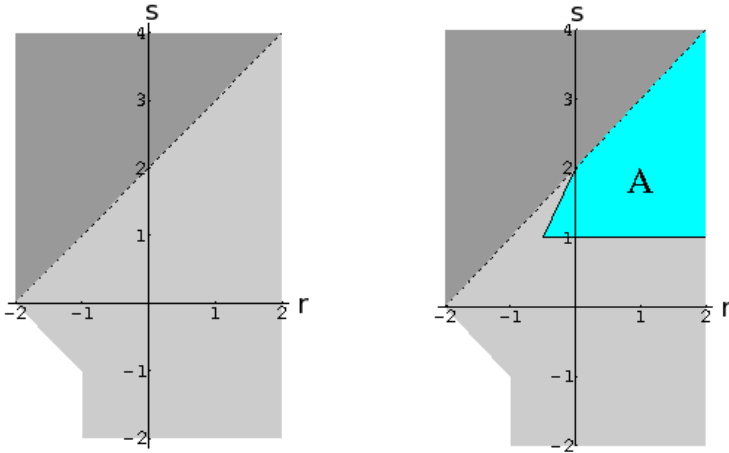


Figure 1: Taken from [12].

The Dominant Energy Condition may be stated as follows:

Definition Calling $T^{\mu\nu}$ the stress-energy tensor, for every future directed time-like vector v^μ the vector $-T^\mu_\nu v^\nu$ is a future directed time-like vector.

This requirement can be loosely restated as saying that the speed of the energy flow of matter is always less than the speed of light: all the Szekeres-Iyer metrics that satisfy such (natural) assumption have a SHPW as Penrose limit. With a complete understanding of the quantum physics of SHPWs one could in principle try to go backwards, “inverting the limit”, thus saying something about more general singularities. As said before, it is much too early for such an attempt, as we do not yet have a thorough comprehension of these special “matrix Big-Bangs”, but we consider the connection between SHPWs and Szekeres-Iyer metrics as a strong motivation for pursuing this line of research.

The non-Abelian Gauge Theory of our matrix Big-Bang

Now that we have sketched what DLCQ is and we have motivated our interest in SHPWs, we discuss our actual theory. As stated before, we want to apply the Seiberg-Sen procedure to the background (4)

$$\begin{cases} ds^2 = -dx^+ dx^- + A_{ab}(x^+) x^a x^b (dx^+)^2 + \delta_{ab} dx^a dx^b \\ e^{2\phi} = (x^+)^{\frac{3b}{b+1}}, \quad b \neq -1. \end{cases} \quad (10)$$

For completeness sake let us say that A_{ab} and the dilatonic field are related because this IIA 10-d solution is obtained by dimensionally reducing an 11-d background (that is actually a SHPW!). All the steps for building the Matrix theory for this background may be found in [9]; we simply present here the final action

$$\begin{aligned} S_{BC} = \int d^2\sigma \text{Tr} \left(-\frac{1}{4} g_{YM}^{-2} \eta^{\alpha\gamma} \eta^{\beta\delta} F_{\alpha\beta} F_{\gamma\delta} - \frac{1}{2} \eta^{\alpha\beta} \delta_{ab} D_\alpha X^a D_\beta X^b + \right. \\ \left. + \frac{1}{4} g_{YM}^2 \delta_{ac} \delta_{bd} [X^a, X^b][X^c, X^d] + \frac{1}{2} A_{ab}(\tau) X^a X^b \right) \end{aligned} \quad (11)$$

where $\tau = x^+$, $g_{YM} \sim e^{-\phi}$ and the X s are *matrix coordinates*.

We want to focus on the case of *strong coupling singularities*, namely when the coupling of the String Theory diverges as the singularity is approached: the string coupling and the dilaton field are related by $g_s \sim e^\phi$, so strong coupling corresponds to requiring $-1 < b < 0$. Notice that in our non-Abelian theory the A_{ab} matrix contains the masses of the coordinate fields X and so one easily deduces that $-1 < b < 0$ implies that some of the X s must be tachyonic (see again [9]).

We said that $g_{YM} \sim e^{-\phi}$; as we chose to study strong string coupling singularities we find that approaching $\tau = 0$, $g_{YM} \rightarrow 0$, while $g_{YM} \rightarrow \infty$ as $\tau \rightarrow \infty$. In our action we have a g_{YM}^2 prefactor in front of the quartic interaction and it is thus reasonable to expect that at late times the coordinate fields choose a commuting configuration in order to compensate the divergence of g_{YM} , while for small times they are free to not commute. Moreover, as the X s are matrix fields, only when they are commuting is it possible to interpret them as coordinates of the ordinary space-time, and it is exactly the ordinary flat space-time that we presume to find away from the singularity (see also[14]): so all in all this picture looks tantalizing, suggesting that near the singularity the space-time is not commuting and that extra degrees of freedom (the off-diagonal elements of the X s) are turned on.

In [10] we wanted to test this picture, reducing the complete Lagrangian to a more manageable toy model. This is achieved by performing the following steps:

1. we compactify on a world-sheet circle of radius L ;
2. we restrict ourselves to two transverse directions (represented by two $\text{su}(2)$ matrices);
3. we pick a Fourier mode for each direction.

The resulting Lagrangian is

$$S = \frac{1}{2} \int dt \text{Tr} \left(|\dot{X}|^2 + |\dot{Y}|^2 - \omega_X(t)^2 |X|^2 - \omega_Y(t)^2 |Y|^2 + \lambda |t|^{2q} |[X, Y]^2 \right) \quad (12)$$

where

$$\omega_{X,Y}(t)^2 = \frac{n_Y^2}{2\pi L} + \frac{n_X^2}{2\pi L} - \frac{p(p+2)}{4t^2}. \quad (13)$$

Basically, we study a system made up of two harmonic oscillators with time-dependent frequency and a quartic coupling; actually as $t \rightarrow 0$ $\omega_{X,Y}(t)^2$ becomes negative and we are in the presence of two *inverted* harmonic oscillators⁴. We work with p and q unrelated, even if q is in our case a simple function of p , because this slight generalization makes our model relevant for other problems discussed in literature [15].

We studied the evolution of this system both classically and quantum mechanically, in both the limits $t \rightarrow 0$ and $t \rightarrow \infty$. In the following we summarize our results.

Classical and quantum analysis for $t \rightarrow 0$

We start from the classical analysis. In [10] we used both a perturbative approach and a numerical one: the result is that near the singularity the coordinates are non-commuting and the degrees of freedom are actually N^2 , but the quartic interaction is subleading and as $t \rightarrow 0$ the evolution is definitely that of N^2 decoupled inverted harmonic oscillators. Such result holds for any value of p and q . This is illustrated in the Figure 2.

At a quantum level we treated again the problem perturbatively, and we found that the quartic interaction is subleading as long as $2q - 2p > -1$ (the case of SHPWs satisfies this condition). We adopted also a numerical

⁴Due to the fact that the X s are tachyonic.

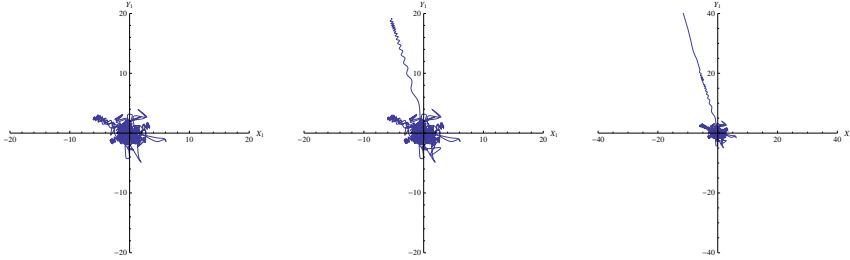


Figure 2: Numerical integration of toy model projected in the X_1, Y_1 plane for $t_i = -100$ and $t_f = -10, -1$ and -0.001 , respectively.

approach, studying the spreading of wave packets initially located near the origin as $t \rightarrow 0$: *their evolution is slow enough that they don't feel the minimum due to the quartic interaction.* Indeed, if the spreading of the packets is small respect to the distance between the minimum and the origin, the evolution is not affected by the presence of the minimum for any values of p and q .

Classical analysis for $t \rightarrow \infty$

We redefine our time and coordinates as

$$X = t^{-\frac{q}{3}}W, \quad Y = t^{-\frac{q}{3}}Z, \quad T \sim t^{\frac{2}{3}q+1} \quad (14)$$

so that

$$S = \frac{1}{2} \int dT \operatorname{Tr} \left(\left| \frac{dW}{dT} \right|^2 + \left| \frac{dZ}{dT} \right|^2 - m^2(|W|^2 + |Z|^2)T^{-4q/(2q+3)} \right. \\ \left. - \left(\frac{4}{3}q(2q+3) - p(p+2) \right) \frac{(|W|^2 + |Z|^2)}{4T^2} - \lambda|[W, Z]|^2 \right) \quad (15)$$

In these new coordinates it is apparent that as $t \rightarrow \infty$ the evolution is driven by a quartic interaction with *time-independent* coupling, so it does not appear likely that the coordinates fall definitely into a commuting configuration. In fact the numerical simulations give results like those in Figure 3

We observed that as t grows larger and larger the coordinates spend progressively more time in a commuting configuration, but the particular configuration is chosen (time by time) in a completely chaotic fashion.

Quantum mechanically the situation is very involved, as one has to deal with both quantum and chaotic effects. This notwithstanding, the La-

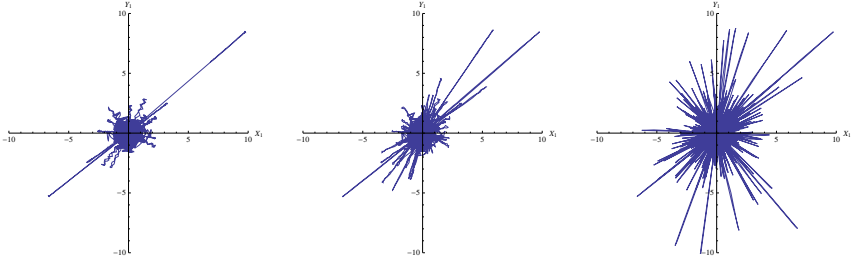


Figure 3: Numerical integration of toy model projected in the X_1, Y_1 plane for $t_i = 100$ and $t_f = 500, 1000$ and 5000 , respectively.

grangian of our system is similar to those studied in the context of quantum chaos [16, 17, 18] and in those cases it is found that the wave function does not remain in one single commuting configuration, but it fragments itself between all possible ones (and these obviously do not mutually commute). Obviously this issue needs to be explored further, as we expect to recover the ordinary flat space-time physics away from the singularity (namely to observe the coordinates settling into a commuting configuration).

Conclusions

In this talk we presented a possible approach to the physics of cosmological singularities in the context of String Theory. We sketched what DLCQ is, we motivated our interest in SHPWs, and we presented a toy model that should retain the main features of our Matrix Big-Bang. We showed that the quartic interaction is negligible near the singularity and thus for the study of the near singularity physics it is enough to take into account the quadratic Lagrangian. On the other hand, we showed that the emergence of the flat-space physics away from the singularity is not automatic, and further study is required. We are currently working in both these directions.

Acknowledgments

I would like to thank the organizers for inviting me to this meeting: it was a great occasion for sharing ideas and making new acquaintances, and especially for learning what is going on in fields different from my own. The location was also extraordinarily beautiful!

References

- [1] S.W. Hawking and R. Penrose, *The Singularities of gravitational collapse and cosmology* Proc. Roy. Soc. Lond. A **314** (1970) 529-548.
- [2] R. Geroch, *What is a singularity in general relativity?*, *Annals of Physics* **48** (1968) 526-540.
- [3] Lorenzo Cornalba and Miguel S. Costa, *A new cosmological scenario in string theory*, *Phys. Rev. D* **66** (2002) 066001.
- [4] Hong Liu, Gregory W. Moore, and Nathan Seiberg, *Strings in a time-dependent orbifold*, *JHEP* **06** (2002) 045.
- [5] Hong Liu, Gregory W. Moore, and Nathan Seiberg, *Strings in time-dependent orbifolds*, *JHEP* **10** (2002) 031.
- [6] Ben Craps, Savdeep Sethi, and Erik P. Verlinde. *A Matrix Big Bang*, *JHEP* **10** (2005) 005.
- [7] Nathan Seiberg, *Why is the matrix model correct?*, *Phys. Rev. Lett.* **79** (1997) 3577-3580.
- [8] Ashoke Sen, *D0 branes on $T(n)$ and matrix theory*, *Adv. Theor. Math. Phys.* **2** (1998) 51-59.
- [9] Matthias Blau and Martin O'Loughlin, *DLCQ and Plane Wave Matrix Big Bang Models*, *JHEP* **09** (2008) 097.
- [10] Martin O'Loughlin and Lorenzo Seri, *The non-Abelian gauge theory of matrix big bangs*, *JHEP* **07** (2010) 036.
- [11] Steven Weinberg, *Dynamics at infinite momentum*, *Phys. Rev.* **150** (1966) 1313-1318.
- [12] Matthias Blau, Monica Borunda, Martin O'Loughlin, and George Papadopoulos, *The universality of Penrose limits near space-time singularities*, *JHEP* **07** (2004) 068.
- [13] Roger Penrose, in *Differential geometry and relativity*, (Reidel, Dordrecht, 1976) 217.
- [14] Ben Craps, *Big bang models in string theory*. *Class. Quant. Grav.* **23** (2006) S849-S881.
- [15] Adel Awad, Sumit R. Das, Suresh Nampuri, K. Narayan, and Sandip P. Trivedi, *Gauge Theories with Time Dependent Couplings and their Cosmological Duals*, *Phys. Rev. D* **79** (2009) 046004.
- [16] B. K. Berger, *Quantum Chaos in the Mixmaster Universe*, *Phys. Rev. D* **39** (1989) 2426-2429.
- [17] T. Furusawa, *Quantum Chaos of Mixmaster Universe*, *Prog. Theor. Phys.* **75** (1986) 59.
- [18] T. Furusawa, *Quantum Chaos of Mixmaster Universe 2*, *Prog. Theor. Phys.* **76** (1986) 67.

t & *m*

Cosmic time with quantum matter?

S.E. RUGH¹ AND H. ZINKERNAGEL^{2*}

¹ *Symposion, 'The Socrates Spirit', Section for Philosophy and the Foundations of Physics, Hellebækgade 27, Copenhagen N, Denmark*

² *Department of Philosophy I, Granada University, 18071 Granada, Spain*

Abstract: In the two papers cited below, we examine the necessary physical underpinnings for setting up the cosmological standard model with a global cosmic time parameter. In particular, we discuss the role of Weyl's principle which roughly asserts that it is possible to set up a comoving reference frame based on an expanding 'substratum' of world lines of galaxies (or 'fundamental particles') which form a spacetime-filling family of non-intersecting geodesics. Although the Weyl principle is often not mentioned explicitly in modern texts on cosmology, it is implicitly assumed and is, we argue, necessary for a physically well-defined notion of cosmic time.

Insofar as the Weyl principle is necessary for the notion of cosmic time in the cosmological standard model, it becomes important to examine whether the properties and motion of matter are compatible with the Weyl principle as we go back in cosmic time. If a point is reached at which this is not the case, then it appears not to be physically justified to contemplate 'earlier' epochs. Doing so would involve extrapolating the standard model in cosmology into a domain where the fundamental assumptions (needed to build up the model) are no longer valid and the model would lose its physical basis. We discuss two important problems:

- Above the electroweak phase transition (before 10^{-11} seconds 'after' the big bang), all constituents are massless and move with velocity c in any reference frame. There will thus be no constituents which are comoving (at rest) and the Weyl principle is not satisfied for any typical particle although one may attempt to introduce fictitious averaging volumes in order to create as-close-as-possible substitutes for "fundamental particles which are at rest" (in a comoving frame). This procedure requires, however, that length scales are available. As discussed in [1], the only option for specifying such length scales, and

* zink@ugr.es

thus for having a cosmic time, above the electroweak phase transition will be to appeal to speculations beyond current well-established physics.

- It is widely assumed that matter in the very ‘early’ phase of the universe can be described exclusively in terms of quantum theory. However, under this assumption there may not be a well-defined notion of particle trajectories (let alone non-crossing particle trajectories) in which case it is difficult to even formulate the Weyl principle (let alone decide whether it is satisfied). In that situation, no cosmic time can be defined and it thus seems difficult to maintain the ‘quantum fundamentalist’ view of an early quantum epoch of the universe [2].

As a mathematical study, the FLRW model may be extrapolated back arbitrarily close to $t = 0$. But as a physical model nobody believes it ‘before’ the Planck time. As mentioned above, however, there are interesting problems with establishing a physical basis for the FLRW model with a cosmic time, even before (in a backward extrapolation from now) we might reach an ‘epoch’ in which theories of quantum gravity may come into play.

References

- [1] S.E. Rugh and H. Zinkernagel, *On the physical basis of cosmic time*, Studies in History and Philosophy of Modern Physics **40** (2009) 1.
- [2] S.E. Rugh and H. Zinkernagel, *Weyl’s principle, cosmic time and quantum fundamentalism*, ed. D. Dieks *et al.* Explanation, Prediction and Confirmation, The Philosophy of Science in a European Perspective series, Springer (2011) 411.

t & *m*

Epistemic and ontic interpretation of quantum mechanics: Quantum information theory and Husserl's phenomenology

T. BILBAN^{1*}

¹ *Institute for Quantum Optics and Quantum Information, Boltzmannngasse 3,
1080 Vienna, Austria*

Abstract: Since the beginning of quantum mechanical description there have been two approaches to its interpretation, the ontic and the epistemic approach. Up to today the approaches have remained unconnected, which is one of the main reasons for the lack of a common, complete interpretation of quantum mechanics. A possibility for exceeding this ontic/epistemic opposition can be offered by quantum information theory, which is essentially based on the epistemic approach, however when connected with Husserl's phenomenology also offers a basis for an epistemic-ontic interpretation. In Zeilinger-Brukner's quantum information theory, Kant's understanding of the relationship between the phenomenon and the "thing-in-itself" has been used as a model for understanding of the relationship between information and the observed. If it is replaced by Husserl's understanding of the relationship between the two, information and the observed can be understood as causally connected – information represents the direct answer to the question about the observed, while the basis for this information is the observed itself. This kind of approach offers the firm answer how to exceed solipsism and gain the common objectivity of quantum mechanical description, without introducing any further realism or loosing any explanatory power of quantum information theory: furthermore, the relationship between the observer, the observed and the observation can be now more thoroughly understood.

Introduction

The opposite between Einstein's and Bohr's approach towards quantum mechanics has been often described as the opposite between an epistemic and an ontic approach. Bohr's approach has emphasized the epistemic

* tina.bilban@univie.ac.at

point of view, otherwise overlooked in physics, while Einstein saw the classical point of view, labeled as scientific realism and apriori excluding the role of the observer, as the only appropriate stand point for physics. The lack of insight that they are approaching the problem from two different philosophical stand points, rather than understanding the same phenomena in the same context in different ways could be one of the main reasons for the lack of connection of their views: "Both Einstein and Bohr did not clearly realize that they addressed different concepts of reality, since they never made their basic viewpoints explicit. Both Bohr's operationalistic and Einstein's ontological concept of reality have their proper places in the study of matter. Both are legitimate and even necessary, but they must not be confused with each other." [1]

On the one hand Bohr's approach had the advantage of originating directly from the experiments and their most direct interpretation, without considering traditional notions about real and existing, and thus became the basis for physical interpretations of quantum mechanics. On the other hand more or less all ontic approaches (e.g. many worlds, hidden variables) originated from the opposition to the epistemic interpretations (most often gathered under the name Copenhagen interpretation) and not from its continuation or complementarity. For example the description of the hidden variable theory and its contribution to understanding of quantum reality in Bohm's and Hiley's book *An Ontological Interpretation of Quantum Theory* emphasizes the lack of ontology in the Copenhagen interpretation. However, they do not try to supplement it, but offer another, ontic instead of epistemic, interpretation: "Or to put it in more philosophical terms, it may be said that quantum theory is primarily directed towards epistemology which is the study that focuses on the question of how we obtain our knowledge [...], it does not give what can be called an ontology for a quantum system. Ontology is concerned primarily with that which is and only secondarily with how we obtain our knowledge about this." [2]

Both approaches stay unconnected within (more or less) all current interpretations, although their difference does not mean they are opposing each other, on the contrary – a complete interpretation should certainly consider both of them. According to Atmanspacher and Primas: "Drawing the distinction between epistemic and ontic descriptions does not imply, though, that the two categories are unrelated to each other. On the contrary, the crucial point is about the relationship between the two frameworks rather than the selection of one at the expense of the other." [1]

An interesting possibility for exceeding this everlasting opposition can be offered by the quantum information theory. Quantum information theory is essentially based on the epistemic approach, but at the same time,

because of its connection with philosophical tradition, offers a possibility for a connection with Husserl's phenomenological approach and therewith a possible basis for an epistemic-ontic interpretation of quantum mechanics.

Epistemic interpretation of quantum mechanics – quantum information theory

Quantum information theory is essentially connected with Bohr's epistemic approach towards physical phenomena, which can be seen in the frequency of citations of the following reported to be Bohr's quotation: "There is no quantum world. There is only an abstract quantum physical description. It is wrong to think that the task of physics is to find out how nature is. Physics concerns what we can say about nature." [3] Quantum information theory is thus based on the hypothesis that "quantum physics is only indirectly a science of reality but more immediately a science of knowledge." [4]

An important connection between the Copenhagen interpretation and its original proponents on the one side and quantum information theory on the other side is certainly Carl Friedrich von Weizsäcker's philosophically-physical interpretation of quantum mechanics. Weizsäcker places the information as a fundamental concept of contemporary science, and thus *Ur*, an atom of information [5], as the basic element of the system. This principle is then used as the basis of quantum information theory. "So, what is the message of the quantum? I suggest we look at the situation from a new angle. We have learned in the history of physics that it is important not to make distinctions that have no basis [...] I suggest that in a similar way, the distinction between reality and our knowledge of reality, between reality and information cannot be made." [6] Our description of nature thus deeply depends on the characteristics of the system of information. The fundamental principle of quantum information theory is, according to Zeilinger, that an elementary system has the information carrying capacity of at most one bit [7] and on this basis fundamental quantum phenomena, such as Heisenberg's uncertainty principle [8] or entanglement [9] are explained.

This merely epistemic approach of quantum information theory also makes its explanation of the collapse of wave function possible: "This, sometimes called reduction of the wave packet or collapse of the wave function, can only be seen as a measurement paradox if one views this change of the quantum state as a real physical process. In the extreme case it is often even related to an instant collapse of some physical wave in

space. There is never a paradox if we realize that the wave function is just an encoded mathematical representation of our knowledge of the system. When the state of a quantum system has a non-zero value at some position in space at some particular time, it does not mean that the system is physically present at that point, but only that our knowledge (or lack of knowledge) of the system allows the particle the possibility of being present at that point at that instant. What can be more natural than to change the representation of our knowledge if we gain new knowledge from a measurement performed on the system? When a measurement is performed, our knowledge of the system changes, and therefore its representation, the quantum state, also changes. In agreement with the new knowledge, it instantaneously changes all its components, even those which describe our knowledge in the regions of space quite distant from the site of the measurement." [10]

But as the approach of the quantum information theory is fundamentally epistemic, the objectivity of the information cannot be taken as self-evident on the basis of the common, from us independently existing outer world, as is the fact in classical physics. The coincidence in quantum-mechanical processes, completely independent from the observer, and extremely high accuracy and objectivity of the estimation of probabilities, indicate that it is not (only) the closed system of the (subjective) observer's information we are talking about, but that they rely on the, from us independent, reality. Nevertheless, the objectivity of the quantum world can be taken into account only on the basis of certain invariants, and of the inter-subjective agreement about the gained information and their meaning. On this basis it is possible to exceed the solipsism and to conclude that a system of information, independent from us, forms the objective reality, so that the outer world (in that sense) exists. "Andererseits kann es sein, dass diese Übereinstimmung zwischen verschiedenen Beobachtungen bedeutet, dass eine Welt existiert. Eine Welt, die so beschaffen ist, dass die Information, die wir besitzen – und wir besitzen nicht mehr –, offenbar in gewisser Weise auch unabhängig vom Beobachter besteht." [8] But still, since this approach is merely epistemic, there is no direct connection between the information and "that something this information is about". On this basis we can speak about an objective inter-subjective world of information, however we cannot speak about an objective outer world that this information is about. If information is all that exist, then there is nothing this information is about. And on this point the supplementation of this complex epistemic approach by a philosophical-ontic interpretation seems fruitful for further and wider investigation.

Connections with philosophical systems

Immanuel Kant

The relationship between the observer, the observation and the observed has not been seen as particularly important in classical physics, where objects of physical observation and their independence from the observer have been taken for granted. On the contrary, this question has always been seen as crucial in philosophy and has very often been built into more complex philosophical systems. Therefore, one could say that quantum mechanics has not really opened a new problem, but has shed light on an old philosophical problem from a physical side. This opens a possibility for more complex processing of the problem, but since all traditional philosophical systems deal with these questions by only considering classical physics, one has to be very careful while transmitting certain philosophical approaches to the quantum field.

An important, complex and systematic philosophical treatment of the question of relationship between the observer and the observed is represented in Kant's Critique of Pure Reason [11]. As Kant's philosophy had an important place in general education at the time this questions were recognized as important in physical field and as his systematic, mainly epistemic approach offered an interesting basis for further reasoning, some parts of his approach have become, more or less directly and complexly, involved in physical reasoning about this questions.

In Critique of Pure Reason Kant emphasizes that what we are observing are not "things-in-themselves", but phenomena ("things-for-us", the observation). For something to become an object of knowledge, it must be experienced, and experience is structured by our minds. Therefore causality, time and space are not the conditions of the experienced world, but are forms of our cognition (space and time are forms of perceiving and causality is a form of knowing). The relationship between "things-in-themselves" and phenomena is therefore not causal. "Also ist es nur die Form der sinnlichen Anschauung, dadurch wir a priori Dinge anschauen können, wodurch wir aber auch die Objekte nur erkennen, wie sie uns (unsern Sinnen) erscheinen können, nicht wie sie an sich sein mögen." [12]

Kant's method, his distinction between phenomena and "things-in-itself", has offered an interesting basis for consideration of the relationship between the observer, the observation, and the observed. However, as Grete Herman already emphasized in the dialog with Heisenberg and Weizsäcker, in Kant's philosophy the place of the physical object is solely on the side of phenomena, therefore the difference between the-thing-in-itself and the phenomena, as developed by Kant, cannot be transmitted to

the relationship between the physical object and the information about it, if one stays in accordance with Kant's philosophical system: "Sie müssen deutlich unterscheiden zwischen dem Ding an sich und dem physikalischen Gegenstand. Das Ding an sich tritt nach Kant in der Erscheinung überhaupt nicht auf, auch nicht indirekt. Dieser Begriff hat in der Naturwissenschaft und in der ganzen theoretischen Philosophie nur die Funktion, dasjenige zu bezeichnen, worüber man schlechterdings nichts wissen kann. [...] Wenn Sie im Sinne der klassischen Physik vom Radium B-Atom "an sich" sprechen, so meinen Sie damit also eher das, was Kant einen Gegenstand oder ein Objekt nennt. Objekte sind Teile der Welt der Erscheinung: Stühle und Tische, Sterne und Atome." [13]

Therefore, although Kant's approach is mainly epistemic, his philosophical system as such is incompatible with quantum physics or at least with its epistemic interpretations, since ontic interpretations are much closer to classical views on the relationship between the observer and the observed. Nevertheless, his method – his refined relationship between the phenomenon and "thing-in-itself" – is compatible with (orthodox) epistemic interpretations of quantum mechanics. His definition of the relationship between the two (although transmitted from the relationship between "thing-in-itself": phenomenon to the relationship observed: information) has been thus, with more or less awareness of its source and more or less completely, frequently integrated into the epistemic quantum interpretations. This can be seen in quantum information theory and its interpretation of the relationship between the information and "that something this information is about".

However, the more than 200 years old Kant's philosophical system has been, since its formation, frequently re-considered within the field of philosophy. The lack of permeability between the "thing-in-itself" and the phenomena, which can not be causally connected, even though some kind of connection between the two exists, has been recognized as one of the most problematic parts of his system, [14] even by Kant himself: "... though we cannot know these objects as things in themselves, we must yet be in a position at least to think them as things in themselves; otherwise we should be landed in the absurd conclusion that there can be appearance without anything that appears." [11]

Because the main features of the relationship between the information and "that-something-this-information-is-about" in quantum information theory are quite similar to Kant's definition of relationship between the phenomena and the "thing-in-itself", the problems that this kind of approach is facing are similar as well. Information is sensible only as long it

is information about something, but if information is everything it is, what is the information about?

Edmund Husserl

In the philosophical field an answer has been provided by Husserl's approach towards the observer and the observed within his phenomenology. His approach is still mainly epistemic, but maintains the permeability between the "thing-in-itself" and the phenomenon. Despite later criticisms and additions to his system, his construct of phenomenon being essentially related to both: to the observer (and his way of observing) and to the observed itself, has remained intact. For Husserl phenomenon means: the object as has been given to me by itself, but essentially to me, in the way to have a meaning (exactly) to me. Husserl's phenomenon still depends on the observer's cognition but at the same time also on the observed. The connection between the two is causal – "Es ist also ein prinzipieller Irrtum zu meinen, es komme die Wahrnehmung (und ihrer Weise jede andersartige Dinganschauung) an das Ding selbst nicht heran. Dieses sei an sich und in seinem Ansich-sein uns nicht gegeben. Es gehöre zu jedem Seiendem die prinzipielle Möglichkeit, es, als was es ist, schlicht anzuschauen und speziell es Wahrzunehmen in einer adäquaten, das leibhaftige Selbst ohne jede Vermittlung durch "Erscheinungen" gebenden Wahrnehmung." [15]

As such Husserl's philosophical approach towards the relationship between the phenomenon and the "thing-in-itself" (again as with Kant it is not the whole philosophical system that is transmitted, but solely his approach towards this relationship) seems as an interesting possibility for the substitution of quantum information theory's description of the relationship between the information and "that something information is about" within quantum reality.

The connection between the quantum information theory and Husserl's phenomenological approach towards the relationship between the observation and the observed gives the following result: Information and "that something this information is about" within the quantum information theory are causally connected – the information represents the direct answer to the question about the observed (information as the "eigen value" in the case of the description of the measurement in Hilbert space), the basis for this information is, however, the observed itself ("quantum system" in the case of the description of the measurement inside Hilbert space). This connection makes the information meaningful (it is information about something, for example value of the position or of the polarization of

the (observed) photon) and supplements the merely epistemic quantum-information approach with an ontic approach, without introducing quantum realism.

Epistemic and ontic interpretation of quantum mechanics – further derivations

Based on the presented possibility of ontic-epistemic interpretations of quantum mechanics some further philosophical-physical issues can be detailed. Beside the relationship between the observation and the observed, also the relationship between the two and the observer has been frequently considered in philosophy, but has not been particularly important in classical physics, while it has been recognized as relevant in quantum physics. The presented ontic-epistemic approach offers following considerations of the relationship between the information and the “that something this information is about” (the observed) on the one side and the observer on the other side – they are both in two ways connected to the observer:

1. To the observer as observer per se, as to the one for whom they have a meaning. There the observer and his way of comprehension can be seen as the answer to the question “Why information”.
2. To the observer as to the part of an environment, as to the one, who, by trying to get any information, already (necessary) has an influence on the observed and on the information about it.

The first connection is merely epistemic. The information has a meaning as information only as long it is information for someone. Most probably the preconditions of our comprehension are those that determine information as the form, in which everything we comprehend is given. (If our cognition is not taken as something pre-given but as something that has evolved itself as an efficient process for survival in our environment, the relationship is ontic-epistemic already at this point. The reason for our cognition being such that it grasps the world in the form of information is that this is one of the (most) suitable ways to survive in this world. This approach offers also a possible answer to the question of why classical physics seems more intuitive as quantum physics. The answer is: because the comprehension of classical systems is far more crucial for survival.) However, the second connection is merely ontic. Since information is always information about something, in the case of the measurement not only our information about the observed system is changed, but the observed system as entangled with the measurement apparatus (and thus

with our classical system) as well. This process has been described by decoherence.

Both connections emphasize the transition from quantum to classical. Decoherence of the observed quantum system and thus its connection with our classical environment makes it possible to describe it in our classical language and to transmit some characteristics of our classical system to it, and can be thus seen as the basis for the ontic description of the transition from quantum to classical description. However, this transition has to be described from the epistemic point of view as well.

Concepts that we know from our every-day experience are classical concepts, since we know they rely on complex systems, but we do not have any basis for connecting them with coherent quantum systems. Any direct observation would cause decoherence and would thus a-priori disable the observation of the coherent quantum system. An abstract mathematical description of the coherent quantum system is a meaningful operationalistic description of the system we are not directly connected to (which is not directly observed). On the other hand, any interpretation of this description based on the usage of classical concepts has no basis. It is meaningless to speak about the "real existence" of the wave function, or to describe coherent quantum system within the concepts of time and space, since these are classical concepts, based on our everyday experiences in the world of complex decohered systems.

However, another important consideration of the transition from quantum to classical is based on the logical postulate that to describe something it is necessary to be outside the described set. This postulate operationalistically explains the cut between quantum and classical in the process of measurement and is thus (more or less) identical to Heisenberg's consideration of this problem known as "Heisenberg cut" [16]. "There arises the necessity to draw a clear dividing line in the description of atomic processes, between the measuring apparatus of the observer which is described in classical concepts, and the object under observation, whose behaviour is represented by a wave function." [17] "This cut can be shifted arbitrarily far in the direction of the observer in the region that can otherwise be described according to the laws of classical physics, [...] the cut cannot be shifted arbitrarily in the direction of the atomic system" [18]. This cut is a necessary condition for the possibility of empirical knowledge and is as such operationalistic, but not arbitrary. On the one hand the choice depends on the nature of experiment, and on the other hand, since quantum description is universal, while classical physics can describe only complex classical systems, the cut cannot be shifted arbitrary in the direction of the atomic system.

Connection with the experiment: Delayed choice entanglement swapping

In the following chapter the above represented interpretation is applied to an experiment in order to offer a clearer representation. The experiment – “Delayed choice entanglement swapping experiment” has been chosen as a recent experiment that deals with the foundational questions and emphasizes some essential characteristics of quantum mechanics, which are often seen as peculiar.

The experiment is based on the swapping of entanglement within two systems of entangled photons: two observers (Alice and Bob) independently prepare two entangled particles. They test one particle of each pair (1 and 4) along an arbitrarily chosen direction and send the other particle (2 and 3) to a third observer, Victor. At a later time (optical delay), Victor decides either to entangle particles 2 and 3 or not and then test them as well. According to his choice of test and to his results, Alice and Bob can sort into subsets the samples that they have already tested, and in the case, when particles 2 and 3 has been entangled, the the data of particles 1 and 4 suggest that they have been entangled as well, although they have never communicated in the past, not even indirectly via other particles. [19, 20, 21]

But the situation seems less peculiar if our understanding originates from the clear distinction between the observed systems and the information about it. Individual values of measurements are our information about the observed, the entanglement witness (the data on the basis of which we conclude that two photons are entangled – see the figure below [21]) represents the relationships between the information. On the one hand information has a meaning only as long it is information about the observed systems – in our case about one of the observed photons (or of the system of two entangled photons). On the other hand our investigation of possible entanglement is not based on direct observation and interpretation of the whole observed system as it was the case in classical physics, but on the measurement, which gives us information about the chosen property of the observed, polarization of the photons in our case, and afterwards on the interpretation of this information (entanglement witness is not information about the relationship between two observed photons, but is the relationship between the information about the photons). Therefore it is meaningless to speak about a causal relationship between the entanglement of the photons 2 and 3 and the nature of relationship between the photons 1 and 4, since (at the last step) it is information about the observed system we are interpreting with and not the observed photons by itself.

This is clearly represented in figure 1: without the left column that connects information with “that-something this information is about”, the interpretation of the information would lose its content. Nevertheless, it is the interpretation of the information within the four columns on the right that gives us the basis to speak about entanglement between photons that have never communicated with each other.

Photon pairs	Measurement i		Measurement ii	
	State fidelity	Entanglement witness	State fidelity	Entanglement witness
2 and 3	0.645 ± 0.031	-0.145 ± 0.031	0.379 ± 0.026	0.120 ± 0.026
1 and 4	0.681 ± 0.034	-0.181 ± 0.034	0.421 ± 0.029	0.078 ± 0.029
1 and 2	0.301 ± 0.039	0.199 ± 0.039	0.908 ± 0.016	-0.408 ± 0.016
3 and 4	0.274 ± 0.039	0.226 ± 0.039	0.864 ± 0.019	-0.364 ± 0.019

Table 1: Delayed choice entanglement swapping experiments results [21].

Conclusions

A reconsideration of a merely epistemic quantum information theory within continental philosophy offers a possibility for an ontic supplementation. If we follow Husserl’s understanding of the relationship between phenomena and “thing-in-itself” when considering the relationship between information and the observed in quantum information theory, information and the observed can be seen as causally connected and information can be understood as information about the observed. This approach thus offers the firm answer how to exceed solipsism and gain common objectivity of quantum mechanical description, without introducing further realism, since everything that we can say about the observed, beside the answer given by the information about it, is that it exists, and it is senseless to speak about any pre-given properties. Thus we avoid a radical epistemic point of view, where everything that exists is solely our knowledge. Thereby we avoid facing the Cartesian way of reduction in which there is no point where someone could stop and recognise something as existing (not even the observer as the one having that knowledge) and thus as the basis for any hypothesis about reality. But at the same instance we also avoid wasteful scientific realism, bringing huge amount of new elements into the description (either variables, worlds or something else), that can be seen as an interesting alternative form physical operationalistic point of view, but certainly as problematic from the philosophi-

cal point of view, since a huge amount of unintuitive, not evidence based elements have been brought into picture on one side, to avoid unintuitiveness on the other side. This small, but fundamental change in philosophical understanding of the ontic status of information and its basis solves important philosophical problems regarding the relationship between the observer, the observation and the observed (as are “what is the information about”, “what exists”, “why this information”, “how to gain objectivity”, etc.) without loosing any explanatory power of quantum information theory. This kind of picture is much more consistent from the philosophical point of view and thus offers a more firm basis for further consideration, therefore some fundamental principles of quantum information theory can now be re-thought within this philosophical context. The prospects of this philosophical approach are thus the reconsideration and supplementary support of the fundamental elements of the theory, as are: the character of information and the principle that an elementary system has the information carrying capacity of at most one bit.

Acknowledgement

This work was supported by a grant from the John Templeton Foundation. I would like to thank Markus Aspelmeyer, Caslav Brukner, Johannes Kofler and Anton Zeilinger for inspiring discussions and helpful comments.

References

- [1] H. Atmanspacher and H. Primas, *Epistemic and Ontic Quantum realities*. In: Time, Quantum and Information, ed. L. Castell and O. Ischebeck, (Springer, Heidelberg, Berlin, New York, 2003) 301-323.
- [2] D. Bohm and B. Hiley, *The Undivided Universe: An Ontological Interpretation of Quantum Theory*, (Routledge, London, New York 1993).
- [3] A. Petersen, Bulletin of the Atomic Scientists **19** (1963) 8.
- [4] C. Brukner and A. Zeilinger, *Quantum Physics as a Science of Information*, in: Quo Vadis Quantum Mechanics?, ed. A. Elitzur *et al.*, (Springer, Berlin, Heidelberg, New York, 2005) 47-63.
- [5] C.F. von Weizsäcker *Aufbau der Physik*, (Carl Hanser Verlag, München, Wien 1985).
- [6] A. Zeilinger, Nature **438** (2005) 743.
- [7] A. Zeilinger, Found. Phys. **29** (1999) 631.
- [8] A. Zeilinger, *Einsteins Schleier*, (Verlag C.H. Beck oHG, München, 2003).
- [9] C. Brukner *et al.*, New Advances in Physics (Journal of Chinese Physical Society), [arXiv:quant-ph/0106119].
- [10] C. Brukner and A. Zeilinger, *Information and fundamental elements of the structure of quantum theory*, in: Time, Quantum and Information, ed. L. Castell and O. Ischebeck, (Springer, Heidelberg, Berlin, New York, 2003) 323-355.

- [11] I. Kant, *Critique of Pure Reason*, transl. P. Macmillan (Macmillan Publishers Limited, Basingstoke, Hampshire, 2010).
- [12] I. Kant, *Prolegomena zu einer jeden künftigen Metaphysik, die als Wissenschaft wird auftreten können*, (Reclam, Dtzingen, 1989).
- [13] W. Heisenberg, *Quantentheorie und Philosophie*, (Reclam, Stuttgart, 1986).
- [14] I. Blecha, transl. J. Vinkler, *Phainomena* **10** (2001) 143.
- [15] E. Husserl, *Ideen zu einer reinen Phänomenologie und phänomenologischen Philosophie*, (Springer, Dordrecht, 1976).
- [16] M.A. Schlosshauer, *Decoherence and the quantum-to-classical transition*, (Springer, Berlin, 2007).
- [17] W. Heisenberg, *Recent changes in the foundations of exact science, in Philosophic Problems in Nuclear Science*, transl. F.C. Hayes, (Faber and Faber, London, 1952).
- [18] W. Heisenberg, *Ist eine deterministische Ergänzung der Quantenmechanik möglich?*, in: Wolfgang Pauli. *Wissenschaftlicher Briefwechsel mit Bohr, Einstein, Heisenberg*, Vol. 1: 1919-1929, ed. A. Hermann *et al.*, (Springer, New York, 1985).
- [19] A. Peres, *J. Mod. Opt.* **47** (2000) 139.
- [20] C. Brukner *et al.*, *Found. Phys.* **35** (2005) 1909, [arXiv:quant-ph/0405036].
- [21] X. Ma, *Nonlocal Delayed-Choice Experiments with Entangled Photons*, *PhD thesis*, (University of Vienna, Vienna, 2010).

t & *m*



Figure 1: Participants of the 3rd International Conference on TIME AND MATTER 2010. From left to right, *standing*: Y.J. Ng, H. Nicolai, M. O'Loughlin, A. Glazov, H. Zinkernagel, T. Bilban, J.-C. Hamilton, A. Creusot, M. Blau, G. Medin, T.C. Paul, B. Lakić, W. Adam, D. Raftopoulos, R. Percacci, D. Veberič, A. Lawrence, S. Stanić, A. Sušnik, D. Zavrtnanik, B.P. Kerševan, and S. Mizrahi, *kneeling*: L. Seri, M. Vonlanthen, P. Kržan, P. Schmidt-Wellenburg, O. Tajima, and R. Lefevre

